Assessment of performance in patients with homonymous visual field defects by analysis of their visual exploration, using standardized, virtual reality environments – a study for critical comparison with the current approach by conventional perimetry.

Dissertation

zur Erlangung des Grades eines Doktors
der Naturwissenschaften

der Mathematisch-Naturwissenschaftlichen Fakultät
und
der Medizinischen Fakultät
der Eberhard-Karls-Universität Tübingen

vorgelegt
von

Papageorgiou Eleni
Aus Larissa, Griechenland

April - 2011

Tag der mündlichen Prüfung:	22. September 2011
Dekan der Math.-Nat. Fakultät:	Prof. Dr. W. Rosenstiel
Dekan der Medizinischen Fakultät:	Prof. Dr. I. B. Autenrieth
1. Berichterstatter:	Prof. Dr. U. Schiefer
2. Berichterstatter:	Prof. Dr. H. Mallot
Prüfungskommission:	Prof. Dr. U. Schiefer
	Prof. Dr. H. A. Mallot
	Prof. Dr. U. Ernemann
	Prof. Dr. U. Ilg
	Prof. Dr. F. Schaeffel

To my parents

Acknowledgements

Though only my name appears on the cover of this dissertation, a great many people have contributed to its production. I owe my gratitude to all those people who have made this dissertation possible and because of whom my doctoral experience has been one that I will cherish forever.

My deepest gratitude is to my advisor, Dr. Ulrich Schiefer. I have been amazingly fortunate to have an advisor who gave me the freedom to explore on my own, and at the same time the guidance to recover when my steps faltered. I hope that one day I would become as good an advisor to my students as Uli has been to me.

My co-advisor, Dr. Hanspeter Mallot, has been always there to listen and give advice. I am deeply grateful to him for the long discussions that helped me sort out the details of my work. I am also indebted to Dr. Gregor Hardiess, for introducing me to virtual reality, reading my reports, commenting on my views and helping me understand and enrich my ideas. This Thesis would not have been possible without his experimental contribution and practical advice.

I am also grateful to Elke Krapp and Dr. Jens Paetzold, former members of the Research Group Visual Pathway at the University of Tübingen, for their various forms of support during my doctorate. I would also like to thank all my colleagues and staff from the Department of Neuro-Ophthalmology with whom I have interacted during the course of my doctoral studies.

I am also indebted to the members of the Department of the Medical Biometry at the University of Tübingen, for introducing me to Statistics. Particularly, I would like to acknowledge Dr. Klaus Dietz, Dr. Birgitt Schoenfisch and Dr. Reinhard Vonthein, for their valuable teachings and statistical guidance in this research.

Most importantly, none of this would have been possible without the love and patience of my family.

Finally, I appreciate the administrative support from Dr. Thomas Wheeler-Schilling and the financial support from the European Union (Marie Curie Fellowship for Early Stage Training) that funded the research discussed in this dissertation.

Table of contents

1. Papageorgiou E, Hardiess G, Schaeffel F, Wiethoelter H, Karnath HO, Mallot HA, Schoenfisch B, Schiefer U. Assessment of vision-related quality of life in patients with homonymous visual field defects. (Graefes Arch Clin Exp Ophthalmol 2007;245:1749-58)

2. Hardiess G, Papageorgiou E, Schiefer U, Mallot HA. Functional compensation of visual field deficits in hemianopic patients under the influence of different task demands. (Vision Res 2010;50:1158-72.)

3. Papageorgiou E, Hardiess G, Ackermann H, Wiethoelter H, Dietz K, Mallot HA, Schiefer U. Collision avoidance in persons with homonymous visual field defects under virtual reality conditions. (in press in Vision Research)

4. Papageorgiou E, Hardiess G, Mallot H.A., Schiefer U. Gaze patterns predicting successful collision avoidance in patients with homonymous visual field defects. (submitted in Vision Research)

5. Papageorgiou E, Ticini L, Hardiess G, Schaeffel F, Wiethoelter H, Mallot HA, Vonthein R, Wilhelm B, Schiefer U, Karnath HO. The pupillary light reflex pathway: cytoarchitectonic probabilistic maps in hemianopic patients. (Neurology 2008;70:956-63)

Synopsis

Assessment of performance in patients with homonymous visual field defects
by analysis of their visual exploration, using standardized,
virtual reality environments – a study for critical comparison
with the current approach by conventional perimetry.

1. Introduction

In developed countries stroke is the third most common cause of death after heart disease and cancer. As stroke mortality rates decline, individuals are increasingly likely to live with their residual impairments [1]. Homonymous visual field defects (HVFDs), the loss of the field of vision in the same relative position in both eyes, are among the most common disorders that occur in the elderly after vascular brain damage and can pose a considerable impact for survivors' subsequent well-being. Approximately 30% of all patients with stroke and 70% of those with stroke involving the posterior cerebral artery suffer from HVFDs [2, 3]. In Germany there is an incidence of approximately 550,000 brain-injured patients per year, 135,000 of them suffer from visual disturbances, mostly HVFDs. Specific functional impairments related to HVFDs have been repeatedly described in the literature. Patients complain mainly of difficulties with reading and scanning scenes fast enough to make sense of things as a whole. Consequently, they fail to notice relevant obstacles or avoid obstacles on their affected side and may collide with approaching people or cars. This has far reaching repercussions on their vocational and private lives [3]. While a variety of methods for quantifying visual field loss exist, there is not enough information about the degree of functional impairment in everyday life and about how homonymous visual field loss relates to patient-reported functioning.

Additionally, the few studies assessing the performance of patients with HVFDs in realistic or experimental driving paradigms report controversial findings. Some authors suggest that performance of patients with HVFDs is significantly worse than that of normal subjects [4-8]. On the other hand, other studies report that there are no performance differences between patients with HVFDs and control subjects, because some patients develop adaptive eye- and head-movements allowing them to efficiently compensate for the visual field loss and the present challenge is to identify them [9-11]. A compensatory strategy that has been observed in tasks, including dot-

counting [7, 12], viewing of natural and degraded images [13] and visual search paradigms is the deviation of the fixation point towards the hemianopic side. However, to date hemianopic gaze patterns have been assessed only on stationary displays, usually limiting the field of view to a computer screen. Although the most demanding tasks for hemianopic patients arise within dynamic – commonly time-constrained – situations in our constantly changing visual world [12], little is known about the exploration strategy applied by those patients when confronted with moving stimuli.

Therefore, the aims of the present work were (i) to describe the vision-targeted, health-related QOL, assessed with the 25-item National Eye Institute Visual Functioning Questionnaire (NEI-VFQ-25) in patients with HVFDs (ii) to assess the performance of patients with HVFDs in comparison to normal-sighted control subjects in a dot-counting task, a comparative visual search paradigm and a dynamic collision avoidance task, (iii) to investigate the underlying factors affecting performance (i.e. visual field measures, age, gender, side of brain injury, compensatory gaze patterns), and (iv) to assess the brain regions associated with impaired performance of patients with HVFDs.

Additionally, an interesting question raised in regard with the presence of a relative afferent pupillary defect (RAPD) in patients with HVFDs due to cerebrovascular lesions in the posterior and middle cerebral artery territories. A RAPD is characterized by diminished pupillary constriction on direct illumination with a normal consensual response to illumination of the contralateral eye. The neural pathway of the pupillary light reflex (PLR) was first described by Wernicke in the 1880s [14]. According to this classical model of a direct retinal-pretectal connection, a RAPD is typically related to lesions within the anterior visual pathways, unilateral or asymmetric bilateral optic nerve disease, optic tract lesions and congenital occipital hemianopia [15-17]. The detection of a RAPD in acute homonymous hemianopias is hence commonly used in differentiating infrageniculate from suprageniculate lesions. However, the presence of a RAPD in acquired suprageniculate lesions and the underlying anatomic pathway are still a matter of debate, mainly because of numerous studies, reporting disturbances of the PLR in patients with HVFDs due to lesions not involving the optic tract. Many theories have been developed to explain these phenomena, the most prominent pointing out that the integrity of the pupillomotor response depends upon or is influenced also by the occipital cortex [18-21]. However,

the anatomic evidence is still limited to make any clear conclusions. Therefore, we extended our study in (v) investigating the association of relative afferent pupillary defect (RAPD) with the location and extent of brain lesions in patients with HVFDs.

2. Summary

2.1. Assessment of vision-related quality of life in patients with homonymous visual field defects. (Graefes Arch Clin Exp Ophthalmol 2007;245:1749-58)

Patients with HVFDs have difficulties in reading [12, 22], may collide with obstacles on the affected side [3], and generally have problems to comprehend entire visual scenes at a glance. However, reports that specifically describe the vision-related QOL of patients with HVFDs after vascular brain damage by using vision-targeted, standardized instruments are missing. Therefore, we described the vision-targeted, health-related QOL, assessed with the 25-item National Eye Institute Visual Functioning Questionnaire (NEI-VFQ-25, www.rand.org) in patients with HVFDs after cerebrovascular lesion [23, 24], and determined the relationship between the NEI-VFQ-25 scores and the characteristics of HVFDs in the binocular visual field, assessed with semi-automated kinetic perimetry (SKP).

Our findings suggest that patients with HVFDs due to cerebrovascular disease experience a reduction in vision-targeted QOL as indicated by 6 of 11 NEI-VFQ-25 subscales: general vision, near vision, vision-specific mental health, driving, colour vision, and peripheral vision. Furthermore, the composite score as well as the general health score were significantly lower in patients than in reference subjects. Homonymous visual field loss is apparently correlated with a general deterioration in perceived visual function. However, the correlation of the composite score with the extent of the HVFD was weak, indicating a tendency for poorer NEI-VFQ-25 scores with increasing visual field defects. This finding suggests that an objective assessment of the visual field alone may not accurately reflect the actual or perceived ability of the patient to function, and highlights the growing need to design clinical tests of vision that better correlate with patient perception. Additional features which could be considered when performing activities of daily living (ADL) are exploratory eye movements and head turns. Especially in patients with homonymous visual field defects, visual exploration through saccadic eye movements and head turns plays a substantial role because it enables the shift of circumscribed (binocular) visual field

defects from relevant to less important areas of the visual environment [25]. Intact exploration ability thus can at least partially compensate for an existing visual field defect [26-28]. These exploratory viewing strategies represent a substantial characteristic of our visual behaviour and should therefore be assessed in any attempt to describe vision-related QOL. A future challenge for investigators is the design of innovative clinical tests in order to quantify visual exploration and its impact on QOL.

2.2. Functional compensation of visual field deficits in hemianopic patients under the influence of different task demands. (Vision Res 2010;50:1158-72.)

Since some hemianopic patients are able to overcome their visual limitation, the deficits mentioned above should be related to the degree of functional compensation. To compensate for HVFDs, patients need appropriate gaze strategies for efficient use of the remaining areas of the visual system, such as the deviation of the fixation point towards the hemianopic side [29]. In the majority of studies concerning the compensatory gaze behavior, the stimuli were presented on computer screens and hence limited the field of view. Additionally, studies investigating one and the same hemianopic collective in different visual tasks in order to analyze their different exploration capabilities are missing. Therefore, we investigated the task performance and the adaptive, gaze-related strategies of patients with long-standing homonymous hemianopia in two experiments differing in their demand concerning cognitive functions. As first experiment, the dot counting task (DC) was applied as visual sampling paradigm but with enlarged stimulus size compared to the original setup [12]. Secondly, a comparative visual search task (CVS) [30, 31] was introduced as a more cognitively challenging paradigm. In this paradigm two almost identical stimulus hemifields (cupboards filled with geometrical objects) had to be explored in order to find the amount of differences between them. To enable a natural field of view combined with the possibility to perform eye and head movements, a large field projection setup for displaying the stimuli was used.

Based on patients' performance in both experiments, two subgroups of HVFD patients could be identified; "adequately" performing $HVFD_A$ patients and "inadequately" performing $HVFD_I$ patients. In the DC task $HVFD_A$ patients showed visual performance in the range of healthy controls while $HVFD_I$ patients performed with increased gaze adaptation, including increased number of fixations, higher

proportion of fixations to the side of HVFD, longer scanpaths, and higher repetition of fixations compared to controls. However, in the more complex CVS task a strikingly different compensatory gaze pattern was identified: even adequately performing patients adopted a compensatory scanning behavior, in order to overcome their visual limitation. The number of fixations and the scanpath length were increased, while the mean amplitude of saccades was decreased. We suggest that the difference between adequately and inadequately performing patients is due to reduced working memory availability in the $HVFD_I$ patients. In the DC task $HVFD_I$ patients therefore need to compensate with eye movements whereas $HVFD_A$ patients can rely on working memory. In the CVS task, working memory is needed for object recognition, such that scanning compensation now has to be achieved via gaze movements also in $HVFD_A$ patients. The $HVFD_I$ patients attempt to compensate by gaze movements for both, scanning and recognition demands, but fail.

A further anatomical analysis identified three lesion sites as unique to $HVFD_I$ patients: mesio-ventral areas of the temporal lobe (i.e. the fusiform gyrus), the inferior occipital lobe, and the parahippocampal gyrus. Regarding the site of brain lesion, our results are consistent with a recent study on visual search of hemianopes [32], which showed that mesio-ventral areas of the temporal lobe were commonly damaged in severely impaired patients but spared in mildly impaired patients. Temporal regions belong to the ventral processing visual stream, thought to be involved in the visual recognition of objects, including color, texture and form information [33] and may also play a role in the control of attention [34, 35]. Lesions of the mesio-ventral temporal areas and V4 might have affected object recognition and subsequently visual search of $HVFD_I$ patients [32]. In addition, we found that the parahippocampal gyrus is commonly affected in $HVFD_I$ patients. Since the parahippocampal gyrus serves as the main input–output pathway between the hippocampus and cortical association areas, its damage can lead to many cognitive deficits including deficits in memory storage or retrieval from other brain areas [36].

2.3. Collision avoidance in persons with homonymous visual field defects under virtual reality conditions. (in press in Vision Research)

In addition to compensatory behavior of hemianopes when confronted with stationary stimuli, we further examined the effect of homonymous visual field defects

(HVFDs) on collision avoidance of dynamic obstacles at an intersection under virtual reality (VR) conditions. Overall performance was quantitatively assessed as the number of collisions. Two difficulty levels including different numbers of dynamic obstacles were used ("densities" of 50% and 75%). We hypothesized that patients with HVFDs would demonstrate poorer performance than normal subjects in terms of collision avoidance at the intersection. However, we speculated that performance would not be solely explained by visual field-related parameters and therefore expected contribution of additional factors, e.g. age, gender, side of brain lesion, time span since brain lesion onset, presence of macular sparing and compensatory behavior.

As hypothesized, subjects with HVFDs experienced more collisions with vehicles approaching from the blind side than the seeing side and had on average more collisions than subjects with normal vision. Advancing visual field defects and increasing age were associated with worse performance. These results suggest that patients with HVFDs are less efficient and experience difficulties in collision avoidance under VR conditions. Our findings are partly in accordance with a recent study [4] reporting significantly lower detection rates of drivers with homonymous hemianopia for stationary pedestrians on the blind side than the seeing side, which were significantly lower than those of drivers with normal vision. We suggest that hemianopics perform on average worse than normal subjects, but may achieve better ratings on collision avoidance tasks with moving obstacles than on detection of stationary targets at intersections, probably due to the Riddoch phenomenon or statokinetic dissociation [37]. The relationship between the extent of the HVFD and the number of collisions was weak, performance of some patients was similar to that of normal subjects and wide variability among subjects was observed. The high degree of between-subject variability in patients with HVFDs in VR or on-road driving tasks has been reported in other studies as well and may reflect the different capacities of each individual to compensate for their visual disability [4, 6, 11, 38]. Therefore, we suggest that perimetric findings per se seem to be inadequate in predicting collision avoidance of hemianopic patients under VR-conditions. Due to this wide between-subject variability, generalization of the findings regarding the impact of HVFDs is misleading and individualized approaches of compensatory functional behavior of patients with HVFDs are necessary. Future studies should attempt to find predictors of visual compensation in realistic tasks and measure not

only the extent of the visual field defect, but also the extent to which impaired individuals adopt compensatory viewing strategies. Assessment of visual exploration (head and eye movements), functioning in everyday life and multimodal approaches (performance in different tasks) may play an important role in determining the visual capacities of patients with homonymous visual field loss.

2.4. Gaze patterns predicting successful collision avoidance in patients with homonymous visual field defects. (submitted in Vision Research)

Recent evidence suggested that efficient oculomotor adaptation to visual field loss is highly specific and task-dependent [39], therefore specialized approaches seem necessary in order to assess visual behavior of hemianopic patients towards dynamic objects in contrast to stationary targets. Based on the wide between-subject variability and our findings from the DC and the CVS task, our next aim was hence to identify efficient compensatory gaze patterns applied by patients with HVFDs in the collision avoidance task. We hypothesized that patients with high success rates in completing the task will demonstrate compensatory scanning patterns, characterized by increased gaze movements especially towards moving objects of interest on their blind side and that this gaze adaptation will be more evident in the more difficult task. Saccades, fixations, mean number of gaze shifts, scanpath length and the area under the curve, defined as the area scanned by eye and head movements, were compared between $HVFD_A$, $HVFD_I$ patients and normal subjects.

According to their performance (i.e. the number of collisions) patients were assigned to either an "adequate" ($HVFD_A$) or "inadequate" ($HVFD_I$) subgroup by the median split method. For both difficulty levels, the gaze pattern of $HVFD_A$ patients in comparison to $HVFD_I$ patients was characterized by more gaze shifts, longer saccadic amplitudes towards the affected and the intact side, more fixations on vehicles but fewer fixations on the intersection, longer scanpaths and larger area under the curve. Scanpath length and number of gaze shifts were similar between $HVFD_A$ patients and normal subjects. Overall, the visual exploration behavior was intensified in the subgroup of adequately performing patients. All patients showed increased fixational behavior compared to normals; however, $HVFD_A$ patients invested additional fixations in looking more often to vehicles, while $HVFD_I$ patients explored the straight ahead direction more often. This compensatory behavior became especially

evident during the more demanding task. A gaze bias to the blind hemifield – in terms of proportion of fixations and the area under the curve – is observed in both patient subgroups; however, adequately compensating patients undertake larger saccadic amplitudes and more gaze shifts than inadequate patients, leading to a scanned area that is even larger than that of normal subjects. These findings confirmed our initial hypothesis that patients with HVFDs who adapt successfully to their visual deficit, display distinct gaze patterns characterized by increased exploratory eye and head movements, particularly towards moving objects of interest on their blind side.

Interestingly, in an ongoing own study, lesion analysis in this patient group showed that the cortical structures associated with impaired collision avoidance were the parieto-occipital region and posterior cingulate gyrus in the *right* hemisphere, and the inferior occipital cortex and parts of the fusiform (occipito-temporal) gyrus in the *left* hemisphere. Therefore, impaired performance of patients with *right*-hemispheric lesions may be associated with damage in the dorsal processing stream and potential impact on the visual spatial working memory, while impaired performance of patients with *left*-hemispheric lesions may be associated with damage in the ventral stream and potential impact on the visual object working memory.

2.5. The pupillary light reflex pathway: cytoarchitectonic probabilistic maps in hemianopic patients. (Neurology 2008;70:956-63)

The pupillary light reflex (PLR) has for a long time been associated with a single subcortical neural pathway. Since then, numerous studies have examined the effect of visual cortical lesions on the PLR. The results – either the presence of papillary hemihypokinesia in the blind part of the visual field or a relative afferent pupillary defect (RAPD) contralateral to the brain lesion, as a response to full-field light stimulation – often contradicted this classic belief and provided evidence that the PLR is not just a pure subcortical pathway [18-20, 40]. However, the exact anatomic pathway remained unknown.

Using a new strategy of lesion analysis by combining established subtraction techniques [41] with the stereotaxic probabilistic cytoarchitectonic atlas developed by the Jülich group [42-45], our findings suggest that a region in the early course of the optic radiation in the temporal white matter, close to the lateral geniculate nucleus (LGN), seems to be associated with the presence of the RAPD. It was demonstrated

that the pupillary light reflex (PLR) depends on the input of suprageniculate neurons, thus supporting the involvement of a cortical pathway also. The site of integration of cortical signals in relation to the PLR into the pupillomotor pathway may be located suprageniculately in the vicinity of the LGN. This finding is consistent with the hypothesis that the connection between visual pathways and pretectal area in the dorsal midbrain is probably closely related to the LGN [40, 46-48]. Moreover, the suggested combination of established lesion analysis techniques with the probabilistic cytoarchitectonic atlas turned out to be a very helpful amelioration of stroke data analyses.

3. Outlook

Assessment of visual exploration (head and eye movements), functioning in everyday life and multimodal approaches (performance in different tasks) may play an important role in determining the visual capacities of patients with homonymous field loss. The next step is the investigation of compensatory strategies applied by patients with homonymous visual field defects under naturalistic, everyday scenarios. The findings of those studies should further enhance the development of rehabilitation tools for patients with visual field defects through training of their exploration ability (eye movements) for clinical use in hospitals and rehabilitation units. Furthermore, such an approach would be extremely useful as a tool for identification of inefficient exploration and subsequently unsuccessful compensatory ability (for example inadequate eye movements), which might have further implications in the field of driving research.

References

1. Haacke C, Althaus A, Spottke A, Siebert U, Back T, Dodel R (2006) Long-term outcome after stroke: evaluating health-related quality of life using utility measurements. Stroke, 37, 193–198.

2. Pambakian AL, Kennard C. (1997). Can visual function be restored in patients with homonymous hemianopia? British Journal of Ophthalmology, 81, 324–328.

3. Zihl J. (2000). Rehabilitation of visual disorders after brain injury. Psychology Press, Hove, East Sussex.

4. Bowers A, Mandel A, Goldstein R, Peli E. (2009). Driving with hemianopia: 1. Detection performance in a driving simulator. Investigative Ophthalmology and Visual Science, 50, 5137-5147.

5. Kooijman A, Brouwer W, Coeckelbergh T, Tant M, Cornelissen F, Bredewoud R, et al. (2004). Compensatory viewing training improves practical fitness to drive of subjects with impaired vision. Visual Impairment Research, 6, 1-27.

6. Lövsund P, Hedin A, Törnros J. (1991). Effects on driving performance of visual field defects: a driving simulator study. Accident; analysis and prevention, 23, 331-342.

7. Tant M, Brouwer W, Cornelissen F, Kooijman A. (2002). Driving and visuospatial performance in people with hemianopia. Neuropsychological rehabilitation, 12(5), 419-437.

8. Szlyk J, Brigell M, Seiple W. (1993). Effects of age and hemianopic visual field loss on driving. Optometry and Vision Science, 70(12), 1031-1037.

9. Martin T, Riley M, Kelly K, Hayhoe M, Huxlin K. (2007). Visually guided behavior of homonymous hemianopes in a naturalistic task. Vision Research, 47(28), 3434-3446.

10. Schulte T, Strasburger H, Muller-Oehring E, Kasten E, Sabel B. (1999). Automobile driving performance of brain-injured patients with visual field defects. American journal of physical medicine & rehabilitation, 78(2), 136-142.

11. Wood J., McGwin G, Elgin J, Vaphiades M, Braswell R, DeCarlo D, et al. (2009). On-road driving performance by persons with hemianopia and quadrantanopia. Investigative Ophthalmology and Vision Science, 50(2), 577-585.

12. Zihl J. (1995). Visual scanning behavior in patients with homonymous hemianopia. Neuropsychologia, 33(3), 287-303.

13. Pambakian A, Mannan S, Hodgson T, Kennard C. (2004). Saccadic visual search training: a treatment for patients with homonymous hemianopia. Journal of Neurology Neurosurgery and Psychiatry, 75(10), 1443-1448.

14. Wernicke C. (1883). Uber hemianopische Pupillenreaktion. Fortschritte Der Medizin, 1,49–53.

15. Savino PJ, Paris M, Schatz NJ, Orr LS, Corbett JJ. (1978). Optic tract syndrome: a review of patients. Archives of Ophthalmology, 96, 656–663.

16. Lowenfeld IE. (1993). The pupil. Anatomy, Physiology and Clinical Applications Vol. 1. Detroit: Wayne State University Press.

17. Newman SA, Miller NR. (1983). Optic tract syndrome: neuroophthalmologic considerations. Archives of Ophthalmology, 101, 1241–1250.

18. Hamann KU, Hellner KA, Muller-Jensen A, Zschocke S. (1979). Videopupillographic and VER investigations in patients with congenital and acquired lesions of the optic radiation. Ophthalmologica, 149, 348–356.

19. Wilhelm H, Kardon R. (1997). The pupillary light reflex pathway. Neuro-Ophthalmology, 6, 219–224.

20. Wilhelm H. Pupille und retrogenikulare Sehbahn. (1996). Ophthalmologe, 93, 319–324.

21. Wilhelm BJ, Wilhelm H, Moro S, Barbur JL. (2002). Pupil response components: studies in patients with Parinaud's syndrome. Brain, 125(Pt 10), 2296–2307.

22. McDonald, S. A., Spitsyna, G., Shillcock, R. C., Wise, R. J. S., & Leff, A. P. (2006). Patients with hemianopic alexia adopt an inefficient eye movement strategy when reading text. Brain, 129, 158–167.

23. Franke GH. (1999). Handbuch zum National Eye Institute Visual Function Questionnaire (NEI-VFQ) - ein psychodiagnostisches Verfahren zur Erfassung der Lebensqualität bei Sehbeeinträchtigten. Eigendruck, Essen.

24. Mangione CM, Lee PP, Gutierrez PR, Spritzer K, Berry S, Hays RD. (2001). Development of the 25-item national eye institute visual function questionnaire. Archives of Ophthalmology 119, 1050–1058.

25. Schiefer U, Hofer R, Vischer PM, Wilhelm H. (2000). Perimetry findings and driving performance. "How much visual field" does a motorist need? [Article in German] Ophthalmologe, 97, 491–497.

26. Coeckelbergh TR, Brouwer WH, Cornelissen FW, Van Wolffelaar P, Kooijman AC. (2002). The effect of visual field defects on driving performance: a driving simulator study. Archives of Ophthalmology, 120, 1509–1516.

27. Meienberg O, Zangemeister WH, Rosenberg M, Hoyt WF, Stark L. (1981). Saccadic eye movement strategies in patients with homonymous hemianopia. Annals of Neurology, 9, 537–544.

28. Zangemeister WH, Utz P. (2002). An increase in a virtual hemianopic field defect enhances the efficiency of secondary adaptive gaze strategies. Current Psychology and Cognition, 21, 281–303.

29. Gassel M, Williams D. (1963). Visual function in patients with homonymous hemianopia II. Oculo-motor mechanisms. Brain, 86, 1–36.

30. Hardiess G, Gillner S, Mallot HA. (2008). Head and eye movements and the role of memory limitations in a visual search paradigm. Journal of Vision, 8(1), 1–13.

31. Pomplun M, Sichelschmidt L, Wagner K, Clermont T, Rickheit G, Ritter H. (2001). Comparative visual search: A difference that makes a difference. Cognitive Science, 25, 3–36.

32. Machner B, Sprenger A, Kompf D, Sander T, Heide W, Kimmig H, et al. (2009). Visual search disorders beyond pure sensory failure in patients with acute homonymous visual field defects. Neuropsychologia, 47, 2704–2711.

33. Ungerleider L, Mishkin M. (1982). Two cortical visual systems. In D. J. Ingle, M. A. Goodale, & R. J. W. Mansfield (Eds.), Analysis of visual behavior. Cambridge, MA: The MIT Press.

34. Goodale M, Milner D. (1996). Separate visual pathways for perception and action. In A. Ellis & A. Young (Eds.), Human cognitive neuropsychology. A textbook with readings. Hove, East Sussex: Psychology Press.

35. Ungerleider L, Pasternak T. (2004). Ventral and dorsal cortical processing streams. In L. Chalupa & J. Werner (Eds.). The visual neurosciences (Vol. 1). Cambridge, MA: The MIT Press.

36. Ploner CJ, Gaymard BM, Rivaud-Péchoux S, Baulac M, Clémenceau S, Samson S, Pierrot-Deseilligny C. (2000). Lesions affecting the parahippocampal cortex yield spatial memory deficits in humans. Cerebral Cortex, 10(12), 1211-1216.

37. Schiller J, Paetzold J, Vonthein R, Hart WM, Kurtenbach A, Schiefer[U. (2006). Quantification of stato-kinetic dissociation by semi-automated perimetry. Vision Research, 46(1-2), 117–128.

38. Racette L, Casson E. (2005). The impact of visual field loss on driving performance: evidence from on-road driving assessments. Optometry and Vision Science, 82(8), 668-674.

39. Schuett S, Kentridge RW, Zihl J, Heywood CA. (2009). Adaptation of eye-movements to simulated hemianopia in reading and visual exploration: Transfer or specificity? Neuropsychologia, 47, 1712-1720.

40. Wilhelm H, Wilhelm B, Petersen D, Schmidt U, Schiefer U. (1996). Relative afferent pupillary defects in patients with geniculate and retrogeniculate lesions. Neuro-Ophthalmology, 16, 219–224.

41. Rorden C, Karnath H-O. (2004). Using human brain lesions to infer function: a relic from a past era in the fMRI age? Nature Reviews Neuroscience, 5, 813–819.

42. Amunts K, Zilles K. (2001). Advances in cytoarchitectonic mapping of the human cerebral cortex. Neuroimaging Clinics of North America, 11, 151–169.

43. Zilles K, Schleicher A, Palomero-Gallagher N, Amunts K. (2002). Quantitative analysis of cyto- and receptor architecture of the human brain. In: Mazziotta JC, Toga A, eds. Brain Mapping: The Methods. Amsterdam: Elsevier; 573–602.

44. Burgel U, Amunts K, Hoemke L, Gilsbach JM, Zilles K. (2006). White matter fiber tracts of the human brain: threedimensional mapping at microscopic resolution, topography and intersubject variability. Neuroimage, 29, 1092–1105.

45. Burgel U, Schormann T, Schleicher A, Zilles K. (1999). Mapping of histologically identified long fiber tracts in human cerebral hemispheres to the MRI volume of a reference brain: position and spatial variability of the optic radiation. Neuroimage, 10, 489–499.

46. Behr C. (1926). Hemianopische Pupillenstarre ohne Hemianopsie. Zeitschrift fuer Praktische Augenheilkunde, 58, 398–406.

47. Johnson RE, Bell RA. (1987). Relative afferent pupillary defect in a lesion of the pretectal afferent pupillary pathway. Canadian Journal of Ophthalmology, 22, 282–284.

48. King JT Jr, Galetta SL, Flamm ES. (1991). Relative afferent pupillary defect with normal vision in a glial brainstem tumor. Neurology, 41, 945–946.

Contribution of Co-Authors

1. Papageorgiou E, Hardiess G, Schaeffel F, Wiethoelter H, Karnath HO, Mallot HA, Schoenfisch B, Schiefer U. Assessment of vision-related quality of life in patients with homonymous visual field defects. (Graefes Arch Clin Exp Ophthalmol 2007;245:1749-58)

Papageorgiou E. examined participants, collected and assembled data, analysed and interpreted data, wrote the paper.
Hardiess G. interpreted data and edited the paper
Schaeffel F. provided study material, and edited the paper.
Wiethoelter H. examined participants, provided study material, and edited the paper.
Karnath HO. conceived and designed the experiment, provided study material (neuropsychological tests), interpreted data, and edited the paper.
Mallot HA. conceived and designed the experiment, interpreted data, and edited the paper.
Schoenfisch B. analysed and interpreted data, and wrote part of the paper (statistical analysis).
Schiefer U. conceived and designed the experiment, examined participants, interpreted data, and edited the paper.

2. Hardiess G, Papageorgiou E, Schiefer U, Mallot HA. Functional compensation of visual field deficits in hemianopic patients under the influence of different task demands. (Vision Res 2010;50:1158-72)

Hardiess G. conceived and designed the experiment, examined participants, collected and assembled data, analysed and interpreted data, wrote the paper.
Papageorgiou E. examined participants, collected and assembled data, analysed data, and wrote part of the paper (lesion analysis).
Schiefer U. conceived and designed the experiment, examined participants, and edited the paper.
Mallot HA. conceived and designed the experiment, analysed and interpreted data, wrote and edited the paper.

3. Papageorgiou E, Hardiess G, Ackermann H, Wiethoelter H, Dietz K, Mallot HA, Schiefer U. Collision avoidance in persons with homonymous visual field defects under virtual reality conditions. (first revision submitted in Vision Research)

Papageorgiou E. examined participants, collected and assembled data, analysed and interpreted data, wrote the paper.
Hardiess G. conceived and designed the experiment, examined participants, collected and analysed data and edited the paper.
Ackermann H. provided study material, and edited the paper.
Wiethoelter H. provided study material, and edited the paper.
Dietz K. analysed and interpreted data, and wrote part of the paper (statistical analysis).
Mallot HA. conceived and designed the experiment, and edited the paper.
Schiefer U. conceived and designed the experiment, examined participants, interpreted data and edited the paper.

4. Papageorgiou E, Hardiess G, Mallot H.A., Schiefer U. Gaze patterns predicting successful collision avoidance in patients with homonymous visual field defects. (ready for submission in Vision Research)

Papageorgiou E. examined participants, collected and assembled data, analysed and interpreted data, and wrote the paper.
Hardiess G. conceived and designed the experiment, examined participants, collected and assembled data, edited the paper.
Mallot HA. conceived and designed the experiment, interpreted data, and edited the paper.
Schiefer U. conceived and designed the experiment, examined participants, interpreted data, and edited the paper.

5. Papageorgiou E, Ticini L, Hardiess G, Schaeffel F, Wiethoelter H, Mallot HA, Vonthein R, Wilhelm B, Schiefer U, Karnath HO. The pupillary light reflex pathway: cytoarchitectonic probabilistic maps in hemianopic patients. (Neurology 2008;70:956-63)

Papageorgiou E. examined participants, collected and assembled data, analysed and interpreted data, and wrote the paper.

Ticini L. analysed and interpreted data, and edited the paper.

Hardiess G. interpreted data and edited the paper.

Schaeffel F. provided study material and approved the final version of the paper.

Wiethoelter H. provided study material and approved the final version of the paper.

Mallot HA. interpreted data and edited the paper.

Bahlo S. provided study material and approved the final version of the paper.

Wilhelm B. provided study material, interpreted data and edited the paper.

Vonthein R. analysed and interpreted data, and wrote part of the paper (statistical analysis).

Schiefer U. conceived and designed the experiment, examined participants, interpreted data, and edited the paper.

Karnath HO. conceived and designed the experiment, analysed interpreted data, and edited the paper.

Graefes Arch Clin Exp Ophthalmol (2007) 245:1749–1758
DOI 10.1007/s00417-007-0644-z

CLINICAL INVESTIGATION

Assessment of vision-related quality of life in patients with homonymous visual field defects

Eleni Papageorgiou · Gregor Hardiess · Frank Schaeffel · Horst Wiethoelter · Hans-Otto Karnath · Hanspeter Mallot · Birgitt Schoenfisch · Ulrich Schiefer

Received: 31 October 2006 / Revised: 20 March 2007 / Accepted: 16 April 2007 / Published online: 25 July 2007

Abstract
Background and purpose Homonymous visual field defects (HVFDs) are among the most common disorders that occur in the elderly after vascular brain damage and can have a major impact on quality of life (QOL). Aims of this study were to describe the vision-targeted, health-related QOL in patients with HVFDs after cerebrovascular lesion, and to determine the relationship between patients' self-reported difficulties and the characteristics of HVFDs in the binocular visual field.

Methods The German version of the 25-item National Eye Institute Visual Functioning Questionnaire (NEI-VFQ-25) was used. NEI-VFQ-25 scores for patients were compared to reference values of healthy German subjects from Franke (Z Med Psychol 7:178–184, 1999). Extent and location of absolute HVFDs were assessed by binocular semi-automated kinetic perimetry (SKP) within the 90° visual field. Correlations of the NEI-VFQ-25 scores of patients with the area of sparing within the affected hemifield (A-SPAR) were estimated by Spearman's r_s.

Results The mean NEI-VFQ-25 composite score for 33 patients (time span after brain injury at least 6 months) was 77.1, which was significantly lower ($p<0.0001$) than the reference value for 360 healthy subjects (composite score= 90.6), and this was also the case for general vision, near activities, vision specific mental health, driving, colour, and peripheral vision. The score for general health was also significantly lower in patients than in reference subjects ($p<0.0001$). A weak correlation of the composite score with A-SPAR ($r_s=0.38$) was observed.

Conclusions Our findings indicate that detectable decrements in vision-targeted, health-related QOL are observed in patients with homonymous visual field loss. A relationship of the perceived visual functioning with objective parameters is by definition difficult; however, understanding what components of visual function affect certain visual tasks, would help in developing more efficient, clinical assessment strategies. The results reveal a tendency for increasing QOL with advancing size of the area of sparing within the affected hemifield (A-SPAR). The lack of a strong correlation between NEI-VFQ-25 subscales and A-SPAR suggests that an assessment of the visual field may not accurately reflect patients' perceived difficulty in visual tasks. Additional consideration of visual exploration via eye and head movements may improve the correlation between visual function and its perception.

This paper was presented at the 2006 annual meeting of the German Ophthalmological Society (DOG) in Berlin, Germany on September 21, 2006.

The NEI-VFQ-25 was developed by the RAND Health Corporation (http://www.rand.org) and was funded by the National Eye Institute.

E. Papageorgiou (✉) · F. Schaeffel · U. Schiefer
Centre for Ophthalmology, Institute of Ophthalmic Research,
University of Tuebingen,
Schleichstrasse 12-16,
72076 Tuebingen, Germany
e-mail: Eleni.Papageorgiou@med.uni-tuebingen.de

G. Hardiess · H. Mallot
Department of Zoology, Lab of Cognitive Neuroscience,
University of Tuebingen,
Tuebingen, Germany

H. Wiethoelter
Department of Neurology, Buerger Hospital,
Stuttgart, Germany

H.-O. Karnath
Section of Neuropsychology, Centre for Neurology,
University of Tuebingen,
Tuebingen, Germany

B. Schoenfisch
Department of Medical Biometry, University of Tuebingen,
Tuebingen, Germany

Keywords Homonymous hemianopia · Homonymous visual field defect · Vascular brain damage · Questionnaire · Exploration · Visual exploration · Quality of life (QOL)

Introduction

In developed countries stroke is the third most common cause of death after heart disease and cancer. As stroke mortality rates decline, individuals are increasingly likely to live with their residual impairments [15]. Homonymous visual field defects (HVFDs) are among the most common disorders that occur in the elderly after vascular brain damage and can pose a considerable impact for survivors' subsequent well-being. Approximately 30% of all patients with stroke and 70% of those with stroke involving the posterior cerebral artery suffer from HVFDs [30]. In Germany there is an incidence of approximately 550,000 brain-injured patients per year, 135,000 of them suffer from visual disturbances, mostly HVFDs.

There have been several studies focussing on stroke-related disabilities mainly assessed with generic questionnaires. Such generic instruments describe health-related quality of life (QOL) in terms of various dimensions including physical, functional, psychological, and social health as well as utility measurements [15]. Specific QOL measures have also been used in order to identify vision-related QOL in patients with binocular visual field defects due to various ophthalmological diseases [6, 14, 16, 17, 25, 31, 39]. However, to our knowledge, reports that specifically describe the vision-related QOL of patients with HVFDs after vascular brain damage by using vision-targeted, standardized instruments are missing. Specific functional impairments related to HVFDs have been repeatedly described in the literature. Patients complain mainly of difficulties with reading and scanning scenes fast enough to make sense of things as a whole. Consequently, they fail to notice relevant obstacles or avoid obstacles on their affected side and may collide with approaching people or cars. This has far reaching repercussions on their vocational and private lives [49]. While a variety of methods for quantifying visual field loss exist, there is not enough information about the degree of functional impairment in everyday life and about how homonymous visual field loss relates to patient-reported functioning.

Since previous research suggests that patients with HVFDs face a considerable degree of disability in everyday life, aims of this study were to describe the vision-targeted, health-related QOL, assessed with the 25-item National Eye Institute Visual Functioning Questionnaire (NEI-VFQ-25) in patients with HVFDs after cerebrovascular lesion, and to determine the relationship between the NEI-VFQ-25 scores and the characteristics of HVFDs in the binocular visual field, assessed with semi-automated kinetic perimetry (SKP).

Material and methods

Forty-five patients with HVFDs were recruited from the Department of Neuro-Ophthalmology at the University of Tuebingen (Germany), the University Neurology Clinic of Tuebingen, as well as the Neurology Clinic of Buerger Hospital in Stuttgart and the Bad Urach Rehabilitation Centre. All patients had a homonymous visual field defect, varying from a complete homonymous hemianopsia to homonymous paracentral scotomas, due to a unilateral vascular brain lesion, which was documented by neuroradiological imaging (magnetic resonance imaging or computerized tomography). In the majority of patients the lesion was located in the area supplied by the posterior cerebral artery. Inclusion criteria were a normal function of the anterior visual pathways, as evaluated by ophthalmologic examination (including ophthalmoscopy and slit-lamp exam), and a best corrected monocular (near and distant) visual acuity of at least 16/20. Exclusion criteria were severe unilateral visual hemi-neglect identified by pathological findings in horizontal line bisection, copying of figures [18], and by means of the "Bells test" [13], as well as evidence of cognitive decline, aphasia, apraxia, visual agnosia or physical impairment.

Since many of the patients with HVFDs show impaired reading performance, reading ability was tested with a German text used in the stroke unit of the University Neurology Clinic of Tuebingen. The text was a short story with a simple vocabulary and was easy to read. It was printed on an A4 page in landscape format and was read with best corrected visual acuity and the age-related addition for presbyopia. Reading distance was 30 cm. The total number of letters was 1614, which was equivalent to 276 words. Reading ability of patients was expressed as reading speed in letters/minute.

Furthermore, hemianopic patients may have difficulties in assessing the presence or absence and the severity of their visual handicap; therefore, anosognosia for hemianopsia was examined using a German translation of the anosognosia scale suggested by Bisiach et al. [4, 19]. The scale is based on direct observation of the patient's behaviour during the clinical examination, filled in by the examiner, with a grading scale as follows: grade 0 (no anosognosia)—the disorder is spontaneously reported or mentioned by the patient following a general question about their complaints; grade 1 — the disorder is reported only following a specific question about the strength of the patient's limbs; grade 2 — the disorder is acknowledged only after demonstrations through routine techniques of neurological examination; and grade 3 — no acknowledgement of the disorder can be obtained.

Finally, in order to check for cerebral achromatopsia, the colour naming test of the "Aachener Aphasie Test" was

applied. However, colour naming is not an adequate tool for cerebral dyschromatopsia, because residual colour perception may allow an approximate categorization of colours despite the inability to make fine judgements about hue and saturation. Therefore the desaturated panel D-15 test was additionally used [37, 47]. The test requires that the subject sorts 15 coloured chips into an orderly progression on the basis of hue. Patients were instructed to sort the hues in the conventional direction, i.e. from left to right, and test scores were calculated as described by Lanthony [22].

The validated German version of the NEI-VFQ-25 in the self-administered format was used in the study population [1, 9]. The NEI-VFQ-25 is a validated, reliable instrument that assesses the dimensions of self-reported, vision-targeted health status that are most important for persons who have chronic eye diseases (http://www.rand.org) [10–12, 26, 27]. The questionnaire focuses on the influence of visual disability and visual symptoms on generic health domains, such as emotional well-being and social functioning, in addition to task-oriented domains related to daily visual functioning. It consists of a base set of 25 vision-targeted questions representing 11 vision-related constructs, plus an additional, single-item, general health rating question. The NEI-VFQ-25 generates the following vision-targeted subscales: global vision rating, difficulty with near vision activities, difficulty with distance vision activities, limitations in social functioning due to vision, role limitations due to vision, dependency on others due to vision, mental health symptoms due to vision, driving difficulties, limitations with peripheral and colour vision, ocular pain as well as a single, general health rating item. Subscales are scored on a 0- to 100-point scale in which 100 indicates the best possible score on the measure and 0 indicates the worst. The composite NEI-VFQ-25 score is the mean score of all the items except for the general health item.

Size and location of absolute HVFDs were assessed by binocular SKP within the 90° visual field (stimulus III4e, background luminance 10 cd/m^2, angular velocity 3°/s) with the OCTOPUS 101 perimeter (HAAG-STREIT Inc., Koeniz, Switzerland). From the visual field data we calculated the area of sparing within the affected hemifield (A-SPAR in degrees^2), the area of visual field loss (A-HVFD) in the binocular visual field, and the distance of the visual field border from the visual field centre along the horizontal axis (in degrees) for stimulus III/4e (Fig. 1). We used the binocular visual field because it provides more realistic information about the visual field a patient uses for performing daily activities. The degree of sparing along the horizontal axis was assessed because it plays a crucial role, in particular, for reading. Furthermore, only the stimulus III/4e was used because this is a functionally relevant target that is typically used to define legal blindness and also the visual field extent in driving license forms in Germany.

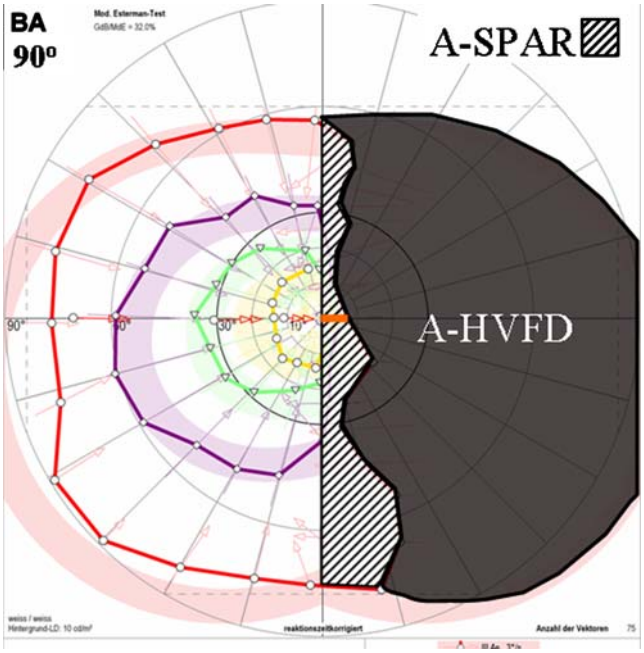

Fig. 1 Binocular visual field of a patient with a homonymous hemianopia to the right. Graphical representation of the area of sparing within the affected hemifield (A-SPAR, *hatched region*), the area of the visual field loss in the binocular visual field (A-HVFD, *black region*, obtained with stimulus III4e, angular velocity 3°/s) and the distance of the visual field border from the visual field centre along the horizontal axis or macular sparing (*orange line*, in degrees)

The research study was performed according to the Declaration of Helsinki and was approved by the Institutional Review Board of the University of Tuebingen, Germany. Following verbal and written explanation of the experimental protocol each subject gave written consent, with the option of withdrawing from the study at any time. None of the patients denied participation in the study and there were no missing data. The study was conducted between September 2005 and August 2006.

Statistical analysis

The patients' NEI-VFQ-25 subscale scores and the composite score were calculated according to the guidelines of the NEI-VFQ-25 manual. NEI-VFQ-25 scores were compared to reference values of a stratified sample of 360 healthy German subjects from Franke [10].

Since the reference values from Franke [10] were obtained from a large population (N=360), we choose one sample tests to compare values from our study group. For each subscale of the NEI-VFQ-25 a one sample Wilcoxon rank test was performed. For multiple testing adjustments we used the Bonferroni correction. Differences in reading speed between two groups of patients were tested with the two-sample Wilcoxon rank test. The distributions of individual NEI-VFQ-25 subscale scores are shown by

boxplots using medians, quartiles, and minimal and maximal values. In order to detect relations of the binocular visual field impairment with the questionnaire scores, correlations of the NEI-VFQ-25 subscale scores with A-SPAR were estimated by Spearman's r_s. We used JMP 5.0.1 (SAS Institute Inc., Cary, NC, USA) for most of the graphics and the correlation coefficient calculations. The boxplots are produced by R 2.2.1 (R foundation for statistical computing, Vienna, Austria) and the package "exactRankTests" of R was used in order to obtain exact values in the presence of ties [34].

Results

Of the 45 recruited patients, 12 were excluded due to the presence of bilateral HVFDs and/or pathological findings of the anterior visual pathways; 33 patients with HVFDs without visual neglect (24 male and 9 female), with a mean age of 51.4 years (SD±15.8; range 21–74) were deemed eligible for participation in the study. Mean time since lesion onset was 2.7 years (range 6 months to 16 years) and exceeded 1 year in the vast majority of patients (27 out of 33 patients). There were 16 patients with right-sided HVFDs and 17 patients with left-sided HVFDs. The distribution of the area of sparing within the affected hemifield (A-SPAR in degrees^2) is shown in Fig. 2.

Patients were divided in three groups: 0–2°, >2–5°, >5° according to the distance of the visual field border from the visual field centre along the horizontal axis (macular sparing, obtained with stimulus III4e, angular velocity 3°/s, Fig. 3). Mean reading speed was slower in right-sided HVFDs (510 letters/min, equivalent to 85 words/min) than in left-sided HVFDs (669 letters/min, equivalent to 112 words/min); however, the difference is not significant (p=0.080). For comparison, the abstract of this paper contains about 350 words. In right HVFDs, reading speed was much lower if macular sparing was 5 degrees or less (Fig. 3).

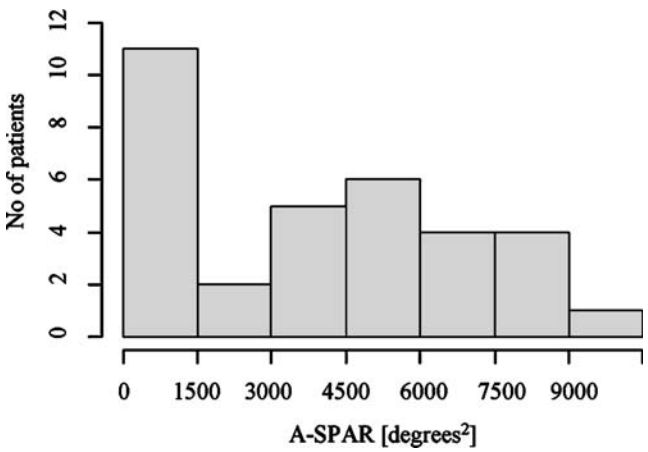

Fig. 2 Distribution of the area of sparing within the affected hemifield (A-SPAR, obtained with stimulus III4e, angular velocity 3°/s)

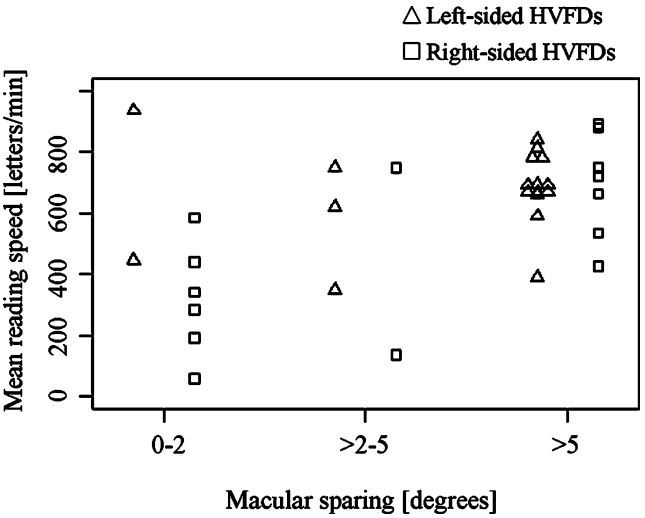

Fig. 3 Scatter plot of mean reading speed (letters/min) in patients with left- and right-sided HVFDs by the degree of macular sparing (distance of the visual field border from the visual field centre along the horizontal axis in degrees, obtained with stimulus III4e, angular velocity 3°/s)

Regarding the presence of anosognosia for hemianopsia in regard to visual field loss, 30 (91%) of the 33 brain-damaged patients mentioned their visual field defect spontaneously following a general question about their symptoms. Only 3 (9%) of the patients had a denial grade of 1, that is, they reported their visual field impairment only following a specific question about their visual complaints.

All patients showed an adequate performance in the colour naming test of the "Aachener Aphasie Test". In 7 (21%) of 33 patients the error score was slightly pathological according to the age-related normal values established by Lanthony [22].

When compared with the reference group, patients with HVFDs had significantly poorer scores on 7 of 12 NEI-VFQ subscales (Table 1): general health, general vision, near activities, mental health, driving, colour vision, and peripheral vision. Furthermore, the composite score was significantly lower in patients (Table 1, Fig. 4).

Female patients had a higher composite score (82.5) in comparison to male patients (75.1), but this difference was not statistically significant (p=0.27). When comparing each subscale of the NEI-VFQ-25 separately, female patients always had slightly higher scores compared to male patients, except for the item regarding self-assessment of driving performance, where the mean value was similar (female 32.4, male 32.6). There was no significant difference between female and male patients when the area of sparing within the affected hemifield (A-SPAR in degrees^2) was considered (p=0.49). There was no influence of time since

Table 1 NEI-VFQ-25 subscale scores for the patient and the reference group and *p* values for one sample Wilcoxon rank test

NEI-VFQ-25 subscales	NEI-VFQ-25 scores		One sample Wilcoxon rank test
	Patients N=33	Reference group *N*=360 resp. 302[a]	
General health	44.7[b]	69.4	<0.0001
General vision	65.5[b]	82.6	<0.0001
Ocular pain	92.0	89.2	0.052
Near activities	78.0[b]	93.3	<0.0001
Distance activities	84.8	94.7	0.057
Social functioning	89.0	96.6	0.369
Mental health	77.8[b]	90.2	0.001
Role difficulties	73.9	91.6	0.024
Dependency	89.9	96.6	0.368
Driving	32.6[b]	92.4	<0.0001
Colour vision	94.7[b]	97.0	0.002
Peripheral vision	69.7[b]	95.6	<0.0001
Composite score	77.1[b]	90.6	<0.0001

Data are presented as mean values
[a] Reference values from Franke [10] (*N*=360 resp., *N*=302 for driving)

injury on either A-SPAR (r_s=−0.21) or on the composite score (r_s=−0.12). Similarly, our data showed no evidence for an effect of age on NEI-VFQ-25 responses (r_s=0.17).

Table 2 shows the correlation coefficients r_s between the area of sparing within the affected hemifield (A-SPAR in degrees^2) for each of the NEI-VFQ-25 subscales.

A moderate correlation was only detected for the subscale social functioning (r_s=0.51). Weak correlations were detected for the subscales near activities (r_s=0.25), distance activities (r_s=0.31), dependency due to vision (r_s=0.25), peripheral vision (r_s=0.26), and for the composite score (r_s=0.38) (Fig. 5). Similarly, there was a weak correlation between reading speed (letters/min) and A-SPAR values (r_s=0.29). The correlation with the NEI-VFQ-25 driving score was moderate (r_s=0.44). However, more than half of the patients (19 out of 33) did not drive a car due to the existing visual field defect, therefore the NEI-VFQ-25 score for the driving item was zero in this subgroup. If we consider the remaining 14 patients, then the correlation with A-SPAR decreased (r_s=0.25, Fig. 6). A similar problem occurred in

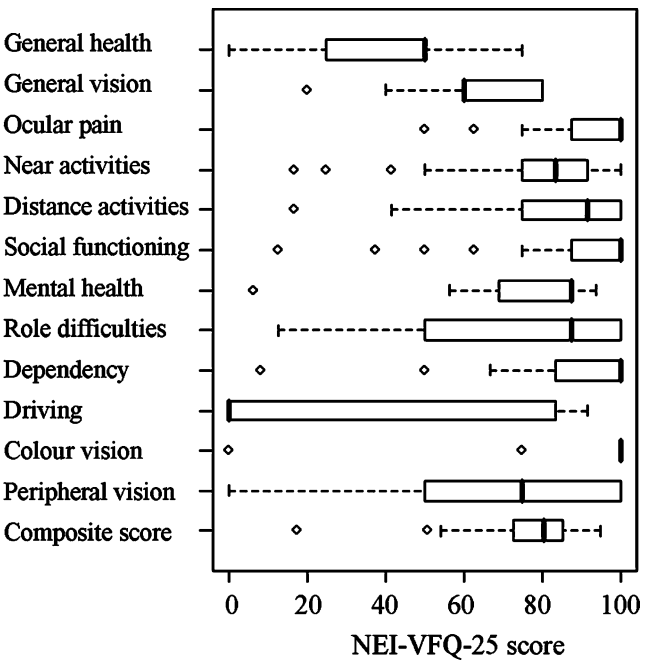

Fig. 4 Boxplots of subscale scores of the NEI-VFQ-25 for 33 patients suffering from homonymous visual field defects (HVFDs)

Table 2 Spearman's correlation coefficients r_s between NEI-VFQ-25 scores and A-SPAR values in patients with HVFDs (*N*=33). Additionally, the correlation coefficient r_s between reading speed (letters/min) and A-SPAR values is shown (r_s=0.29)

Rating items	Correlation coefficient r_s
General health	−0.04
General vision	0.13
Ocular pain	−0.12
Near activities	0.25
Distance activities	0.31
Social functioning	0.51
Mental health	0.15
Role difficulties	0.11
Dependency	0.25
Driving	0.44
Colour vision	0.02
Peripheral vision	0.26
Composite score	0.38
Reading speed	0.29

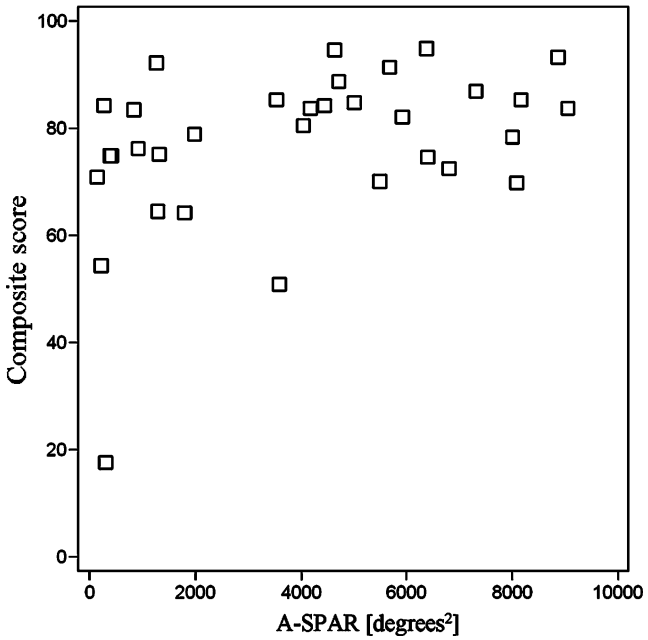

Fig. 5 Scatterplot of the area of sparing within the affected hemifield (A-SPAR, obtained with stimulus III4e, angular velocity 3°/s) with the NEI-VFQ-25 composite score for 33 patients. A weak trend for increasing QOL by advancing A-SPAR is depicted (r_s=0.38)

the social functioning and dependency subscales, where identical values (score=100%) occurred in 21 and 14 out of 33 patients, respectively. Due to the presence of ties in these subscales the correlation coefficients are of limited value.

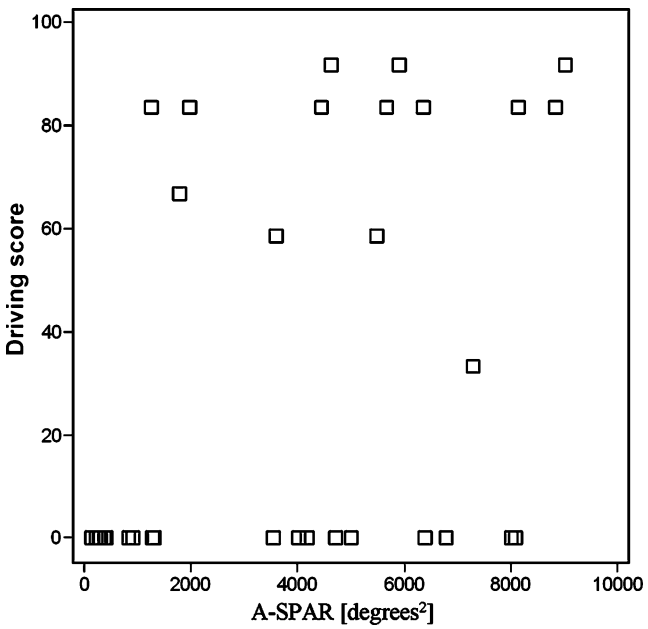

Fig. 6 Scatterplot of the area of sparing within the affected hemifield (A-SPAR, obtained with stimulus III4e, angular velocity 3°/s) with the NEI-VFQ-25 driving score (r_s=0.44) for 33 patients. If the patients who are not driving (N=19, score=0) are excluded, r_s decreases to 0.25

Discussion

Our findings suggest that patients with HVFDs due to cerebrovascular disease experience a reduction in vision-targeted QOL as indicated by 6 of 11 NEI-VFQ-25 subscales: general vision, near vision, vision-specific mental health, driving, colour vision, and peripheral vision. Furthermore, the composite score as well as the general health score were significantly lower in patients than in reference subjects. Homonymous visual field loss is apparently correlated with a general deterioration in perceived visual function. Especially regarding near vision, NEI-VFQ-25 includes three items that assess reading ability, difficulties in near activities (e.g. cooking or using hand tools), and finding objects on crowded shelves (http://www.rand.org). It is likely that the decrease in the subscale "near vision" is due to an impairment of reading performance. Reading ability is commonly affected in homonymous visual field loss and patients with HVFDs have reading difficulties that reflect the laterality of the visual field defect and depend on the degree of macular sparing (Fig. 1). Fluent reading demands at least 2° of visual angle to the left and right of the central fixation point and 1° above and below [2, 42, 43]. Reading disorders of patients with HVFDs result from the loss of parafoveal field regions which form a "perceptual window" for reading, subserving letter identification [49]. In western societies this reading window extends 3–4 characters to the left of fixation and 7–11 characters to the right of it; due to the asymmetry of this perceptual window right-sided HVFDs cut a larger part of the reading window and therefore impair reading more than left-sided HVFDs (approximately 5° vs. 2°), and reading speed improves with increasing distance to the visual field centre [21, 42, 49]. Left HVFDs cause difficulties with eye movements required to find the beginning of a new line, resulting in omissions of the first word or syllables of the line. Right HVFDs cause more severe reading difficulties, with loss of the anticipatory parafoveal scanning process, increased number of saccades, and significant reduction of reading speed, which result in a characteristic reading disorder termed "hemianopic dyslexia", which in some patients is nearly equivalent to spelling [2, 23, 24, 42, 43, 49]. Our results are consistent with other studies, suggesting that patients with right-sided HVFDs are more handicapped than those with left-sided HVFDs and reading speed improves with increasing degree of macular sparing (Fig. 3) [42, 49]. The weak correlation of reading speed and of the near vision item with A-SPAR also indicates this tendency (Table 2). However, when the patients are divided into further subgroups based on the degree of macular sparing, the number of patients remaining in each group is limited. Therefore, these results can only be descriptive and can show some trends (Fig. 3). Impaired reading ability

clearly causes a significant decline in QOL, because a considerable amount of the information acquired at educational, professional, and social levels is transferred by written documents.

Driving with HVFDs is one of the critical issues in traffic ophthalmology. Up to 90% of the information input regarding driving is visual [40]. Consequently, impairments in the binocular visual field will lead to deficits in nonvisual activities (cognition and motor control) [21]. Due to the unilateral peripheral affection of the visual field, patients with HVFDs show similar problems in daily activities demanding the use of peripheral vision (e.g. for detecting vehicles or persons to avoid collisions or falls [21]). Many of these patients do not feel safe enough to drive a car. Others do not meet the minimum standards for a driving license, since traffic safety regulations in the European Union require a horizontal extent of the binocular visual field of 120 degrees [41]. According to the recommendations of the German Ophthalmological Society for patients with HVFDs, the central 20 degrees of the binocular visual field, as well as 10 degrees above and below the horizontal meridian at 30 degrees eccentricity, should be unaffected [36]. Since driving represents the primary mode of travel in most western societies and is commonly linked to personal independence, one could imagine the socio-economic aspects as well as the individual impact on personal autonomy.

In poststroke patients, besides physical functioning, neuropsychological sequelae such as depression and cognitive impairment contribute to a reduced QOL and can be associated with a handicap that affects the ability to work and diminished social activity [7, 15, 32, 33]. These limitations — potentially combined with an impaired reading ability — could give a possible explanation for the decline in perceived mental and general health, as observed in the patient group. Our results indicate clearly that homonymous visual field loss can create a remarkable amount of subjective inconvenience in everyday life, since vision is one of the major input channels to memory, and the most important medium in the workplace in our visually and PC-dominated world.

However, in most of the scales we failed to demonstrate strong correlations with the extent of the binocular visual field assessed by kinetic perimetry. We calculated the area of sparing within the affected hemifield (A-SPAR) and demonstrated its relation with the questionnaire scores because the central 30 degrees of the visual field are thought to play an outstanding role in performing activities of daily living (ADL) [36]. When calculating the correlation coefficients of the questionnaire scores with the area of the visual field loss in the binocular visual field (A-HVFD, Fig. 1), we obtained analogous inverse correlations, which indicated a tendency for poorer NEI-VFQ-25 scores with increasing visual field defects. This result was expected, since the values A-SPAR and A-HVFD are complementary indices of the affected hemifield (Fig. 1); therefore, only the results for correlations with A-SPAR were demonstrated.

The findings suggest that an objective assessment of the visual field alone may not accurately reflect the actual or perceived ability of the patient to function. Over the past several years increased awareness of the effect of ophthalmic disease upon QOL has led many investigators to evaluate vision-related QOL for various ophthalmic conditions, such as glaucoma and retinitis pigmentosa, and their relation to binocular visual field loss [25, 29, 31, 38, 44]. A study by Gutierrez et al. showed that a steady decline characterized the relation between visual field loss and health related QOL in glaucoma assessed by the NEI-VFQ-25 [14]. Other studies also indicated a good association between some types of perceived visual disability and the severity of binocular visual field loss in glaucoma and in retinitis pigmentosa [25, 29, 31, 35, 38, 44]. However, the correlation with measures of the binocular visual field was in some cases moderate or modest and was only detected for some of the examined subscales [31]. It was also observed that some glaucoma patients with visual field loss did not have any limitations in visual function [25]. Moreover, some investigators reported a poor correlation of subjective QOL values with the Esterman score in glaucoma patients and suggested that clinical tests and QOL assessments only partially characterize the effect of glaucoma damage and thus provide complementary information [17]. Although these studies are not directly comparable to ours because of substantial differences in the etiology and pattern of binocular visual field loss, they provide evidence that subjective visual limitations are not always related to the total amount of visual field loss. Reports on vision-related QOL of patients with HVFDs are, to our knowledge, currently missing; however, the need to design clinical tests of vision that better correlate with patient perception is growing. Additional features which could be considered when performing ADL are exploratory eye movements and head turns. Particularly in driving, no strong correlation between perceived disability and A-SPAR could be detected. This leads to the hypothesis that there is great interindividual variability and that the extent of the HVFD per se is not a good predictor of the perceived disability in driving. Especially in patients with homonymous visual field defects, visual exploration through saccadic eye movements and head turns plays a substantial role because it enables the shift of circumscribed (binocular) visual field defects from relevant to less important areas of the visual environment [36]. Intact exploration ability thus can at least partially compensate for an existing visual field defect [8, 28, 45, 48]. These exploratory viewing strategies represent a substantial characteristic of our visual behaviour and should therefore be assessed in any attempt

to describe vision-related QOL. A future challenge for investigators is the design of innovative clinical tests in order to quantify visual exploration and its impact on QOL.

According to the anosognosia scale of Bisiach et al., 9% of the patients should be classed as having "mild anosognosia" [4]; however, analysis of the verbal responses showed that all three patients rated grade I complained spontaneously about other neurological deficits such as speed arrest, loss of concentration, and tiredness, which were real and are indeed common in poststroke patients. When the examiner asked about their visual complaints, all three patients immediately acknowledged the homonymous visual field loss. Thus our results are consistent with those of a former study by Baier et al., suggesting that patients in denial grade I did not appear to have a problem in accepting their hemianopsia, but simply perceived other symptoms as being more prominent, when asked a general question about their complaints [3]. Thus these patients were not considered as suffering from general anosognosia.

In patients with bilateral occipitotemporal injury, colour vision may be moderately affected in the entire visual field, or in rare cases may even be completely lost (cerebral achromatopsia). After unilateral occipitotemporal brain injury colour vision may be lost in the contralateral hemifield or the upper quadrant (cerebral hemiachromatopsia or hemidyschromatopsia). Foveal colour vision may also be affected [47, 49]. The performance of 7 out of 33 patients in the desaturated panel D-15 test was, compared to normative data, only slightly pathological, and indicated a mild form of cerebral dyschromatopsia with foveal involvement. The NEI-VFQ-25 score for colour vision however was significantly lower indicating that the desaturated panel D-15 test may not be sensitive enough to detect less severe cerebral disturbances of colour vision. A more detailed hue discrimination test may be necessary [47]. On the other hand, colour vision in the NEI-VFQ-25 is assessed by only one item:"Because of your eyesight, how much difficulty do you have picking out and matching your own clothes?" One could question the relevance of this item, since it addresses colour discrimination only in an indirect way and assesses at most a global impairment. Moreover, it has been reported that not all patients with moderately impaired colour vision after unilateral posterior brain injury are aware of their deficit and therefore will not mention it [49]. An alternative test is the questionnaire for the subjective assessment of cerebral visual disorders, developed and validated in the German language by Kerkhoff et al. [20]. Disturbances of colour vision are assessed here with a more specific question: "Do you perceive colours as saturated and clear as earlier? Yes or no? If not, are they now brighter, desaturated or strange?"

It was not expected that time since brain injury would influence A-SPAR or the NEI-VFQ-25 responses because the time span after lesion onset was at least 6 months. Recent quantitative studies of visual field recovery suggest that spontaneous improvement of homonymous hemianopsia is seen in at least 50% of patients within 1 month of injury and in most cases the improvement occurs within the first 3 months after injury [30, 46]. After this period spontaneous field recovery is very rare. Therefore an improvement in the visual field, which could have an impact on QOL, would be rather unlikely.

This study has several limitations. First, we considered a rather small sample size with a wide range of visual field impairment, which reduces the generalizability of the results. The time span between brain injury and data collection was at least 6 months, so our results are valid for patients with HVFDs existing longer than 6 months. Furthermore, our patient group is not representative of the general poststroke population, because we only included nonhospitalized subjects with HVFDs, who could be examined perimetrically in the outpatient care unit and thus had only minor motor or cognitive deficiencies. This fact could provide evidence that our patient sample has probably reported a higher QOL in comparison with the general poststroke population with HVFDs. Further research should concentrate on larger population samples, because individuals may respond to questions in an overly positive or overly negative manner, depending on idiosyncratic personality styles, motivations, or incentives [38].

In general, a relationship of the perceived visual functioning with objective parameters is by definition difficult [5]; however, understanding what components of visual function affect certain tasks, would help in developing more efficient, clinical assessment strategies [38]. Different tasks may emphasize different aspects of visual function, therefore we aimed at observing trends about the activities with which patients have perceived difficulty and about which tests of visual function best relate to these activities. The development of the clinical tests that best predict self-reported functioning would be important to better define practical, and perhaps more efficient, clinical assessment strategies for the evaluation of patients with HVFDs [38].

In conclusion, our results indicate that there is a trend for decreasing QOL with advancing HVFDs. However perceived difficulty is not strongly related to the extent of the binocular visual field. Conventional clinical measures such as visual field assessments do not seem to fully capture the influence of visual disability on daily functioning and on abilities to perform ADL that are valued by patients. From a functional point of view, additional assessment of visual exploration by means of eye and head movements should be helpful in evaluating global, vision targeted QOL in order to improve the correlation between visual function and its perception.

Acknowledgements The authors thank the Rehabilitation Centre Bad Urach, European Union (PERACT- Marie Curie Early Stage Training MEST-CT-2004-504321) and RAND Health Corporation for their support for this study. The authors are also indebted to one of the referees of this manuscript for providing some control values and to PD Dr. Anne Kurtenbach for helpful comments on the manuscript.

References

1. Adler M, Naskar R, Thanos S, Groppe M (2004) Validation of German-language versions of visual function indexes (VF-14 and VFQ-25). 102. Annual meeting of the German Ophthalmological Society, Berlin
2. Aulhorn E (1953) Über Fixationsbreite und Fixationsfrequenz beim Lesen gerichteter Konturen. Pflügers Arch 257:318–328
3. Baier B, Karnath HO (2005) Incidence and diagnosis of anosognosia for hemiparesis revisited. J Neurol Neurosurg Psychiatry 76:358–361
4. Bisiach E, Vallar G, Perani D, Papagno C, Berti A (1986) Unawareness of disease following lesions of the right hemisphere: anosognosia for hemiplegia and anosognosia for hemianopia. Neuropsychologia 24:471–482
5. Bradley E, Bradley D, Bartley G (2006) Evaluating health-related quality of life in ophthalmic disease. Arch Ophthalmol 124:121–122
6. Cahill MT, Stinett SS, Banks AD, Freedman SF, Toth CA (2005) Quality of life after macular translocation with 360 degrees peripheral retinectomy for age-related macular degeneration. Ophthalmology 112:144–151
7. Carod-Artal J, Egido JA, Gonzalez JL, Varela de Seijas E (2000) Quality of life among stroke survivors evaluated 1 year after stroke: experience of a stroke unit. Stroke 31:2995–3000
8. Coeckelbergh TR, Brouwer WH, Cornelissen FW, Van Wolffelaar P, Kooijman AC (2002) The effect of visual field defects on driving performance: a driving simulator study. Arch Ophthalmol 120:1509–1516
9. Franke G, Esser J, Voigtlaender A, Maehner N (1998) Erste Ergebnisse zur psychometrischen Prüfung des NEI-VFQ (National Eye Institute Visual Function Questionnaire), eines psychodiagnostischen Verfahrens zur Erfassung der Lebensqualität bei Sehbeeinträchtigten. Z Med Psychol 7:178–184
10. Franke GH (1999) Handbuch zum National Eye Institute Visual Function Questionnaire (NEI-VFQ) - ein psychodiagnostisches Verfahren zur Erfassung der Lebensqualität bei Sehbeeinträchtigten. Eigendruck, Essen
11. Franke GH, Esser J, Reimer J, Maehner N (2002) Vision targeted quality of life under different degrees of visual impairment. Rev Port Psicossom 4:39–49
12. Franke GH, Maehner N, Reimer J, Voigtlaender-Fleiss A, Esser J (2003) Ein psychodiagnostischer Zugang zur Erfassung der Einbuβen an gesundheitsbezogener Lebensqualität bei verringerter Sehkraft. Z Med Psychol 12:57–62
13. Gauthier L, Dehaut F, Joannette Y (1989) The bells test: a quantitative and qualitative test for visual neglect. Int J Clin Neuropsychol 11:49–54
14. Gutierrez P, Wilson MR, Johnson C, Gordon M, Cioffi GA, Ritch R, Sherwood M, Meng K, Mangione CM (1997) Influence of glaucomatous visual field loss on health-related quality of life. Arch Ophthalmol 115:777–784
15. Haacke C, Althaus A, Spottke A, Siebert U, Back T, Dodel R (2006) Long-term outcome after stroke: evaluating health-related quality of life using utility measurements. Stroke 37:193–198
16. Hall TA, MacGwin G, Searcey K, Xie A, Hupp SL, Owsley C, Kline LB (2006) Health-related quality of life and psychosocial characteristics of patients with benign essential blepharospasm. Arch Ophthalmol 124:116–119
17. Jampel HD, Schwartz A, Pollack I, Abrams D, Weiss H, Miller R (2002) Glaucoma patients' assessment of their visual function and quality of life. J Glaucoma 11:154–163
18. Johannsen L, Karnath HO (2004) How efficient is a simple copying task to diagnose spatial neglect in its chronic phase? J Clin Exp Neuropsychol 26:251–256
19. Karnath HO (2002) Anosognosie. In: Hartje W, Poeck K (eds) Klinische Neuropsychologie, 5th edn. Thieme, Stuttgart, pp 361–371
20. Kerkhoff G, Schaub J, Zihl J (1990) Assessment of cerebral visual disorders by patient-questionnaire. Nervenarzt 61:711–718
21. Kerkhoff G (2000) Neurovisual rehabilitation: recent developments and future directions. J Neurol Neurosurg Psychiatry 68:691–706
22. Lanthony P (1987) Assessment of desaturated panel D-15 II: comparison between desaturated panel D-15 and Farnsworth 100-hue tests. J Fr Ophtalmol 10:579–585
23. Leff AP, Crewes H, Plant GT, Scott SK, Kennard C, Wise RJ (2001) The functional anatomy of single-word reading in patients with hemianopic and pure alexia. Brain 124:510–521
24. Leff AP, Scott SK, Crewes H, Hodgson TL, Cowey A, Howard D, Wise RJ (2000) Impaired reading in patients with right hemianopia. Ann Neurol 47:171–178
25. Lu DW, Azuara-Blanco A, Spaeth G, Collur S, Speicher MA, Araujo S (1998) Visual limitations assessment in patients with glaucoma. Br J Ophthalmol 82:1347
26. Mangione CM, Lee PP, Gutierrez PR, Spritzer K, Berry S, Hays RD (2001) Development of the 25-item national eye institute visual function questionnaire. Arch Ophthalmol 119:1050–1058
27. Mangione CM, Lee PP, Pitts J, Gutierrez P, Berry S, Hays RD (1998) Psychometric properties of the national eye institute visual function questionnaire (NEI-VFQ). Arch Ophthalmol 116:1496–1504
28. Meienberg O, Zangemeister WH, Rosenberg M, Hoyt WF, Stark L (1981) Saccadic eye movement strategies in patients with homonymous hemianopia. Ann Neurol 9:537–544
29. Nelson P, Aspinall P, O'Brien C (1999) Patients' perception of visual impairment in glaucoma: a pilot study. Br J Ophthalmol 83:546–552
30. Pambakian AL, Kennard C (1997) Can visual function be restored in patients with homonymous hemianopia? Br J Ophthalmol 81:324–328
31. Parrish RK, Gedde SJ, Scott IU, Feuer WJ, Schiffman JC, Mangione CM, Montenegro-Piniella A (1997) Visual function and quality of life among patients with glaucoma. Arch Ophthalmol 115:1447–1455
32. Pohjasvaara T, Erkinjuntti T, Vataja R, Kaste M (1997) Comparison of stroke features and disability in daily life in patients with ischemic stroke aged 55 to 70 and 71 to 85 years. Stroke 28:729–735
33. Pohjasvaara T, Leppavuori A, Siira I, Vataja R, Kaste M, Erkinjuntti T (1998) Frequency and clinical determinants of poststroke depression. Stroke 29:2311–2317
34. R Development Core Team (2005) A language and environment for statistical computing. R Foundation for Statistical Computing, Vienna, Austria. http://www.R-project.org
35. Ringsdorf L, McGwin G, Owsley C (2006) Visual field defects and vision-specific health-related quality of life in African Americans and Whites with glaucoma. J Glaucoma 15:414–418
36. Schiefer U, Hofer R, Vischer PM, Wilhelm H (2000) Perimetry findings and driving performance. "How much visual field" does a motorist need? [Article in German] Ophthalmologe 97:491–497
37. Stasheff SE, Barton JJ (2001) Deficits in cortical visual function. Ophthalmol Clin North Am 14:217–242
38. Szlyk JP, Fishman GA, Alexander KR, Revelins BI, Derlacki DJ, Anderson RJ (1997) Relationship between difficulty in performing daily activities and clinical measures of visual function in patients with retinitis pigmentosa. Arch Ophthalmol 115:53–59
39. Szlyk JP, Fishman GA, Grover S, Revelins BI, Derlacki DJ (1998) Difficulty in performing everyday activities in patients with

juvenile macular dystrophies: comparison with patients with retinitis pigmentosa. Br J Ophthalmol 82:1372–1376
40. Taylor JF (1982) Vision and driving. Practitioner 226:885–889
41. Rijn LJ (Ed) (2005) New standards for the visual functions of drivers. Report of the Eyesight Working Group, http://ec.europa.eu/transport/home/drivinglicence/fitnesstodrive/index_en.htm
42. Trauzettel-Klosinski S, Reinhard J (1998) Eye movements in reading with hemianopic field defects: the significance of clinical parameters. Graefe's Arch Clin Exp Ophthalmol 236:91–102
43. Trauzettel-Klosinski S, Reinhard J (1998) The vertical field border in hemianopia and its significance for fixation and reading. Invest Ophthalmol Vis Sci 39:2177–2186
44. Viswanathan AC, McNaught AI, Poinoosawmy D, Fontana L, Crabb DP, Fitzke FW, Hitchings RA (1999) Severity and stability of glaucoma: patient perception compared with objective measurement. Arch Ophthalmol 117:450–454
45. Zangemeister WH, Utz P (2002) An increase in a virtual hemianopic field defect enhances the efficiency of secondary adaptive gaze strategies. Curr Psychol Cogn 21:281–303
46. Zhang X, Kedar S, Lynn MJ, Newman NJ, Biousse V (2006) Natural history of homonymous hemianopia. Neurology 66:901–905
47. Zihl J (1988) The influence of homonymous visual field disorders on colour sorting performance in the FM 100-hue test. Neuropsychologia 26:869–876
48. Zihl J (1995) Visual scanning behavior in patients with homonymous hemianopia. Neuropsychologia 33:287–303
49. Zihl J (2000) Rehabilitation of visual disorders after brain injury. Psychology Press, Hove, East Sussex

Vision Research 50 (2010) 1158–1172

Contents lists available at ScienceDirect

Vision Research

journal homepage: www.elsevier.com/locate/visres

Functional compensation of visual field deficits in hemianopic patients under the influence of different task demands

Gregor Hardiess [a,*], Eleni Papageorgiou [b], Ulrich Schiefer [b], Hanspeter A. Mallot [a]

[a] Faculty of Biology, Cognitive Neuroscience, University of Tuebingen, Germany
[b] Department of Pathophysiology of Vision and Neuro-Ophthalmology, Centre for Ophthalmology, University of Tuebingen, Germany

ARTICLE INFO

Article history:
Received 21 April 2009
Received in revised form 29 January 2010

Keywords:
Homonymous hemianopia
Functional compensation
Comparative visual search
Visual sampling
Eye movements
Head movements

ABSTRACT

We investigated the task-specific role of eye and head movements as a compensatory strategy in patients with homonymous visual field deficits (HVFDs) and in age-matched normal controls. All participants were tested in two tasks, i.e. a dot counting (DC) task requiring mostly simple visual scanning and a cognitively more demanding comparative visual search (CVS) task. The CVS task involved recognition and memory of geometrical objects and their configuration in two test fields. Based on task performance, patients were assigned to one of two groups, "adequate" ($HVFD_A$) and "inadequate" ($HVFD_I$); the group definitions based on either task turned out to be identical. With respect to the gaze related parameters in the DC task we obtained results in agreement with previous studies: the gaze pattern of $HVFD_A$ patients and normal controls did not differ significantly, while $HVFD_I$ patients showed increased gaze movement activity. In contrast, for the more complex CVS task we identified a deviating pattern of compensatory strategy use. Adequately performing subjects, who had used the same gaze strategies as normals in the DC task, now changed to increased gaze movement activity that allowed coping with the increasing task demands. Inadequately performing patients switched to a novel pattern of compensatory behavior in the CVS task. Different compensatory strategies are discussed with respect to the task-specific demands (in particular working memory involvement), the specific behavioral deficits of the patients, and the corresponding brain lesions.

1. Introduction

Movements of eye and head (i.e. gaze), together with attentional shifts are a key element of visual behavior in complex environments. Patterns of gaze shifts will depend on a number of factors, including the size and layout of the visual field, central visual processing capacities, short-term and long-term memory, and specific task demands. Generally, the efficiency of gaze movement strategies is determined by the acquired perceptual database (see Boothe, 2002) and the adequacy of this database for the current task. Studies with patients suffering from visual field deficits are instrumental in assessing the gaze strategies and their adaptation to reduced information intake and maybe reduced processing capacities. As compared to healthy subjects, patients' strategies may differ with respect to scanpath pattern and memory involvement, leading to various levels of functional compensation. In this study, we investigated the functional compensation achieved by homonymous hemianopes and the dependence of the used gaze strategies on tasks constraints and visual field limitations.

Patients with homonymous visual field defects (HVFDs) are impaired by a restricted visual field due to scotomas caused by unilateral post-chiasmal brain damage (Zihl, 1994). Common causes are cerebrovascular accident, traumatic brain injury, and tumors (e.g. Kerkhoff, 1999; Zihl, 2000). The visual system of these patients lacks up to one hemifield (in case of complete homonymous hemianopia). Consequently, these patients have difficulties in reading (e.g. McDonald, Spitsyna, Shillcock, Wise, & Leff, 2006; Zihl, 1995a), may collide with obstacles on the affected side (Zihl, 2000), and generally have problems to comprehend entire visual scenes at a glance.

However, some hemianopic patients are able to compensate for the visual limitation, at least to a certain extent, by performing additional, adaptive eye and head movements leading to an efficient use of the remaining visual field. Ishiai, Furukawa, and Tsukagoshi (1987) describe one obvious adaptation used by hemianopic patients. When viewing simple pattern, normal controls focus mainly to the centre of a display while hemianopic patients concentrate on the side of their visual field defect. The shift of the fixation point towards the hemianopic side brings more of the visual scene into the seeing hemifield (Gassel & Williams, 1963).

* Corresponding author. Address: Department of Biology, Cognitive Neuroscience, University of Tübingen, Auf der Morgenstelle 28, 72076 Tübingen, Germany. Fax: +49 (0) 7071 292891.
E-mail address: gregor.hardiess@uni-tuebingen.de (G. Hardiess).

0042-6989/$ - see front matter © 2010 Elsevier Ltd. All rights reserved.
doi:10.1016/j.visres.2010.04.004

Furthermore, Meienberg, Zangemeister, Rosenberg, Hoyt, and Stark (1981) identified different compensatory strategies in HVFD patients when faced with simple visual targets which were presented in a predictable or unpredictable fashion. In more detail, compensatory effects identified in many studies showed that patients spend more (search) time in the stimulus half corresponding to their visual loss, perform generally more saccades but with decreased amplitudes when directed into the area of the visual loss, and differed therefore in their scanpath pattern as compared to healthy subjects (e.g. Kerkhoff, 1999; Pambakian et al., 2000; Tant, Cornelissen, Kooijman, & Brouwer, 2002; Zangemeister, Meienberg, Stark, & Hoyt, 1982; Zangemeister & Oechsner, 1996; Zihl, 1995b, 1999, 2000). Also in visual search tasks, hemianopes exhibited longer total search times, shorter and more frequent fixations, and shorter saccades than healthy subjects (Chedru, Leblanc, & Lhermitte, 1973; Machner et al., 2009). Overall, the HVFD patients' bias toward the blind hemifield has been suggested to be a compensatory strategy that aims to partially overcome the loss of input from the affected side (Zihl, 1995b).

With the introduction of a visual sampling task (i.e. the dot counting paradigm, see below), Zihl (1995b) was able to subdivide the investigated collective of patients into two groups, depending on whether their search time exceeded the highest value found in the group of normal subjects (these patients were denoted as "pathologic hemianopics") or not (this group was denoted as "normal hemianopics"). Interestingly, for the "normal hemianopics" the author identified effective search patterns comparable to healthy subjects. In contrast, the scanpaths of the "pathologic" group were significantly longer and showed a higher number of fixations not only in the affected but also in the "intact" hemifields. Furthermore, it was concluded (Zihl, 1999, 2000) that the presence, time since, and severity of the HVFDs could not sufficiently explain the observed scanning deficit, and that additional factors are crucial for explaining the impaired oculomotor scanning. In general, it seems that patients with the same amount of visual field loss, as assessed by perimetry, show different degrees in their functional compensation and behavioral performance.

In the majority of studies concerning the oculomotor compensatory behavior, the stimuli were presented on computer screens and were therefore limited in field of view. The most prominent paradigm used to objectively and quantitatively assess oculomotor compensational behavior is the dot counting task introduced by Zihl (1995b, 1999, 2000). This counting task assesses the process of visual scanning without the primary involvement of more complex visual functions (Zihl, 1999).

Little is known about the visual exploration strategies applied by individual patients when dealing with different and cognitively more demanding tasks. Such studies are needed to understand the way how the visual system chooses among different compensation strategies and to better evaluate the performance of hemianopic patients. Therefore, the main focus of the present study was to investigate the task performance and the gaze related strategies of patients with long lasting homonymous hemianopia in two visual experiments differing in their demands concerning visual processing. We established an innovative experimental setup with a large projection display (i.e. full field of view) and simultaneous measurements of eye and head movements. In the first experiment, we used a dot counting task with an enlarged stimulus size as compared to the original setup (cf. Zihl, 1995b). The aim of this experiment was to validate the new setup with a standard paradigm and to extend previous results including the oculomotor compensation strategies (Zihl, 1995b, 1999) to larger fields of view. The second experiment used a comparative visual search task (Hardiess, Gillner, & Mallot, 2008; Pomplun et al., 2001) as a more cognitively challenging paradigm. In this paradigm two almost identical stimulus hemifields (i.e. cupboards filled with geometrical objects) have to be explored in order to find the number of differences between them. For both experiments, two patient groups were defined according to task performance. While previous group classifications were based on comparisons of the performance of patients with healthy controls (Zihl, 1995b) or on patients' behavior in everyday life (Zihl, 1999), we developed a procedure based only on intrinsic task performance (i.e. error rate and response time) in each experiment. For the resulting patient groups, task performance together with the applied gaze strategies was analyzed and compared to the results from healthy controls in order to identify functional compensation patterns employed by the HVFD patients. We will point out that patients of both groups show different degrees and strategies of visual compensation in the different tasks. These differences are discussed in terms of brain lesions and cognitive task demands.

2. Methods

2.1. Experimental setup

To enable standardized and completely programmable experimental environments, all experiments were performed applying virtual reality (VR) technology programmed in C++ using OpenGL® libraries. The computed VR stimuli were presented on a large, curved projection screen as shown in Fig. 1. The geometrical shape of the projection screen was that of a conic shell with a vertical axis, an upper radius of 1.83 m, and a lower one of 1.29 m. Subjects were seated upright with their back tightly at the chair and with their head in the axis of the conical screen (eye level was adjusted at 1.2 m with 1.62 m screen distance). The screen provided a horizontal field of view of 150° and a vertical one of 70° (45° downwards plus 25° upwards). To illuminate the whole projection screen, two video projectors each with 1024 by 768 pixel resolution and a fixed 60 Hz frame rate were used. The light in the experimental lab was dimmed nearly to complete darkness to avoid disturbing cues from the surround.

The projection setup was running on a 2.6 GHz PC under Linux RedHat 9.0 as operating system (graphic card: NVIDIA® Quadro4® 980XGL with dual video projector connection). The spatial resolution of the generated images was 2048 by 768 pixels. The SGI® OpenGL Performer™ was used to render the virtual environments as well as to handle the programs for the experimental tasks.

Fig. 1. Image of the curved projection screen and the displayed comparative visual search paradigm (cupboard task). Subjects sit comfortably in a high adjustable seat while performing the experiments. Small picture: ASL501 eye tracker with fixed rigid body enabling head tracking.

Eye-in-head movement recordings were realized with an infrared light based, head mounted and lightweight eye tracker (bright pupil type, model 501 from Applied Science Laboratories, Bedford, USA). The tracker uses the pupil-corneal-reflection method and enables an accuracy two degrees or better, depending on the eccentricity of the eye position. Real time delay was 50 ms. To record head-in-space movements, an infrared light based tracker system (ARTtrack/DTrack from ART GmbH, Weilheim, Germany) with 6 degrees of freedom, 0.1° accuracy, and a real time delay of 40 ms was used. A configuration of four light reflecting balls fixed to the eye tracker device and thus to the head (see Fig. 1) provided the tracking target for the head tracking system. Both trackers had a fixed temporal sampling frequency of 60 Hz. The online position recordings from eyes and head were transmitted via socket connection to an experimental PC for storage.

2.2. Experimental tasks

2.2.1. Dot counting

Visual sampling was assessed using the dot counting (DC) task introduced by Zihl (1995b). This task probes pure visual sampling without any further (top-down) identification of the stimulus material (Zihl, 1999), or the primary involvement of other complex high-order visual functions (Tant et al., 2002). The memory demands during the DC task are small and restricted to spatial memory of the scanpath.

To perform the DC task in the present study, subjects had to scan consecutively three different dot patterns. Each pattern included 20 bright dots scattered randomly over the projection screen. The background color was dark grey. The dots were presented within a field of 60° horizontally by 40° vertically; this differs from the original study (Zihl, 1995b, 1999) where 40° by 32° were used. All dots were arranged with a minimal spatial separation of 7° and the diameter of a single dot was 54 min of arc. For reasons of comparability with Zihl's work, only eye movements were allowed and recorded whereas head movements were restricted by using a chin rest.

Subjects were instructed to scan the pattern and to count dots in silence as quickly and reliably as possible and to terminate each trial by pressing a button on a joystick. Afterwards they were asked to report verbally the number of dots. No instruction was given how to proceed during scanning. Each trial started with the fixation phase to the fixation cross (see below) after pressing the joystick button.

2.2.2. Comparative visual search

Comparative visual search (CVS) requires observers to sample, identify, store, and compare corresponding portions of two display halves, which involves processes such as visual search, eye movements, and visual working memory (Gottlob, 2006). CVS differs from (non-comparative) visual search in the way in which distracters are defined: In (non-comparative) visual search, targets are distinguished from distracters by some physical (bottom-up) feature dimensions which may be pre-attentively apparent as in feature search, or may require a minimal set of computations as in conjunction search (Wolfe, 1994). In contrast, CVS target pairs can be identified only by comparison of the display halves, requiring memory and gaze shifts. Targets are defined by a lack of correspondence across the two halves of the display. Thus, this task addresses a number of components tested neither by the DC task nor by standard visual search, including: (i) storage of a collection of objects or features in visual working memory, (ii) gaze movements to acquire "snapshots" for the purposes of comparison, and (iii) a "comparator mechanism" to signal when corresponding items differ in shape and/or color. In conclusion, we argue that CVS involves visual working memory much more than visual search or counting of dots.

In the present CVS paradigm (cf. Hardiess et al., 2008; Pomplun et al., 2001), two cupboards equally filled with simple objects in four geometrical shapes (triangles, circles, diamonds, and squares) and four different colors (green, blue, yellow, and black) were used as stimuli (see Fig. 2). Each cupboard included 20 objects in four shelves. Each shelf included five objects in a row and one cupboard subtended 30° of the subjects' horizontal field of view. The diameter of each object was 3°, the horizontal separation between two objects was 5°, and the vertical separation between shelves was 11°. The horizontal separation between the centers of both cupboards was 60° (±30 distance from the subject's straight ahead direction).

The object configuration in the two cupboards was either completely equal (zero target condition) or differed at one or two positions (one and two target conditions, respectively). Target objects differed in shape only whereas all other object pairs had identical features (functioning as distracters). A maximum number of two targets were introduced, to avoid premature trial completion. Since subjects did not know the number of targets, they could not terminate the comparative search after detecting the first target. A complete cupboard task session consisted of 21 trials presented in random order (three target conditions × seven repetitions). The object configuration regarding targets and distracters was randomized for each trial. Contrary to the DC task, subjects were free to move their head together with eyes to find the number of targets (i.e. zero, one, or two) as quickly and reliably as possible. No instruction was given how to proceed with searching. Subjects had to terminate each trial by pressing a joystick button and reported the number of targets verbally. Each trial started with a fixation phase to the fixation cross (see below) after pressing the button. Participants were free to take breaks in between trials if desired.

2.3. Procedure

Subjects were seated in the chair and the eye tracker was calibrated by displaying a 9-point calibration pattern on the projection screen. For the procedure, head movements were prevented with a chin rest. The target for head movement tracking was calibrated also with fixed head. After completion of the calibration procedure, subjects started to perform the DC paradigm. During the task the head remained on the chin rest to avoid head movements. Immediately after finishing the first experiment, subjects had to proceed with the CVS experiment. For that task the head was set free and unrestricted head movements became also possible.

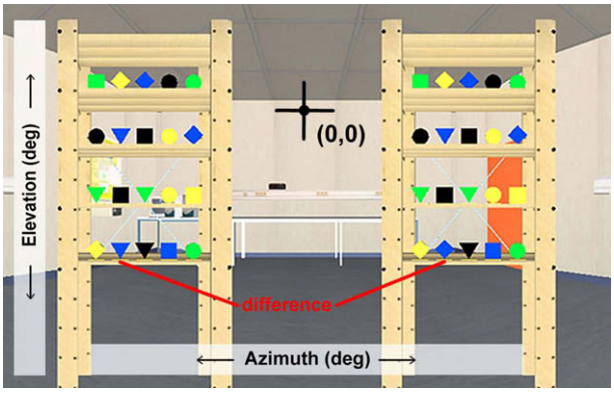

Fig. 2. Screenshot of the cupboard experiment as used in the comparative visual search task. In this example trial a one target condition is shown. Gaze position is expressed in angles (azimuth, α and elevation, β) with respect to the point of origin.

In both paradigms, each single experimental trial started with a five second fixation phase during which a fixation cross was displayed at eye level (1.2 m elevation) in the center of the projection screen (point of origin, cf. Fig. 2). During this phase participants had to rotate the head to align the naso-occipital axis with the fixation cross (automatically assured by chin rest in DC task), followed by fixating the cross with the eyes. All gaze (eye movement and heading) measurements are reported relative to this point of origin. After the fixation phase the cross disappeared automatically and the dots (in case of the DC task) or the two cupboards (in case of the CVS task) became visible.

2.4. Subjects

Twelve homonymous visual field defect (HVFD) patients without visual neglect (age: 45.2 ± 16.1 mean ± SD, range: 22–71 years; see Table 1) and twelve normally sighted control subjects (age: 44.4 ± 15.8 mean ± SD, ages in ascending order: 20, 24, 27, 30, 40, 41, 42, 45, 50, 64, 65, and 66 years) participated in this study. Patients were recruited from the Department of Neuroophthalmology at the University of Tübingen (Germany), the University Neurology Clinic of Tübingen, as well as the Neurology Clinic of Burger Hospital in Stuttgart and the Bad Urach Rehabilitation Centre. All patients had normal function of the anterior visual pathways, as evaluated by orthoptic and ophthalmologic tests (fundus and slit-lamp examinations). Best corrected monocular visual acuity was at least 16/20 (near and far). Patients with unilateral visual hemi-neglect were excluded from the study by testing horizontal line bisection (Stone, Halligan, Wilson, Greenwood, & Marshall, 1991), copying of figures (Johannsen & Karnath, 2004), reading ability, and by means of the "Bells test" (Gauthier, Dehaut, & Joannette, 1989). Furthermore, the patients investigated in this study showed no evidence of cognitive decline, aphasia, apraxia, visual agnosia, or physical impairment. Clinical and demographic data of all patients are summarized in Table 1. After the visual field evaluation (see below) patients were interviewed about their everyday life difficulties using the standardized 25-item National Eye Institute (NEI) Visual Function Questionnaire (VFQ-25, version 2000; see Mangione et al., 1998, 2001). The NEI-VFQ-25 focuses on the influence of visual disability and visual symptoms on generic health and task-oriented domains related to daily visual functioning. The questionnaire includes twelve vision-targeted subscales (i.e. eleven subscales related to vision: global rating, difficulty with near activities, difficulty with distance activities, limitations in social functioning, role of limitations, dependency on others, mental health symptoms, driving difficulties, limitations with peripheral and color vision, ocular pain; and one general health rating item). Subscales are scored on a 0- to 100-point scale in which 100 indicated the best possible score on the measure and 0 the worst. The composite NEI-VFQ-25 score was the mean score of all items except for the general health item.

Normal-sighted control subjects were recruited from the Department of Neuroophthalmology at the University of Tübingen and were in many cases patients' relatives. They had normal or corrected to normal vision, normal-appearing fundus, normal visual fields, normal orthoptic status, and no physical or cognitive impairment. The research study was performed according to the Declaration of Helsinki and was approved by the independent ethics committee of the University of Tübingen (Germany). Following verbal and written explanation of the experimental protocol each subject gave their written consent, with the option of withdrawing from the study at any time.

2.5. Visual field evaluation and brain lesion analysis

Assessment of the patients' visual fields was carried out by monocular supraliminal automated static perimetry within 30°-area, binocular supraliminal automated static perimetry within 90°-area as well as binocular semi-automated 90° kinetic perimetry obtained with the OCTOPUS 101-perimeter (Fa. HAAG-STREIT, Koeniz, Switzerland). Visual fields of control subjects were assessed with binocular supraliminal automated static perimetry within 90°-area and binocular semi-automated 90° kinetic perimetry. A summary of all perimetric and MRI results of all patients is given in Table 7.

For analysis of the brain lesions, patients' lesions were mapped on normalized brain scans using MRIcro software (Rorden & Brett, 2000) and SPM5 (Statistical Parametric Mapping, http://www.fil.ion.ucl.ac.uk/spm). MRIcro software was used to map the lesion on transversal slices of the T1-template MRI from the MNI (www.bic.mni.mcgill.ca/cgi/icbm_view) distributed with MRIcro. For anatomic analysis the left-sided lesions were mirrored and superimposed on the right side of the brain template. For each group of patients (i.e. $HVFD_I$ and $HVFD_A$), lesions were overlapped onto the template brain. Subtraction plots directly contrasted $HVFD_I$ and $HVFD_A$ patients. Since subtractions were made between groups of different sizes proportional values were used. Finally, mask analysis was performed in order to indicate regions that are more frequently damaged in $HVFD_I$ patients than in $HVFD_A$ patients.

Table 1
Clinical and demographic data of all 12 HVFD subjects.

Pat. ID	Sex	Age (year)	Δt (year)	Aetiology	Site/extent of lesion	Side of brain lesion	Type of HVFD	A-HVFD (deg^2)	A-SPAR (deg^2)	D (deg)	RT (ms)
ECG	Male	33	1	Brain surgery	Parieto-occipital	Right	Left cHH; mac. sparing	9559	414	3.2	1062
ANE	Male	40	4.9	Ischemia	Occipital	Right	Left cHH; mac. sparing	9258.9	923.7	2.3	299
AIH	Female	46	16	Ischemia	Parietal	Left	Right cHH; mac. sparing	9881	391	2.1	442
ULH	Male	64	0.7	Ischemia	Occipital	Right	Left upper iQA	2837	6790.6	7.8	348
FRH	Male	65	0.5	Ischemia	Occipital	Left	Right iHH; mac. sparing	7720.4	1986.6	15.4	518
URF	Male	71	1	Ischemia	Occipital	Left	Right iHH; mac. sparing	4739.4	4632	19	305
ARG	Female	36	11.2	Ischemia	Occipital	Left	Right cHH; mac. sparing	9003.3	1335	7	344
ARJ	Male	31	1.6	Hemorrhage (Aneurysm)	Parietal	Left	Right cHH; mac. sparing	10342.5	149.4	0	357
AYC	Female	33	1.1	Ischemia	Occipital	Left	Right cHH; mac. sparing	9370.8	845.5	4.5	260
TRH	Female	40	2.7	Ischemia	Occipital	Left	Right upper iQA	567.8	8853.2	4.7	311
TTC	Female	22	3.9	Ischemia	Parieto-occipital	Left	Right upper cQA	5867	4710.7	1.7	267
CKF	Male	61	3.6	Ischemia	Occipital	Right	Left upper iQA	2748.1	5496.4	8	387
Mean ± SD		45.2	4.02					6824.6	3044.0	6.3	408.3
		16.1	4.80					3358.6	2935.7	5.7	218.6

Δt – time since brain lesion and neuro-ophthalmological examination; Type of HVFD – characterization of homonymous visual field defect (HH: homonymous hemianopia, QA: quadrantanopia, c: complete, i: incomplete); A-HVFD – area of the visual field loss in the binocular visual field for stimulus III/4e; A-SPAR – area of the spared visual field in the affected hemifield for stimulus III/4e; D – minimum linear distance between the central fixation point and the defect border; RT – perimetric reaction time.

2.6. Data analysis and statistics

The MATLAB® software (MathWorks Company, Natick, USA) was used to analyze the recorded experimental data. Based on head and eye tracking data, the gaze vector was calculated in angles with an azimuth and an elevation component (α and β, respectively) with respect to the point of origin (see Fig. 2). Thus, the gaze vector includes both the head-in-space and the eye-in-head vectors. Object fixations were defined as sections of the gaze trajectory where gaze velocity did not exceed 100°/s for at least 120 ms. A gliding window procedure was used to distinguish such gaze fixations (stable gaze position related to the processed stimulus region) from gaze saccades (cf. Hardiess et al., 2008).

Task performance was quantified in terms of response times and error rates. In the DC task, error rate was defined as the unsigned difference of the reported and true dot number (20) in percent. In the CVS task, we distinguish two types of error, miss and false alarm, corresponding to a lower or higher number of reported targets than were actually presented. Misses and false alarms will be pooled to a total error rate.

To compare patient's ability to solve the two experimental tasks, a rank order was calculated based on the two task performance parameters response time and error rate independently. To get the final rank order, both rank numbers (i.e. for error rate and response time) were multiplied and the results of all 12 patients were ordered consecutively from 1 (i.e. best task performance) to 12 (i.e. worst task performance). In order to compare the patients task performance with their statements related to the quality of life questionnaire (VFQ-25; cf. Papageorgiou et al., 2007) the calculated final scores of the VFQ-25 were also ranked from 1 (i.e. best quality of life) to 12 (i.e. worst quality of life).

A distinction between adequate and inadequate patients was made with the median splitting method. Independently for each task both performance parameters (i.e. error rate and response time) were used to span a two dimensional co-ordinate system (see Figs. 3 and 4). All 12 data points from the patients' experimental performance were mapped into this system. The medians of both parameters were used to divide the co-ordinate system into four quadrants. Patients with error rate and response time above the respective medians (upper right quadrant) were assigned to the "inadequate" group while all remaining patients constitute the "adequate" group ($HVFD_I$ and $HVFD_A$, respectively). Contrary to previous grouping methods (cp. Zihl, 1995b, 1999), the median splitting approach employs an intrinsic criterion based on the patients' own data rather than on a comparison with the healthy subjects' performance. Only after separating patients into two groups the task performance comparisons between each of these groups and the control subjects were analyzed.

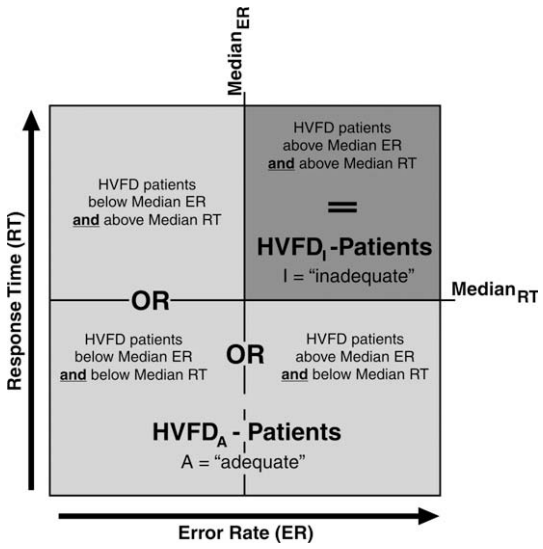

Fig. 3. Scheme for illustrating the median splitting method. The both task performance variables error rate and response time span a two dimensional co-ordinate system. Independently for each task the data of all 12 HFVD patients were added to this system. The medians of the patients data related to error rate and response time divide the sample into four quadrants. All patients whose data points are located into the quadrant labeled as above median ER and RT fall into the patients group called $HVFD_I$. All other patients are grouped to $HVFG_A$.

Parametric statistics were applied for the majority of the data. For some variables lacking standard distribution, data were transformed via $\log_{10}(x)$ operation to reach normally distributed values. For all other variables nonparametric statistics were applied.

3. Results

3.1. Task performance analysis

3.1.1. Rank comparisons

The task performance values for all subjects represented by the parameters error rate and response time are plotted in Fig. 4. The dotted lines indicate the medians for error rate and response time of the homonymous visual field defect (HVFD) patients. Also the assigned rank number (from 1 to 12) determined independently for each task (see below) is plotted for each subject. Interestingly, the data distributions of patients and controls overlap to a great extend for the dot counting (DC) task. Only three patients performed with a higher error rate than controls whereas no differences regarding response time are apparent. In contrast, in the comparative visual search task (CVS), the data distribution of all control subjects was localized within the lower left quadrant. Hence, the overlap between patients and control was much less in this task (see Fig. 4, right side). Additionally, the data distribution of patients in the CVS paradigm showed an increased variance compared with the controls. In both tasks, the same four patients (ECG, ULH, ANE, and AIH) cluster in the upper right quadrant, leading to identical adequate and inadequate groups for both tasks. However, the two groups appear clearly separated in the CVS tasks whereas the patients' data in the DC task are organized rather continuously.

To enable a comparison between the homonymous hemianopes' task performance in the DC and in the CVS task, all 12 patients were ranked independently for each task (cf. Section 2.6). These ranks show a significant correlation (Rho-S = 0.63, $p < 0.05$; see Fig. 5). This analysis also confirms the definition of the "inadequate" group initially derived from the un-ranked performance data (grey disk in Fig. 5).

Fig. 6 shows the relation between functional deficits (task performance) and reported quality of life parameters (VFQ-25), expressed in terms of the respective ranks. For both experimental tasks, weak but not significant statistical relations were found (Rho-S = 0.48 for the DC task and Rho-S = 0.29 for the CVS task comparison).

3.1.2. Task performance comparisons

Interestingly, the group of $HVFD_A$ patients accomplished the DC task with the same performance level as control subjects, as judged from both, error rate and response time (see Fig. 7A and C). In contrast, statistical analysis confirmed that $HVFD_I$ patients performed significantly worse than controls with respect to error rate ($p < 0.05$, two-sided Mann–Whitney–U test; cf. Fig. 7A) and response time ($F(2, 60) = 6.32$, MSE = 11.63, $p < 0.01$, $eta_p^2 = 0.17$; post-hoc comparison between controls and $HVFD_I$ subjects, $p < 0.01$; cf. Fig. 7C). In the CVS task, the comparison between each

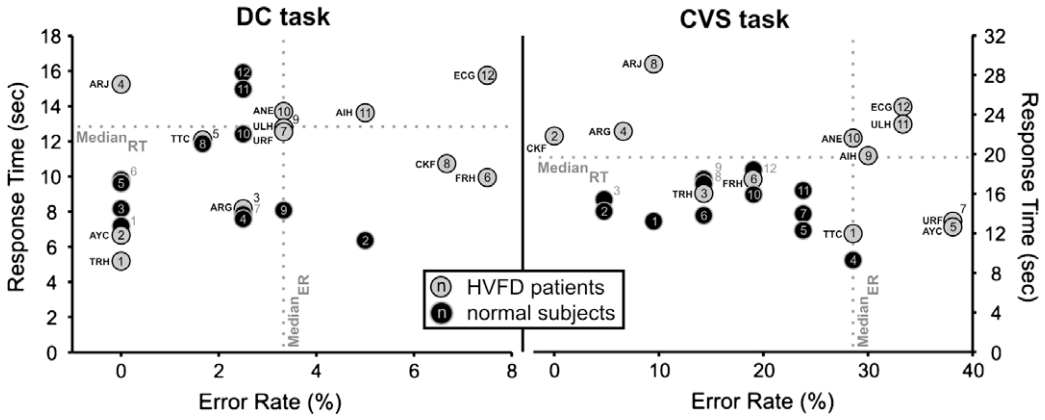

Fig. 4. The two task performance parameters error rate and response time plotted separately for each task (left: dot counting, right: comparative visual search) and for all subjects (grey circles: HVFD patients, black circles: normal subjects). The numbers within or beside each circle denote the given rank number calculated separately for each task and for the two subject groups. For reasons of comparison patients' labels are presented beside the circles.

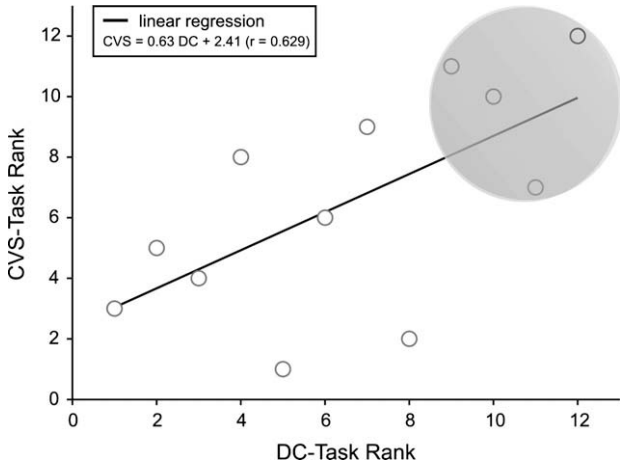

Fig. 5. Patients' task performance correlation based on the ranking method between the DC and the CVS task. Regression indicates a linear relation with a correlation coefficient $r = 0.63$. The four patients with the highest ranks in both tasks marked with the grey circle are indicated as inadequate patients ($HVFD_I$).

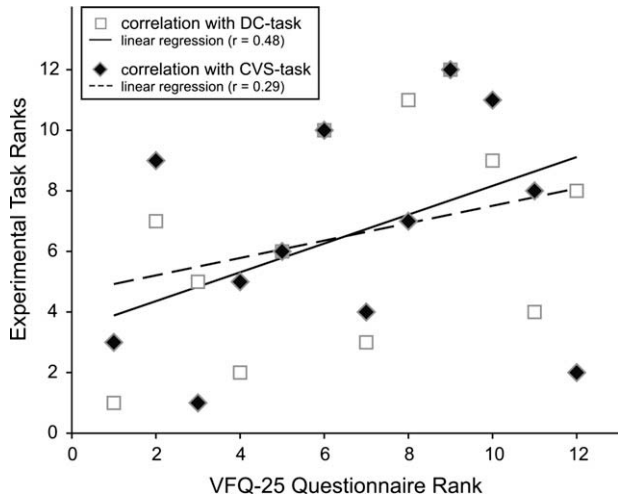

Fig. 6. Correlations between the patients' ranks due to the VFQ-25 questionnaire and their performance ranks in both experimental tasks (DC and CVS). Regressions indicate for weak relations with correlation coefficients $r = 0.48$ (correlation with DC-task) and $r = 0.29$ (correlation with CVS-task).

patient group and the controls showed that $HVFD_I$ patients made more errors than controls ($p < 0.01$, two-sided Fisher's exact test), whereas the error rate of $HVFD_A$ patients was similar to that of controls (see Fig. 7B). However, the analysis of variance of response time between the three subject groups revealed a significantly increased search time for the two patient groups ($F(2, 501) = 59.84$, MSE = 22.34, $p < 0.001$, $eta_p^2 = 0.19$; see Fig. 7D).

Tables 2 and 3 show the errors in more detail. For the DC task (Table 2), the normals tended to overcount the number of dots while both patient groups underestimate the dot number. This tendency is most pronounced in the $HVFD_I$ patients. Table 3 shows the proportions of different error types within the total number of errors for all groups concerning the CVS task. No obvious differences in error distribution were found between these groups. The most common error for all subjects was a miss error when in fact there were two targets presented. False alarm errors when no target was presented occurred fewest of all.

3.2. Scanpaths

The difference between $HVFD_A$ and $HVFD_I$ patients concerning task performance became also evident in their respective scanpath patterns. Fig. 8 shows representative recordings of individual scanning patterns in a normal subject, in a $HVFD_A$, and in a $HVFD_I$ patient for both tasks. In the DC task there are no apparent differences regarding the scanpaths between the normal subject and the adequately performing patient (see Fig. 8A and B). Both participants showed a systematic scanning behavior covering the stimulus field but not fixating each individual dot. In contrast, the $HVFD_I$ patient (cf. Fig. 8C) performed with a highly increased number of small saccades. The scanpath appears rather un-systematic and time-consuming. For the CVS task, similar differences were found (see Fig. 8D–F). However, due to a rather organized layout of the geometrical objects within the shelves, all subjects applied an overall structured search pattern. This pattern type was also apparent for the $HVFD_I$ patient (see Fig. 8F), but with a larger number of fixations and an increased positional scatter. In comparison, the $HVFD_A$ patient showed an organized scanning pattern similar to that of the unimpaired normal subject (cf. Fig. 8D and E).

3.3. Gaze performance analysis

3.3.1. Dot counting

To identify the strategies used for visual field compensation in both patient groups, relevant oculomotor parameters were calculated and compared with the data of the control group (Fig. 9).

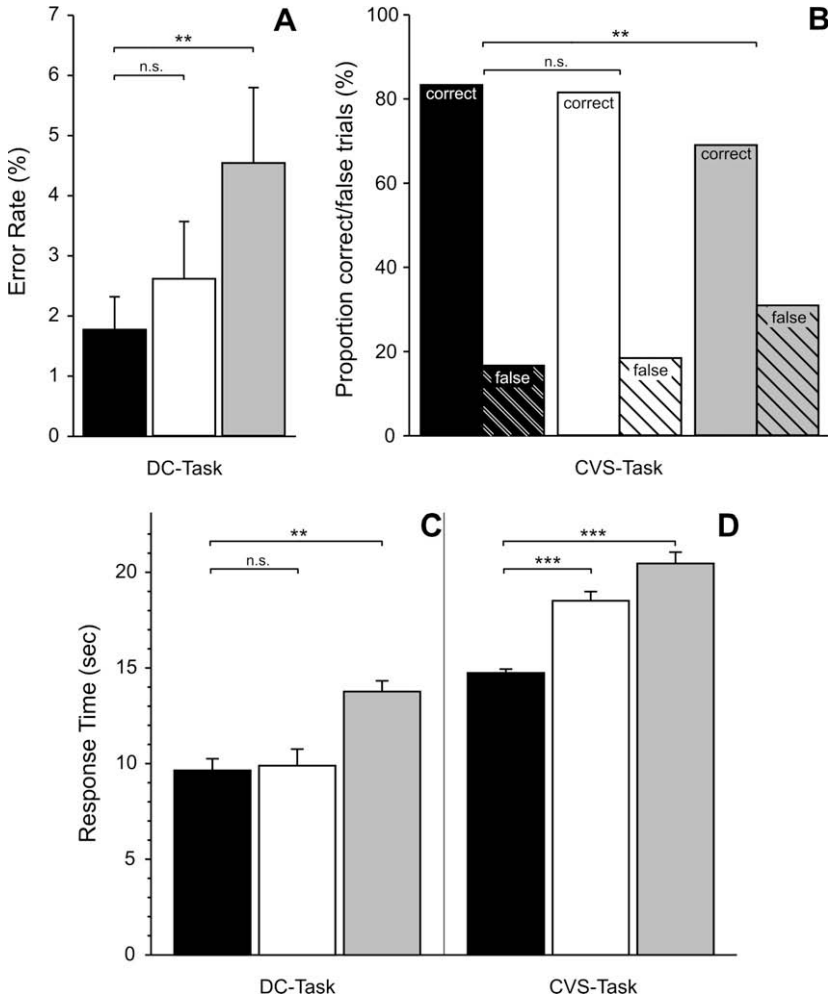

Fig. 7. Task performance comparison (A and B: error rate; C and D: response time) between normal subjects (black bars) and the $HVFD_A$ (white bars) respectively the $HVFD_I$ (grey bars) patient group. Post-hoc analysis was calculated to identify significance between the control subjects and each of the patients' group (Bonferroni: $^{*}p < 0.05$, $^{**}p < 0.01$, $^{***}p < 0.001$, and n.s. denotes not statistically significant). Error bars indicate standard error of the mean.

Table 2
Comparison of the type of counting errors (i.e. number of over- or undercounted dots in percent) in the DC task between controls, $HVFD_A$, and $HVFD_I$ patients.

Condition	Controls	$HVFD_A$	$HVFD_I$
# Dots overcounted per trial	0.30	0.19	0.27
# Dots undercounted per trial	0.06	0.33	0.64

For a better overview, all statistical results related to the analyzed oculomotor parameters are summarized in Table 4.

In comparison to normal controls, $HVFD_I$ patients showed an increased number of fixations (Fig. 9A), a higher proportion of fixations towards the impaired visual field (Fig. 9B), increased total scanpath length (Fig. 9C), and a higher proportion of refixations (calculated as the number of fixations made within 1° of an earlier one; Fig. 9D). Tendencies for increase fixation duration (Fig. 9E) and smaller saccadic amplitudes (Fig. 9F) are apparent but did not reach significance. In contrast to the $HVFD_I$ patients, $HVFD_A$ patients showed no significant differences from the normal controls in any of the investigated parameters.

3.3.2. Comparative visual search

For the CVS task, we considered the same gaze parameters as before, except for the fixation repetition rate which seems to be of little interest given the narrow spacing of target objects in the "shelves" stimulus. Instead, the number of gaze shifts between the two stimulus halves (cupboards) was evaluated as an indicator for working memory involvement (Fig. 10D). The statistical results for all gaze parameters are summarized in Table 5. Unlike the DC task, the cognitively more demanding CVS task leads to significant

Table 3
Comparison of the type of search errors (i.e. proportion of false alarm and miss trials due to the three target conditions in percent) in the CVS task between controls, $HVFD_A$, and $HVFD_I$ patients.

Condition	Controls		$HVFD_A$		$HVFD_I$	
	False alarm (%)	Miss (%)	False alarm (%)	Miss (%)	False alarm (%)	Miss (%)
Zero target trial	0.00	–	9.68	–	5.13	–
One target trial	7.69	30.77	16.13	22.58	20.53	17.95
Two target trial	–	61.54	–	51.61	–	56.41

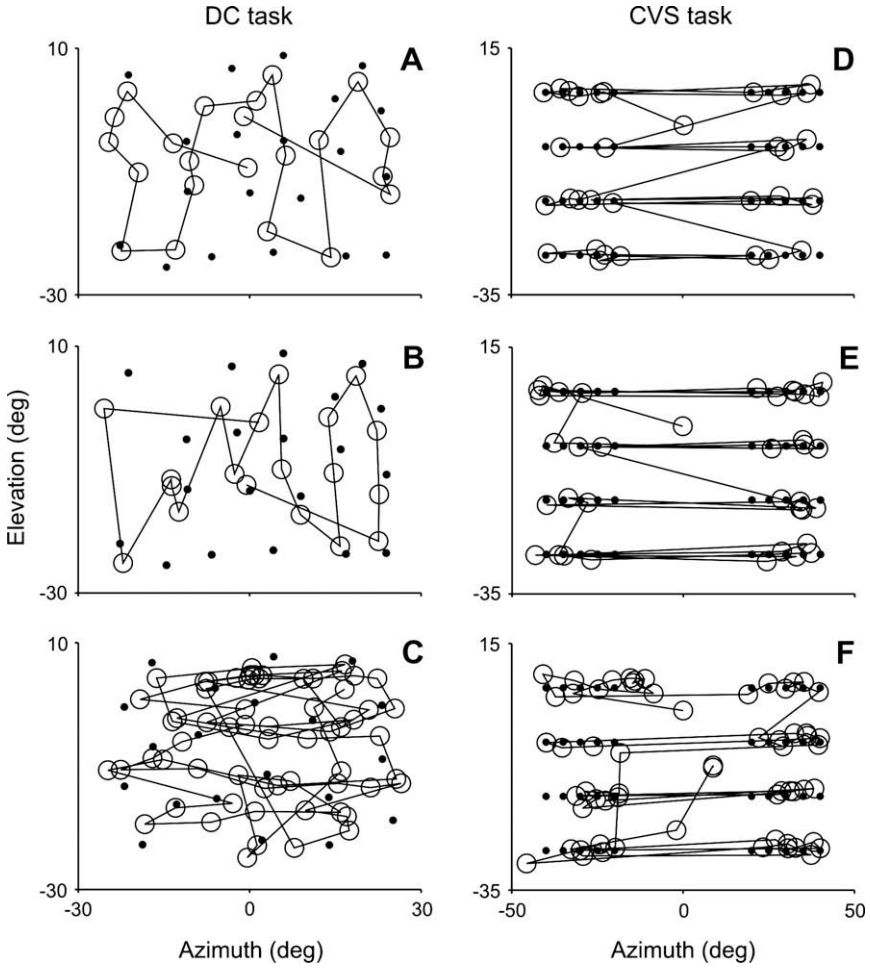

Fig. 8. Scanning pattern (scanpaths) examples for both tasks of a normal subject (A and D), of a $HVFD_A$ patient (B and E) and of a $HVFD_I$ patient (C and F). Black filled circles mark the dot position for the DC task and the object position for the CVS task. The open black circles indicate for the averaged gaze positions during fixations and the black lines illustrate the rapid gaze changes between fixations (saccades).

effects also for the $HVFD_A$ patients, including increased fixation number (Fig. 10A), increased scanpath length (Fig. 10C), and decreased saccadic amplitude (Fig. 10F). For the $HVFD_I$ patients, the effects of fixation number (Fig. 10A) and proportion of fixations to impaired visual field (Fig. 10B) are reproduced. As additional effects, we found increased fixation duration (Fig. 10E) and decreased saccadic amplitudes (Fig. 10F). For the scanpath length, the performance pattern of the three groups differed from the pattern found with the DC task. For this parameter, we found an increase in the $HVFD_A$ patients but not in the $HVFD_I$ patients (Fig. 10C). Here, the normal values for overall scanpath length together with the simultaneous increase in fixation number may be explained by the reduced number of long distance, inter-hemifield gaze shifts reported for the $HVFD_I$ patients but not for the $HVFD_A$ patients in Fig. 10D.

In the free-head comparative visual search task all subjects performed maximum head movements in a range of ±3° and ±20°. The average maximum amplitudes were larger for $HVFD_I$ patients (14.13 ± 8.0 mean ± SD), while for $HVFD_A$ patients they were within a range (8.89 ± 4.78 mean ± SD) similar to the one of normal subjects (9.12 ± 5.0 mean ± SD). Interestingly, all $HVFD_I$ patients showed significant differences for maximum head amplitudes to the left and right side (see Fig. 11). In more detail, the three left sided $HVFD_I$ patients (i.e. ECG, ANE, and ULH) used larger head movements to the left, while the only right sided $HVFD_I$ patient (AIH) displayed larger amplitudes to the right. This effect of different maximum head amplitudes between movements to the left and to the right could not be obtained for the majority of the $HVFD_A$ patients (see Fig. 11). Only three patients from this group (FRH, ARJ, and CKF) showed significantly different amplitudes but the effect sizes (between 0.62 and 0.82) were relatively low compared to those of the inadequate patient group (between 2.21 and 3.53). Five of the $HVFD_A$ patients showed no asymmetry in head movement amplitude.

3.4. Lesion analysis

Seven out of eight $HVFD_A$ patients had left-sided brain lesions, while three out of four $HVFD_I$ patients had right-sided brain lesions. MRI scans were available for six out of eight $HVFD_A$ patients and for three out of four $HVFD_I$ patients (see Table 7). In order to identify the anatomic structures that might be affected in $HVFD_I$ patients but spared in $HVFD_A$ patients, overlapping, subtraction and mask lesion analyses were performed using the MRIcro software (Fig. 12).

Fig. 12 illustrates simple lesion overlay plots for the group of $HVFD_A$ patients (Fig. 12A) and the group of $HVFD_I$ patients (Fig. 12B) respectively. In the subtraction analysis the superimposed lesions of the $HVFD_A$ group were subtracted from the $HVFD_I$ group, revealing percentage overlay plots (Fig. 12C). The focus of the subtracted lesion overlap (yellow and light orange) occurs at mesio-ventral areas of the temporal lobe (i.e. the fusiform gyrus)

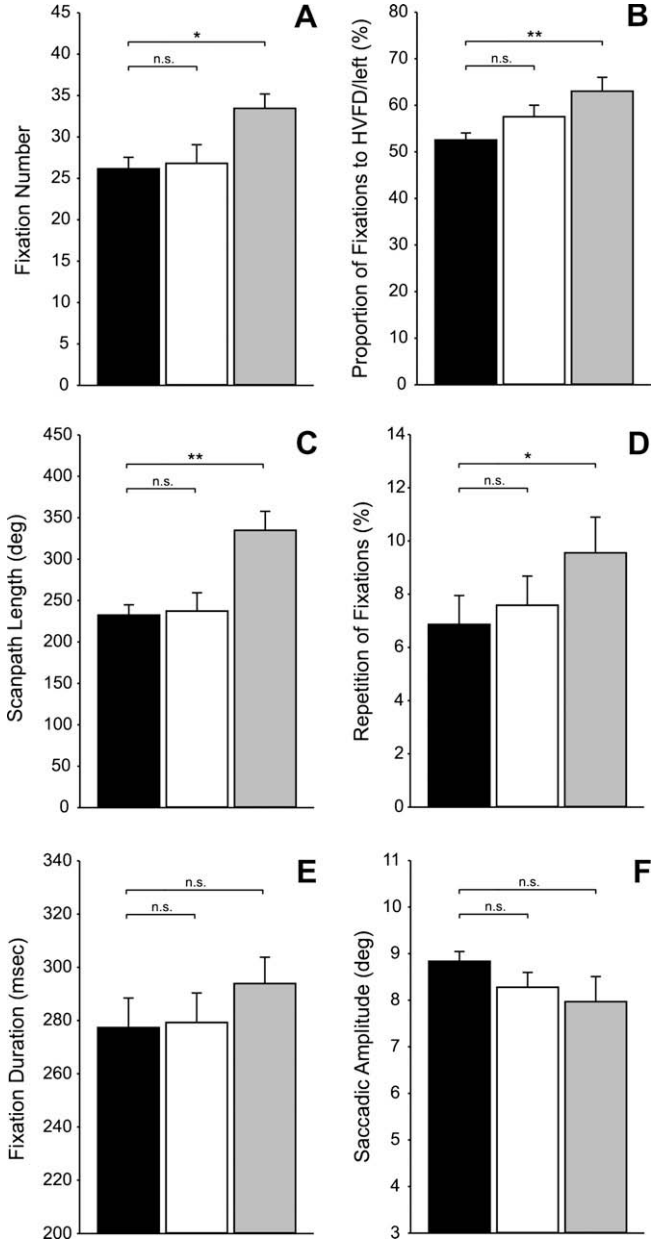

Fig. 9. Oculomotor performance of all subjects showed in the DC task. Comparisons were analyzed between the normal subjects (black bars) and the both patient groups (white bars: $HVFD_A$ patients, grey bars: $HVFD_I$ patients) related to different oculomotor parameters (A: number of fixations; B: proportion of fixations to the patients' impaired side or the control subjects' left side; C: length of the scanpath; D: percentages of repetition of fixations; E: duration of fixations; F: amplitude of saccades). Post-hoc analysis was calculated to identify significances between the controls and each of the patients' group (Bonferroni: $^{*}p < 0.05$, $^{**}p < 0.01$, $^{***}p < 0.001$, and n.s. denotes not statistically significant). Error bars indicate standard error of the mean.

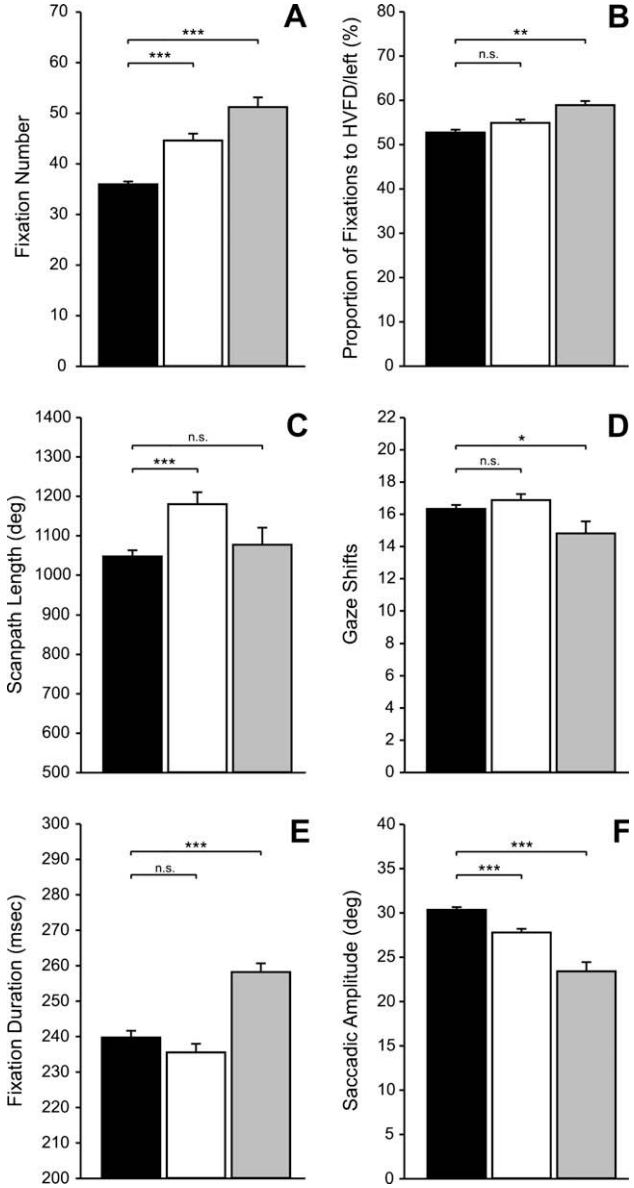

Fig. 10. Gaze performance of all subjects showed in the CVS task. Comparisons were analyzed between the normal subjects (black bars) and the both patient groups (white bars: $HVFD_A$ patients, grey bars: $HVFD_I$ patients) related to different gaze parameters (A: number of fixations; B: proportion of fixations to the patients' impaired side or the control subjects' left side; C: length of the scanpath; D: number of gaze shifts between the two cupboards; E: duration of fixations; F: amplitude of saccades). Post-hoc analysis was calculated to identify significances between the controls and each of the patients' group (Bonferroni: $^{*}p < 0.05$, $^{**}p < 0.01$, $^{***}p < 0.001$, and n.s. denotes not statistically significant). Error bars indicate standard error of the mean.

Table 4
Summary of the statistical results for all gaze performance parameters analyzed in the DC task.

Parameter	Statistical data	Significance
Fixation number[a]	$F(2, 60) = 4.18$, MSE = 0.014, $eta_p^2 = 0.12$	$p < 0.05$
Prop. of fixations to HVFD	$F(2, 60) = 5.07$, MSE = 94.725, $eta_p^2 = 0.14$	$p < 0.01$
Scanpath length[a]	$F(2, 60) = 7.32$, MSE = 0.017, $eta_p^2 = 0.2$	$p < 0.01$
Repetition of fixation	Median test: $\chi^2 = 6.07$	$p < 0.05$
Fixation duration	Median test: $\chi^2 = 2.98$	$p = 0.23$
Saccadic amplitude	$F(2, 60) = 1.97$, MSE = 1.938	$p = 0.15$

[a] This parameter was $\log_{10}(x)$ transformed to reach normally distributed values.

Table 5
Summary of the statistical results for all gaze performance parameters analyzed in the CVS task.

Parameter	Statistical data	Significance
Fixation number	$F(2, 462) = 44.2$, MSE = 177.43, $eta_p^2 = 0.16$	$p < 0.001$
Prop. of fixations to HVFD	$F(2, 462) = 12.93$, MSE = 85.04, $eta_p^2 = 0.053$	$p < 0.001$
Scanpath length	$F(2, 462) = 8.49$, MSE = 99446, $eta_p^2 = 0.035$	$p < 0.001$
Gaze shifts	$F(2, 462) = 5.02$, MSE = 21.7, $eta_p^2 = 0.021$	$p < 0.01$
Fixation duration[a]	$F(2, 462) = 17.89$, MSE = 0.0026, $eta_p^2 = 0.072$	$p < 0.001$
Saccadic amplitude	$F(2, 462) = 43.22$, MSE = 32.43, $eta_p^2 = 0.16$	$p < 0.001$

[a] This parameter was $\log_{10}(x)$ transformed to reach normally distributed values.

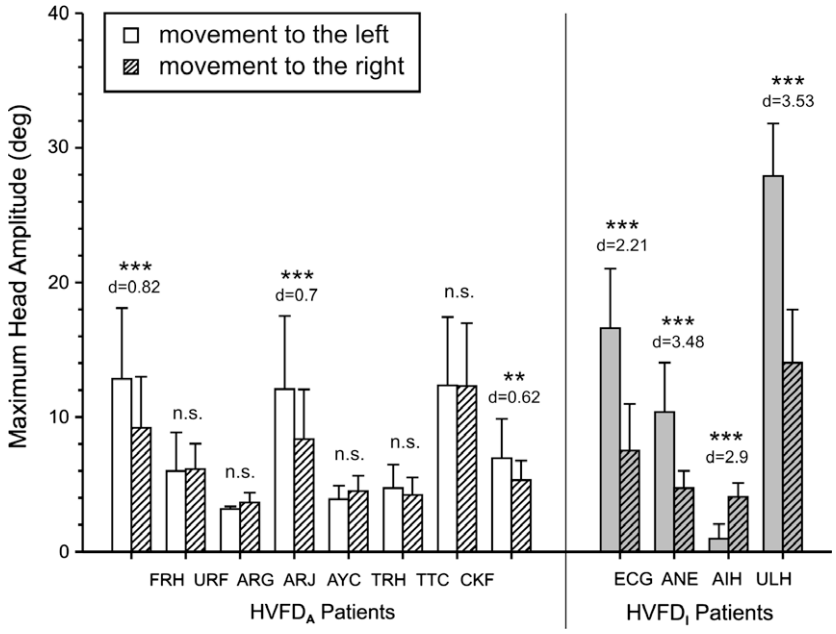

Fig. 11. Comparison of the averaged maximum amplitudes for horizontal head movements to the left (solid bars) and to the right side (striped bars) between the HVFD$_A$ (white bars) and HVFD$_I$ patients (grey bars) in the CVS task. Error bars indicate standard deviations. Statistical results for unpaired group comparisons are shown (unpaired *t*-tests: $^{*}p < 0.05$, $^{**}p < 0.01$, $^{***}p < 0.001$, and n.s. denotes not statistically significant). The effect size of these statistics is marked as d.

and the inferior occipital lobe, that are damaged at least 60% more frequently in HVFD$_I$ patients than in HVFD$_A$ patients (Fig. 12C). The subsequent mask analysis, which identifies deficits that are unique to HVFD$_I$ patients, confirms this finding and reveals additional involvement of the parahippocampal gyrus (Fig. 12D).

4. Discussion

The purpose of the present study was to compare the compensatory gaze strategies of hemianopes occurring in two visual scanning tasks with different cognitive and visual processing demands. The results show (i) that patients can be grouped on the basis of task performance and that the assignment to the adequate and inadequate groups correlates between the different tasks; the performance level of the adequate group is not significantly different from that of normal controls. Grouping also correlates with the patients' brain lesions with more occipital lesion sites in the HVFD$_I$ patients. (ii) Compensatory gaze movements alone do not explain the performance differences between the two groups. In the dot counting (DC) task, HVFD$_I$ patients show longer and more detailed scanning behavior without reaching the performance level of normals or of HVFD$_A$ patients, who solve the task without obvious gaze adaptation. (iii) In the two tasks, different patterns of compensatory gaze movements are found. While HVFD$_A$ patients show no compensatory movement in the DC task, they turn to such behavior in the comparative visual search (CVS) task. HVFD$_I$ patients seem to switch to different compensation strategies in the CVS task. We suggest that this is related to an increased working memory involvement.

4.1. Differences in task performance among HVFD patients

Following the classification approach of Zihl (1995b, 1999) we divided the collective of HVFD patients into two groups (i.e. HVFD$_A$ and HVFD$_I$ patients; **A** = adequate task performance, **I** = inadequate task performance). But, instead of relating the patients' task performance to that of healthy controls (cf. Zihl, 1995b) or using their behavior in everyday life evaluated by questionnaires (cf. Zihl, 1999), we split up the patients based on their intrinsic task performance (i.e. error rate and response time) in both experiments. Interestingly, the majority of HVFD patients could reach adequate performance (i.e. HVFD$_A$ patients) and only 33% of our subjects were assigned to the HVFD$_I$ patient group. This is in line with the results from Zihl (1995b, 1999) who could identify a high number of adequately performing patients as well. In these investigations about one half of the subjects showed search times in the range

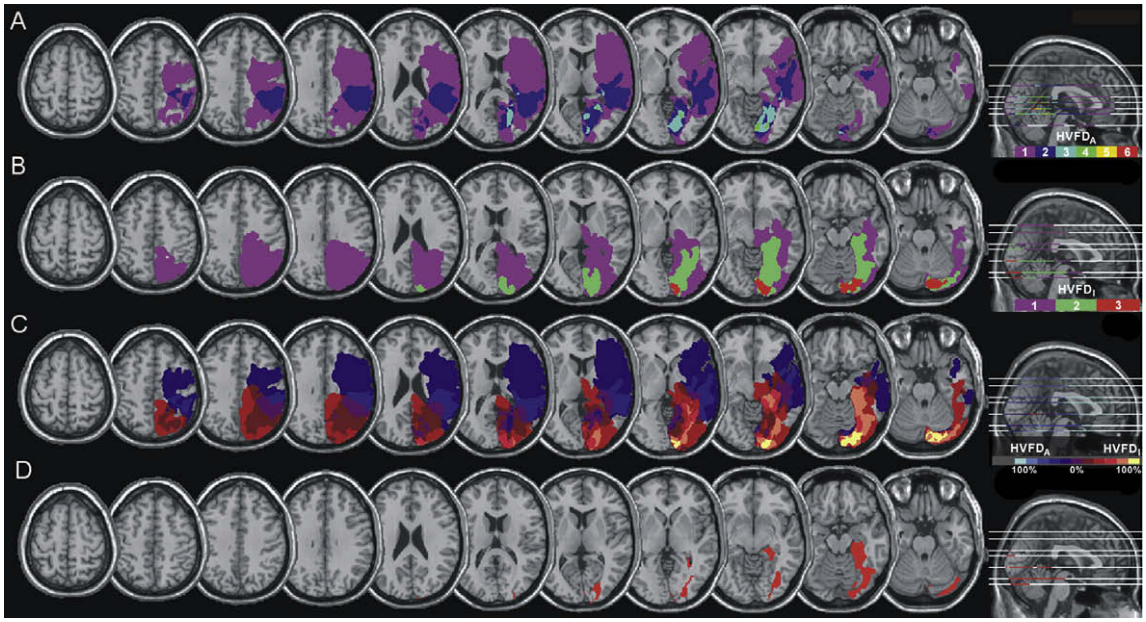

Fig. 12. Overlapping, subtraction and mask lesion analyses. The lesion overlay plots, show the degree of involvement of each voxel in the lesions of the group of HVFD$_A$ patients (A) and the group of HVFD$_I$ patients (B). Overlapping lesions are color-coded with increasing frequency, which indicates the absolute number of patients: from violet ($n = 1$) to red ($n = 6$) for HVFD$_A$ patients and accordingly from violet ($n = 1$) to red ($n = 3$) for HVFD$_I$ patients. (C) Subtraction of the superimposed lesions of HVFD$_A$ patients from the overlap image of the HVFD$_I$ patients. The center of the subtracted lesion overlap (yellow and light orange area) shows regions damaged at least 60% more frequently in HVFD$_I$ patients than in HVFD$_A$ patients. (D) Subtraction overlap and the subsequent mask analysis, which indicates regions that are unique to HVFD$_I$ patients, reveal that the occipitotemporal (fusiform) gyrus, the parahippocampal gyrus and parts of the inferior occipital lobe are commonly damaged in HVFD$_I$ patients but spared in HVFD$_A$ patients.

of healthy subjects or was labeled as "unimpaired" because of their almost normal behavior in everyday life. Our results confirm the general conclusion that hemianopics' oculomotor performance should be analyzed in relation to task performance.

The comparison of both patient groups with the task performance of the unimpaired healthy subjects suggests that HVFD$_A$ patients reached normal performance level at least in the DC task. In the CVS task, this group also performed in the range of normal controls with respect to error rates. The increased time requirements of this group was due to their compensatory gaze behavior during the comparative search, that is, a significantly elevated number of fixations and increased scanpath length (cf. Section 4.2). Error rates and search times of healthy subjects and HVFD$_A$ patients found in the present study are similar to those reported previously (cf. Tant et al., 2002; Zihl, 1995b, 1999). The group of HVFD$_I$ patients performed significantly worse than controls in both tasks. Still, the search times and errors rates reported here are smaller than those found in the studies mentioned above. This could be due to our small sample of only four inadequate patients.

Overall, the performance data supported the assumption that the CVS task was the more difficult one. The two data distributions of controls and patients in the DC task were overlapping widely. In contrast, the performance values (response time and error rate) of all controls in the more complex CVS task were below the respective medians of the patients' data distribution. Consequently, patients had more problems reaching normal performance levels in visual search than in dot counting.

The group assignments, derived from both response time and error rate, correlated highly both between these two measures and between the DC and CVS tasks; this hints towards a stable performance level across tasks for each patient. One reason for the task-independent performance could be the subject-specific use of effective compensatory strategies developed during everyday life tasks. Also, clinical and demographic characteristics could influence the ability to adequately perform the tasks. However, none of the demographic and clinical parameters listed in Table 1 was correlated with the task performance of the patients (data not shown). These findings are supported by other studies. Zihl (1999, 2000) concluded that the presence, time since and severity of the HVFDs could not sufficiently explain the observed deficit. Also Pambakian et al. (2000) analyzed a task concerning viewing of naturalistic pictures and found that neither the location nor the size of the visual loss correlates with any of the analyzed oculomotor parameters. Additionally, in an ongoing own study investigating the HVFD patients' performance in a dynamic collision avoidance task, none of the clinical or demographic parameters could explain the patients' task performance (Papageorgiou et al., Submitted for publication).

4.2. Task demands and compensation strategies

The interpretation of task specific compensatory gaze behavior has to take into account three questions: what are the processing steps needed to solve a given task, how are these steps affected by hemianopia, and to what extend can gaze movements help overcome these processing deficits. Both tasks, DC and CVS, require scanning the visual field for target objects. Additionally, in the CVS task, objects and local object configurations have to be memorized and compared among each other. For the scanning part, compensatory gaze movements are likely to show increased scanpath length, increased number of fixations, and reduced saccadic amplitudes. In order to compensate for recognition deficits, increased fixation durations and therefore reduced scanpath lengths can be expected (Hardiess et al., 2008).

In accordance with previous findings (Tant et al., 2002; Zihl, 1995b, 1999, 2000) we found no significant differences in any of the investigated gaze parameters between subjects from the HVFD$_A$ group and healthy subjects in the DC task. This is in spite of the larger stimulus size of 60° by 40° used in our study. HVFD$_I$ patients showed significantly increased gaze parameters, including

Table 6
Significance comparisons of all gaze performance parameters between the two patient groups and healthy subjects for both experiments ($^{*}p < 0.05$, $^{**}p < 0.01$, $^{***}p < 0.001$, and n.s. denotes not statistically significant).

Gaze parameter	DC task (mean ± sem)			CVS task (mean ± sem)		
	Controls	$HVFD_A$	$HVFD_I$	Controls	$HVFD_A$	$HVFD_I$
Fixation number	26.2 (1.4)	26.8 (2.3)	33.5 (1.7)	36.0 (0.6)	44.6 (1.4)	51.2 (2.0)
Significance		n.s.		*	***	***
Scanpath length	232.5 (12.3)	237.4 (22.0)	335.0 (22.8)	1047.6 (15.5)	1180.0 (30.3)	1077.2 (43.1)
Significance		n.s.		**	***	n.s.
Saccadic amplitude	8.8 (0.2)	8.3 (0.3)	8.0 (0.5)	30.4 (0.3)	27.8 (0.4)	23.4 (1.1)
Significance		n.s.		n.s.	***	***
Fixation duration	277.4 (11.1)	279.3 (11.1)	293.9 (9.9)	30.4 (0.3)	27.8 (0.4)	23.4 (1.1)
Significance		n.s.		n.s.	n.s.	***
Prop. of fixations to HVFD	52.6 (1.5)	57.5 (2.5)	63.0 (3.0)	52.8 (0.6)	54.9 (0.7)	58.9 (0.9)
Significance		n.s.		**	n.s.	**
Repetition of fixation (DC)/gaze shifts (CVS)	6.9 (1.1)	7.6 (1.1)	9.6 (1.3)	16.3 (0.3)	16.9 (0.4)	14.8 (0.8)
Significance		n.s.		*	n.s.	*

number of fixations, proportion of fixations to the side of HVFD, scanpath length, and repetition of fixations (cf. Table 6).

A completely different result was obtained for the cognitively more demanding comparative visual search paradigm. Here, the group of adequately performing patients also showed significant differences in their gaze behavior as compared to controls (cf. Table 6). The number of fixations and the scanpath length were increased, while the mean amplitude of saccades was decreased. It seems that $HVFD_A$ patients adapted by performing more fixations within each cupboard (CVS hemifield) while executing the same number of inter-hemifield gaze shifts as the controls. In a study conducted by Martin, Riley, Kelly, Hayhoe, and Huxlin (2007), hemianopes also performed a cognitively demanding task, i.e. the assembling of wooden models. In this study, all patients showed performance parameters comparable with those of healthy subjects while no conspicuity due to saccade dynamics or spatial distribution of gaze were found. The authors suggest that in naturalistic situations, hemianopes may be able to compensate quite effectively for their visual loss, perhaps by more strongly relying on visuo-spatial memory. Since peripheral visual information, which guides saccade targeting, is missing, patients used more memory-guided saccades and look-ahead fixations. Furthermore, they fixated the target of an upcoming reach and apparently irrelevant locations more often than controls. Such behavior is thought to reflect increased updating of spatial information in visual working memory, on which homonymous hemianopes might rely to a greater degree than controls. Our results in the CVS task differ from the findings of Martin et al. (2007) in that compensatory gaze movements were found also in the $HVFD_A$ patients. Still, we suggest that the memory effects discussed above also play a role in the CVS task, most notably in the processing related to recognition of objects and object configurations. Gaze adaptations of the $HVFD_A$ patients are like to be related to scanning demands.

The CVS specific gaze adaptations found in the $HVFD_I$ patients can be divided in a subset related to scanning (i.e. increased number of fixations, increased proportion of fixations to deficit side and reduced saccadic amplitude) and a second subset consisting of a reduced number of inter-hemifield gaze shifts and longer fixation durations. This second pattern was also found in an earlier study on CVS gaze adaptations where different costs were associated with inter-hemifield gaze shifts (Hardiess et al., 2008). With this gaze strategy subjects increased the involvement of visual working memory to avoid gaze saccades while memorizing larger chunks of information. We therefore suggest that in the present study, $HVFD_I$ patients attempt to solve the CVS task also with increased working memory involvement. The fact that they don't succeed thus hints towards a working memory problem. Lesion evidence for working memory deficits will be discussed below (cf. Section 4.3).

In conclusion, the gaze movement pattern reported here can be interpreted as follows: in the DC task, adequate patients perform on the level of normals without gaze movement compensation. We therefore assume that this compensation is brought about by increased working memory involvement. Inadequate subjects attempt compensation by gaze movements suitable for scanning tasks, but still do worse than the adequate patients, presumably due to insufficient working memory use. In the CVS task, compensation for both scanning and object recognition components must be achieved. Adequate patients use compensatory gaze movements of the scanning type and are thus able to reach normal performance levels. It can therefore be assumed that the effect of HVFD on object recognition is again compensated by working memory processes. If it is true that inadequate patients suffer from working memory deficits, they might attempt to compensate for both, scanning and recognition deficits simultaneously, thereby producing a novel pattern of gaze movement adaptations.

With respect to head movements in HVFD patients, previous studies reported smaller head movement proportion in combined head-eye saccades (Zangemeister, Dannheim, & Kunze, 1986; Zangemeister et al., 1982; Schoepf & Zangemeister, 1992, 1993). It was argued that head movement programming, which is more complex than eye movement programming alone, takes more time for HVFD patients. Consequently, the head movement proportion is reduced due to a malfunctioning coordination of the eye and head. In contrast, we found in the head unrestricted CVS task, that head amplitudes of $HVFD_A$ patients were within the same range as those of healthy controls (i.e. about ±9.0°). Furthermore, the group of $HVFD_I$ patients used a wider range of head movements (i.e. about ±14.0°). Interestingly, the proportion of head movement towards the impaired hemifield was larger in the $HVFD_I$ patients than in the $HVFD_A$ patients. One difference in experimental design that might account for the results from our and previous studies may be the large stimulus area used for the CVS task (i.e. up to ±45°). In any case, we suggest that HVFD patients use head movements in order to achieve additional compensation in a task specific manner.

4.3. Brain lesions and lateralization effect

We found a tendency for a lateralization effect related to the task performance between both HVFD patient groups. All except one patient in the poorly performing $HVFD_I$ group have lesions in the right brain hemisphere. However, this hemisphere is affected

Table 7
Magnetic resonance images (MRIs) of the head, monocular supraliminal automated static perimetry within 30°-area, and binocular semi-automated 90° kinetic perimetry obtained with the OCTOPUS 101-perimeter of all 12 HVFD patients. For three patients MRI data are not available.

Pat. ID	Head MRIs (Talairach z-coordinates: 60, 50, 40, 32, 24, 10, 8, 0, -8, -10, -24)	30°-NO	90°-SKP
ECG	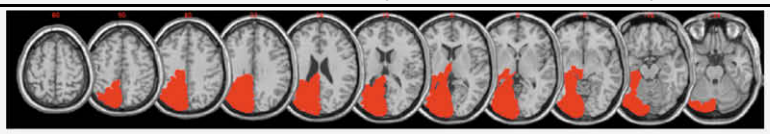	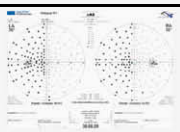	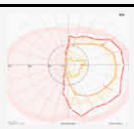
ANE	MRI data not available	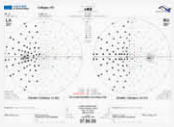	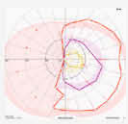
AIH	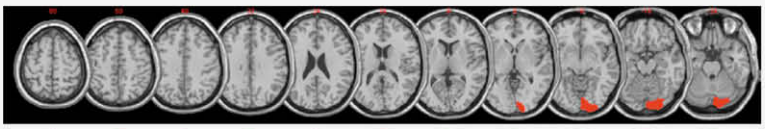		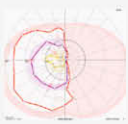
ULH	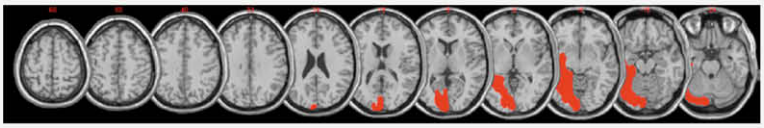		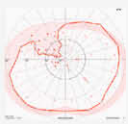
FRH	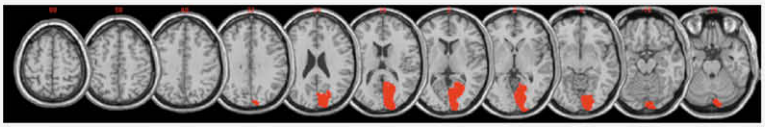		
URF	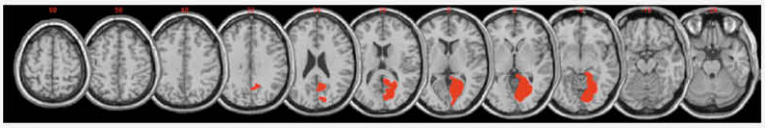		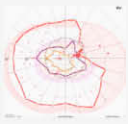
ARG	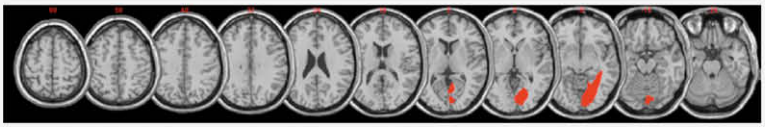		
ARJ	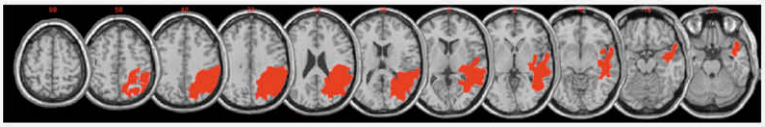		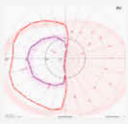
AYC	MRI data not available		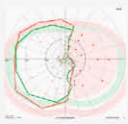
TRH	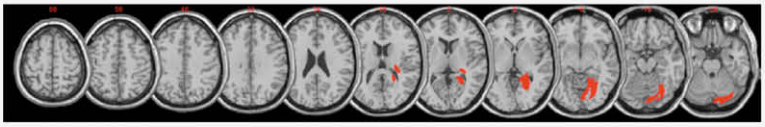		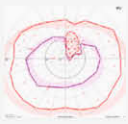
TTC	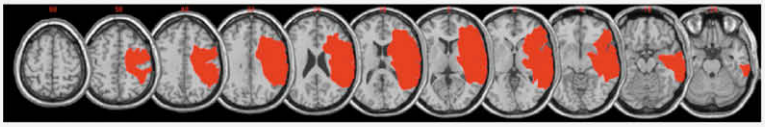	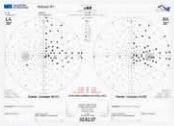	
CKF	MRI data not available		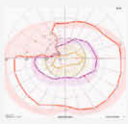

in only one of the $HVFD_A$ patients. Similarly, other studies indicated that patients with right-hemispheric lesions do less well on performance measures and driving tasks (Korner-Bitensky, Mazer, & Sofer, 2000; Mazer, Korner-Bitensky, & Sofer, 1998; Meerwaldt & Van Harskamp, 1982). In a dot counting paradigm Tant et al. (2002) reported that patients with left-sided hemianopia had increased error rates and search times. This lateralization effect was also visible in healthy subjects with simulated visual field loss, indicating that lateralization is not a result of lateralized brain damage. Therefore, the role of lateralization for visual scanning deficits remains elusive.

Zihl (1995b) suggested that the variability in HVFD compensation depends on the extent of brain injury and that parieto-occipital and posterior thalamic lesions may be responsible for insufficient compensation. On the other hand, Tant et al. (2002) observed clear parallels between simulated and real homonymous hemianopes, suggesting that hemianopic scanning behavior is primarily visually elicited, namely by the HVFD, and not by the additional brain damage. However, both studies refer to a simple laboratory task, i.e. dot-counting. For cognitively more demanding tasks, such as CVS or block assembly (Martin et al., 2007), an involvement of other brain regions, especially regions dealing with visuo-spatial memory, seems possible.

In our study, performance differences between $HVFD_I$ and $HVFD_A$ patients were much higher in the CVS than in the DC task. The inadequately performing patients have more difficulties in solving the more complex visual search task. Concerning visual processing there is clear evidence in the literature that spatial working memory performance interferes with visual search. This could be shown for the visuo-spatial sketchpad as part of working memory (Oh & Kim, 2004; Soto & Humphreys, 2008; Woodman & Luck, 2004) as well as for the central executive component (Han & Kim, 2004; Peterson, Beck, & Wong, 2008). Furthermore, results from other groups demonstrate that damage to the right posterior parietal cortex (rPPC) leads to a generalized deficit in visual working memory across a range of stimuli and encoding tasks (see Berryhill & Olson, 2008; Smith & Jonides, 1998; Todd & Marois, 2004). These results seem to suggest that the $HVFD_I$ patients' particularly poor performance in the CVS task might be due to an impairment of their spatial memory resulting from lesions of the rPPC. However, we found a rPPC lesion only in one (ECG) of the four $HVFD_I$ patients. The other $HVFD_I$ patients have visual field defects based on occipital lesions (ANE and ULH) or the left parietal region (AIH). Thus, the lesion analysis does not support the assumed role of spatial memory for the inadequate performance of this group of patients.

A further anatomical analysis identified three lesion sites as unique to $HVFD_I$ patients: mesio-ventral areas of the temporal lobe (i.e. the fusiform gyrus), the inferior occipital lobe, and the parahippocampal gyrus. Regarding the site of brain lesion, our results are consistent with a recent study on hemianopes in visual search (Machner et al., 2009), which showed that mesio-ventral areas of the temporal lobe were damaged in at least half of the severely impaired patients but spared in the mildly impaired patients. Temporal regions belong to the ventral processing visual stream, thought to be involved in the visual recognition of objects, including color, texture and form information (Ungerleider & Mishkin, 1982) and may also play a role in the control of attention (Goodale & Milner, 1996; Ungerleider & Pasternak, 2004).

Lesions of the mesio-ventral temporal areas and V4 might have affected object recognition and subsequently visual search of $HVFD_I$ patients as also suggested by Machner et al. (2009). Disturbance of attentional modulation within the ventral processing stream and damage of its connections with temporal lobe areas and the prefrontal cortex might be a further reason for impaired visual search, through deficits in visuo-spatial memory. In addition, we found that the parahippocampal gyrus is commonly affected in $HVFD_I$ patients. Since the parahippocampal gyrus serves as the main input–output pathway between the hippocampus and cortical association areas, its damage can lead to many cognitive deficits including deficits in memory storage or retrieval from other brain areas.

However, these findings are still subject to interpretation, because our lesion-mapping analysis has some limitations. First, our results are derived from a small number of patients with available MRI scans and the two groups of patients had unequal sizes. Secondly, the brain lesions were mirrored onto the right hemisphere (as in the study of Machner et al., 2009), in order to perform overlapping and subtraction analysis in a greater number of patients. However, the side of the brain lesion, as suggested by many studies and our results above (lateralization effect), might be decisive when studying visual exploration. Therefore, analysis in a larger group of patients separately for right- and left- sided lesions is needed. Yet, our findings are in accordance with previous studies which suggested that the occipitotemporal gyrus, and presumably the parahippocampal gyrus, might be involved in disturbances of visual search after unilateral vascular brain damage.

5. Conclusions

By analyzing the adaptive gaze behavior of patients with HVFDs, we identified two groups of patients differing in their capability to solve two different visual scanning tasks. The $HVFD_A$ patients spontaneously and adequately compensate for their visual field loss in the cognitively unchallenging sampling task as well as in the more demanding comparative visual search task. Although their oculomotor parameters in the DC task did not differ from those of healthy subjects, the $HVFD_A$ patients' gaze (eye and head movement) behavior showed increased compensational adaptations in the CVS task. For the inadequately performing patients (i.e. $HVFD_I$ patients) the pattern of compensational gaze movements differed from the $HVFD_A$ patients' pattern. Still, regardless of their increased adaptations, these patients failed to perform the two scanning tasks as accurately as controls or adequate patients.

We suggest that the difference between adequately and inadequately performing patients is due to reduced working memory availability in the $HVFD_I$ patients. In the DC task $HVFD_I$ patients therefore need to compensate with eye movements whereas $HVFD_A$ patients can rely on working memory. In the CVS task, working memory is needed for object recognition, such that scanning compensation now has to be achieved via gaze movements also in $HVFD_A$ patients. The $HVFD_I$ patients attempt to compensate by gaze movements for both, scanning and recognition demands, but fail. In terms of cortical lesions, losses unique for $HVFD_I$ patients are found mostly in the ventro-mesial temporal lobe.

In general, we argue that comparative studies using visual tasks with varying processing demands are needed to understand gaze movement behavior in hemianopes. Such tasks will require realistic, large field stimulus displays and simultaneous measurements of head and eye movements.

Acknowledgments

The authors thank the Rehabilitation Centre Bad Urach, the Neurology Clinic of Burger Hospital in Stuttgart and the European Union (PERACT – Marie Curie Early Stage Training MEST-CT-2004-504321) for their support for this study. We also thank the anonymous reviewers for their constructive criticisms and comments.

References

Berryhill, M. E., & Olson, I. R. (2008). The right parietal lobe is critical for visual working memory. *Neuropsychologia, 46*(7), 1767–1774.

Boothe, R. G. (2002). *Perception of the visual environment*. New York: Springer-Verlag.

Chedru, F., Leblanc, M., & Lhermitte, F. (1973). Visual searching in normal and brain-damaged subjects (contribution to the study of unilateral inattention). *Cortex, 9*, 94–111.

Gassel, M. M., & Williams, D. (1963). Visual function in patients with homonymous hemianopia II. Oculo-motor mechanisms. *Brain, 86*, 1–36.

Gauthier, L., Dehaut, F., & Joannette, Y. (1989). The bells test: A quantitative and qualitative test for visual neglect. *International Journal of Clinical Neuropsychology, 11*, 49–54.

Goodale, M., & Milner, D. (1996). Separate visual pathways for perception and action. In A. Ellis & A. Young (Eds.), *Human cognitive neuropsychology. A textbook with readings*. Hove, East Sussex: Psychology Press.

Gottlob, L. R. (2006). Aging and comparative search for feature differences. *Aging Neuropsychology and Cognition, 13*, 435–457.

Han, S. H., & Kim, M. S. (2004). Visual search does not remain efficient when executive working memory is working. *Psychological Science, 15*(9), 623–628.

Hardiess, G., Gillner, S., & Mallot, H. A. (2008). Head and eye movements and the role of memory limitations in a visual search paradigm. *Journal of Vision, 8*(1), 1–13.

Ishiai, S., Furukawa, T., & Tsukagoshi, H. (1987). Eye-fixation patterns in homonymous hemianopia and unilateral spatial neglect. *Neuropsychologia, 25*, 675–679.

Johannsen, L., & Karnath, H. O. (2004). How efficient is a simple copying task to diagnose spatial neglect in its chronic phase? *Journal of Clinical and Experimental Neuropsychology, 26*(2), 251–256.

Kerkhoff, G. (1999). Restorative and compensatory therapy approaches in cerebral blindness – A review. *Restorative Neurology and Neuroscience, 15*, 255–271.

Korner-Bitensky, N. A., Mazer, B. L., & Sofer, S. (2000). Visual testing for readiness to drive after stroke: A multicenter study. *American Journal of Physical Medicine and Rehabilitation, 79*, 253–259.

Machner, B., Sprenger, A., Kömpf, D., Sander, T., Heide, W., Kimmig, H., et al. (2009). Visual search disorders beyond pure sensory failure in patients with acute homonymous visual field defects. *Neuropsychologia, 47*, 2704–2711.

Mangione, C. M., Lee, P. P., Gutierrez, P. R., Spritzer, K., Berry, S., & Hays, R. D. (2001). Development of the 25-item National Eye Institute Visual Function Questionnaire. *Archives of Ophthalmology, 119*, 1050–1058.

Mangione, C. M., Lee, P. P., Pitts, J., Gutierrez, P., Berry, S., & Hays, R. D. (1998). Psychometric properties of the National Eye Institute Visual Function Questionnaire (NEI-VFQ). *Archives of Ophthalmology, 116*, 1496–1504.

Martin, T., Riley, M. E., Kelly, K. N., Hayhoe, M., & Huxlin, K. R. (2007). Visually-guided behavior of homonymous hemianopes in a naturalistic task. *Vision Research, 47*, 3434–3446.

Mazer, B. L., Korner-Bitensky, N. A., & Sofer, S. (1998). Predicting ability to drive after stroke. *Archives of Physical Medicine and Rehabilitation, 79*, 743–750.

McDonald, S. A., Spitsyna, G., Shillcock, R. C., Wise, R. J. S., & Leff, A. P. (2006). Patients with hemianopic alexia adopt an inefficient eye movement strategy when reading text. *Brain, 129*, 158–167.

Meerwaldt, J. D., & Van Harskamp, F. (1982). Spatial disorientation in right-hemisphere infarction. *Journal of Neurology, Neurosurgery, and Psychiatry, 45*, 586–590.

Meienberg, O., Zangemeister, W. H., Rosenberg, M., Hoyt, W. F., & Stark, L. (1981). Saccadic eye movement strategies in patients with homonymous hemianopia. *Annals of Neurology, 9*, 537–544.

Oh, S., & Kim, M. (2004). The role of spatial working memory in visual search efficiency. *Psychonomic Bulletin and Review, 11*(2), 275–281.

Pambakian, A. L., Wooding, D. S., Patel, N., Morland, A. B., Kennard, C., & Mannan, S. K. (2000). Scanning the visual world: A study of patients with homonymous hemianopia. *Journal of Neurology, Neuro-surgery, and Psychiatry, 69*, 751–759.

Papageorgiou, E., Hardiess, G., Ackermann, H., Karnath, H., O., Wiethoelter, H., Vonthein, R., Schoenfisch, B., Mallot, H. A. & Schiefer, U. (submitted for publication). Driving performance in patients with homonymous visual field defects and healthy subjects in a standardized virtual reality environment.

Papageorgiou, E., Hardiess, G., Schaeffel, F., Wiethölter,H., Karnath, H. O., Mallot, H. A., Schönfisch, B., & Schiefer, U. (2007). Assessment of vision-related quality of life in patients with homonymous visual field defects. *Graefe's Archive for Clinical and Experimental Ophthalmology*, July 25, 2007 .

Peterson, M. S., Beck, M. R., & Wong, J. H. (2008). Were you paying attention to where you looked? The role of executive working memory in visual search. *Psychonomic Bulletin & Review, 15*, 372–377.

Pomplun, M., Sichelschmidt, L., Wagner, K., Clermont, T., Rickheit, G., & Ritter, H. (2001). Comparative visual search: A difference that makes a difference. *Cognitive Science, 25*, 3–36.

Rorden, C., & Brett, M. (2000). Stereotaxic display of brain lesions. *Behavioural Neurology, 12*, 191–200.

Schoepf, D., & Zangemeister, W. H. (1992). Eye and head reading path in hemianopic patients. In S. F. Wright, & R. Groner (Eds.), *Facets of dyslexia and its remediation, studies in visual information processing* (pp. 267–291). Amsterdam, New York.

Schoepf, D., & Zangemeister, W. H. (1993). Correlation of coordinated gaze strategies to the status of adaptation in patients with hemianopic visual field defects. *Annals of the New York Academy of Sciences, 682*, 404–409.

Smith, E. E., & Jonides, J. (1998). Neuroimaging analyses of human working memory. *PNAS, 95*(20), 12061–12068.

Soto, D., & Humphreys, G. W. (2008). Stressing the mind: The effect of cognitive load and articulatory suppression on attentional guidance from working memory. *Attention, Perception & Psychophysics, 70*, 924–934.

Stone, S. P., Halligan, P. W., Wilson, B., Greenwood, R. J., & Marshall, J. C. (1991). Performance of age-matched controls on a battery of visuo-spatial neglect tests. *Journal of Neurology, Neurosurgery, and Psychiatry, 54*, 341–344.

Tant, M. L. M., Cornelissen, F. W., Kooijman, A. C., & Brouwer, W. H. (2002). Hemianopic visual field defects elicit hemianopic scanning. *Vision Research, 42*, 1339–1348.

Todd, J. J., & Marois, R. (2004). Capacity limit of visual short-term memory in human posterior parietal cortex. *Nature, 428*(6984), 751–754.

Ungerleider, L., & Mishkin, M. (1982). Two cortical visual systems. In D. J. Ingle, M. A. Goodale, & R. J. W. Mansfield (Eds.), *Analysis of visual behavior*. Cambridge, MA: The MIT Press.

Ungerleider, L., & Pasternak, T. (2004). Ventral and dorsal cortical processing streams. In L. Chalupa & J. Werner (Eds.). *The visual neurosciences* (Vol. 1). Cambridge, MA: The MIT Press.

Wolfe, J. M. (1994). Guided search 2.0: A revised model of visual search. *Psychonomic Bulletin and Review, 1*, 202–238.

Woodman, G. F., & Luck, S. J. (2004). Visual search is slowed when visuospatial working memory is occupied. *Psychonomic Bulletin & Review, 11*, 269–274.

Zangemeister, W. H., Dannheim, F., & Kunze, K. (1986). Adaption of gaze to eccentric fixation in homony–mous hemianopia. In E. L. Keller & D. S. Zee (Eds.), *Adaptive processes in visual and oculomotor systems*. Pergamon Press.

Zangemeister, W. H., Meienberg, O., Stark, L., & Hoyt, W. F. (1982). Eye-head coordination in homony–mous hemianopia. *Journal of Neurology, 226*, 243–254.

Zangemeister, W. H., & Oechsner, U. (1996). Evidence for scanpaths in hemianopic patients shown through string editing methods. In W. H. Zangemeister, H. S. Stiehl, & C. Freska (Eds.), *Visual attention and cognition* (pp. 197–220). Amsterdam: Elsevier Science.

Zihl, J. (1994). Rehabilitation of visual impairments in patients with brain damage. In A. C. Kooijman, P. L. Looijestijn, J. A. Welling, & G. J. van der Wildt (Eds.), *Low vision. Research and new developments in rehabilitation* (pp. 287–295). Amsterdam and Oxford: IOS Press.

Zihl, J. (1995a). Eye movement patterns in hemianopic dyslexia. *Brain, 118*, 891–912.

Zihl, J. (1995b). Visual scanning behavior in patients with homonymous hemianopia. *Neuropsychologia, 33*, 287–303.

Zihl, J. (1999). Oculomotor scanning performance in subjects with homonymous visual field disorders. *Visual Impairment Research, 1*(1), 23–31.

Zihl, J. (2000). *Rehabilitation of visual disorders after brain injury*. Hove, East Sussex: Psychology Press Ltd.

Collision avoidance in persons with homonymous visual field defects under virtual reality conditions

Authors: Eleni Papageorgiou[a,*], Gregor Hardiess[b], Hermann Ackermann[c], Horst Wiethoelter[d], Klaus Dietz[e], Hanspeter A. Mallot[b], Ulrich Schiefer[a]

Institutions

[a]Center for Ophthalmology, Institute for Ophthalmic Research, University of Tübingen, Germany

[b]Department of Neurobiology, Lab of Cognitive Neuroscience, University of Tübingen, Germany

[c]Rehabilitation Center, Bad Urach, Germany

[d]Department of Neurology, Bürger Hospital, Stuttgart, Germany

[e]Department of Medical Biometry, University of Tübingen, Germany

***Corresponding author**

Eleni Papageorgiou, Center for Ophthalmology, University of Tübingen, Schleichstraße 12-16, 72076, Tübingen, Germany

E-mail: Eleni.Papageorgiou@med.uni-tuebingen.de

Tel: +49-7071-29-80726

Fax: +49-7071-29-5038

Abbreviations

HVFD: homonymous visual field defect

VR: virtual reality

A-SPAR: area of sparing within the affected hemifield

HH: homonymous hemianopia

QH: homonymous quadrantanopia

Word Count: 6390 words

Number of figures: 8, **Number of tables**: 2, **Supplementary data**: 1 (Appendix.pdf)

ABSTRACT

Aim of the present study was to examine the effect of homonymous visual field defects (HVFDs) on collision avoidance of dynamic obstacles at an intersection under virtual reality (VR) conditions. Additional factors that may affect visual behavior of patients towards moving obstacles at intersections with focus on age and brain lesion were investigated. Our findings were analyzed in relation to previous studies assessing performance of patients with HVFDs in interactive driving scenarios. Overall performance was quantitatively assessed as the number of collisions in a virtual intersection paradigm at two difficulty levels. HVFDs were assessed by binocular semi-automated kinetic perimetry within the 90° visual field, stimulus III4e and the area of sparing within the affected hemifield (A-SPAR in degrees^2) was calculated. The effect of A-SPAR, age, gender, side of brain lesion, time since brain lesion and presence of macular sparing on the number of collisions, as well as performance over time were investigated. Thirty patients (10 female, 20 male, age range: 19-71 years) with HVFDs due to unilateral vascular brain lesions and 30 group-age-matched subjects with normal visual fields were examined. The mean number of collisions was higher for patients. Lower A-SPAR and increasing age were associated with worse performance. However, in agreement with previous studies, wide variability in performance among patients with identical visual field defects was observed and performance of some patients was similar to that of normal subjects. Both participant groups displayed equal improvement of performance over time in the more difficult level. The extent of the HVFD – expressed as area of sparing within the affected hemifield (A-SPAR) – was weakly related to performance in this VR scenario. However, wide variability among patients suggests that visual-field related parameters per se are inadequate in predicting successful collision avoidance. Our results underscore the importance of individualized compensatory-based approaches in order to understand functional behavior of patients with HVFDs in dynamic tasks.

Keywords: collision avoidance, driving simulator, virtual reality, homonymous visual field defects, aging

1. Introduction

Homonymous visual field defects (HVFDs), the loss of the field of vision in the same relative position in both eyes, are among the most frequent disorders after unilateral injury of the postchiasmatic visual pathway. Nearly 80% of patients with unilateral postchiasmatic brain lesions suffer from HVFDs (Zihl, 1995). Most common causes of HVFDs are strokes and, to a lesser extent, traumatic brain injury and tumors (Zihl, 2000). HVFDs create a marked amount of subjective inconvenience in everyday life (Papageorgiou et al., 2007; Gall et al., 2009). Patients with HVFDs may show persistent and severe impairments of reading, visual exploration and navigation, collide with people or objects on their blind side and may be deemed unsafe to drive (Trauzettel-Klosinski & Reinhard, 1998; Zihl, 2000, 2003). This has led to the belief that homonymous visual field loss is per se associated with functional impairment.

Driving has been considered to be problematic for patients with HVFDs; therefore several research groups have assessed function of patients with HVFDs in comparison to subjects with normal visual fields either in driving simulators or on-road. The few studies assessing the performance of patients with HVFDs in realistic or experimental driving paradigms report a variety of findings. Some authors suggest that performance of patients with HVFDs is significantly worse than that of normal subjects (Table 1, Bowers et al., 2009; Kooijman et al., 2004; Lövsund et al., 1991; Tant et al., 2002; Szlyk et al., 1993). On the other hand, other studies report that there are no performance differences between patients with HVFDs and control subjects (Table 1, Martin et al., 2007; Schulte et al., 1999; Wood et al., 2009). The majority of studies have highlighted poor steering control, incorrect lane position and difficulty in gap judgment as the primary problems of drivers with HVFDs (Tant et al., 2002; Szlyk et al., 1993; Wood et al., 2009; Bowers et al., 2009). A secondary question concerned the underlying factors affecting performance of patients with HVFDs. It has been a matter of debate whether performance of patients with longstanding HVFDs is primarily determined by visual field measures, e.g. the extent of the visual field along the horizontal meridian, the Esterman score, the presence of macular sparing (Johnson & Keltner, 1983), or affected by additional factors, such as ageing, side of brain injury and compensation by eye and head movements (Pambakian et al., 2000; Zihl, 1995; Wood et al., 2009).

Rather than making general statements on the average performance of patients with HVFDs, recent evidence suggests that functional processes to judge each patient individually should be introduced, because a significant portion of patients have the potential to compensate and wide variability among them occurs (Bowers et al., 2009; Hardiess et al., 2010; Wood et al., 2009). In order to enable individual assessments in driving scenarios, it has been argued that studies should address specific questions at specific road segments and in relation to specific visual impairments (Mandel et al., 2007). One aspect of driving behavior which has not been studied adequately is performance of patients with HVFDs at intersections. Therefore, Bowers et al. (2009) investigated detection of stationary pedestrians at intersections and along the roadside at city and rural roads in a driving simulator, and found that HH drivers exhibited significantly lower pedestrian detection rates on their blind side at intersections. However, collision avoidance ability of patients with HVFDs at intersections, in terms of detecting and appropriately responding to a dynamic collision-relevant obstacle, has not been studied yet.

Therefore, the aims of the present study were (i) to assess the performance of patients with HVFDs in comparison to normal-sighted control subjects in a dynamic collision avoidance task, and (ii) to investigate whether performance can be explained by the extent of the visual field defect. We evaluated performance of patients with longstanding HVFDs due to cerebrovascular lesions, in a collision avoidance task under virtual reality (VR) conditions and compared them to normal-sighted age-matched subjects. We hypothesized that patients with HVFDs would demonstrate poorer performance in terms of collision avoidance at an intersection. In particular, we expected that patients would collide more often with vehicles on the hemianopic than the seeing side and there would probably be no difference in collision rates between the seeing side of patients and the normal-sighted subjects. However, we speculated that performance would not be solely explained by visual field-related parameters and therefore expected contribution of additional factors, e.g. age, presence of macular sparing, side of brain lesion and time span since lesion onset. Literature on spatial cognition often reports gender differences, with males typically performing better in tasks involving mental rotation, three-dimensional figures and spatial orientation (Voyer et al., 1995; Wolf et al., 2010). Therefore the effect of gender on collision avoidance was also investigated.

Virtual reality was used in order to achieve standardized, repeatable and completely programmable experimental conditions and avoid any safety concerns and driving licensure issues encountered in previous on-road assessments. A driving scenario was chosen as a paradigm that concerns a familiar everyday situation. Driving consists of several subtasks; therefore we have segregated one central aspect, namely collision avoidance, in order to systematically address one type of error and relevant visual behavior. Collision avoidance is associated with further daily living tasks, like crossing a road, walking in a crowd, or driving through an intersection, which often require pedestrians and drivers to adapt their behavior to the displacement of other objects in their environment (Lobjois et al., 2008). At an intersection, a driver must estimate the time interval that it will take for his car to cross the road before an oncoming vehicle will arrive there (i.e. time to collision, TTC), (Lobjois et al., 2008; Matsumiya & Kaneko, 2008; Schiff & Detwiler,1979; Schiff & Oldak, 1990). This task requires oculomotor adaptation, head movements and visuo-motor calibration, which consists of perceiving the size of the gap between the cross-traffic vehicles in terms of time to act (Lee, 1976, Simpson et al., 2003). Yet the effect of homonymous visual field loss on the completion of such a cognitively challenging task has not been assessed previously. The intersection paradigm with incoming roads from the left and right was considered appropriate to detect performance deficits in patients with HVFDs, because target detection in their blind side is thought to be impaired (Bowers et al., 2009).

Author	Study participants	Experimental setup	Results	Remarks
Wood et al. (2011)	22 patients with HH 8 patients with homonymous quadrantanopia (QH) 30 controls	On-road test (interstate and non-interstate)	Patients rated as safe made larger eye movements and more head movements into their blind hemifield	Eye and head movements were assessed qualitatively by means of video footage, rather than by using a formal eye and head tracker system.
Bowers et al. (2010)	12 patients with HH 12 controls	Driving simulator	Drivers with HH took a lane position that increased the safety margin on their blind side	Absolute lane position varied as the steering maneuver and location of the risk from oncoming traffic changed with road segment type.
Hardiess et al. (2010)	12 patients with HVFDs 12 controls	Virtual reality (dot counting task and comparative visual search task)	8/12 patients could reach adequate performance in both tasks	In the two tasks, different patterns of compensatory gaze movements were found.
Bowers et al. (2009)	12 patients with homonymous hemianopia (HH) 12 controls	Driving simulator	HH drivers had significantly lower pedestrian detection rates on the HH-side	Wide variability among subjects and age the main factor for that. The relationship of simulator-based measures to on-road performance has yet to be established.
Wood et al. (2009)	22 patients with HH 8 patients with homonymous QH 30 controls	On-road test (interstate and non-interstate)	73% of HH and 88% of QH patients received safe ratings	10 HH and 1 QH patients did not drive on the interstate, 44% of initially eligible patients did not participate in the study
Bowers et al. (2008)	43 patients with HH	Follow-up questionnaires evaluating functional benefits for mobility	47% of patients were wearing the prism glasses after 12 months reporting significant benefits for obstacle avoidance	Objective measures of functional performance with and without prisms and a control or comparison treatment were not included
Martin et al. (2007)	3 patients with HH 4 controls	Naturalistic task (assembly of wooden models on a table)	No significant differences in task performance, saccade dynamics, spatial distribution of gaze	Small sample
Szlyk et al. (2005)	10 patients with HH due to occipital lobe lesions	Comparison of Fresnel prisms and Gottlieb system in the laboratory, on-road and in a simulator	Prism lenses and training in their use improved performance on visual functioning and driving-related skills	Need for data on the long-term safety of peripheral enhancement devices while driving
Racette et al. (2005)	13 patients with HH 7 patients with QH	Retrospective chart review of occupational therapists' assessments of on-road driving test	Localized visual field loss (VFL) in the left hemifield and diffuse VFL in the right hemifield associated with impaired performance, patients with QH received no unsafe ratings	No control group, different therapists, retrospective design, lack of standardized route
Kooijman et al. (2004)	28 patients with HVFDs	On-road driving test pre- and post-training on a driving simulator	Only 4/28 patients with HVFDs passed the on-road test	No control group, referral of patients due to suspected driving safety concerns
Tant et al. (2002)	28 patients with HH	On-road driving test and neuropsychological visuospatial test performance	Only 14% of patients passed the test	Recruitment of patients whose driving was suspected to be unsafe by the caregiver or the patients themselves
Schulte et al. (1999)	6 patients with HVFDs 10 controls	Driving simulator	No differences in performance (driving speed, driving error rate, reaction time)	Small sample
Zihl (1995)	60 patients with HH 16 controls	Dot counting task on a screen	40% of patients showed normal scanning behavior	Time since brain damage was at least 6 weeks

Szlyk et al. (1993)	6 patients with HVFDs 7 age-matched controls 31 younger controls	Driving simulator	Performance of patients worse than or similar to the older control group	3 patients had hemi-neglect, the study was performed 2 months after stroke
Lövsund et al. (1991)	26 patients with HVFDs 20 controls	Detection of stimuli in a driving simulator at 24 positions	Only 3/26 patients with HVFDs were found able to compensate	Wide variation in the individual reaction time

Table 1: List of studies assessing performance of patients with HVFDs (in descending chronological order).

2. Material and Methods

2.1 Subjects

Potential participants with hemianopia or quadrantanopia were recruited from the Department of Neuro-Ophthalmology and the Neurology Clinic at the University of Tübingen (Germany), as well as the Neurology Clinic of the Bürger Hospital in Stuttgart and the Bad Urach Rehabilitation Centre. Normal-sighted control subjects were recruited from the Tübingen region and comprised group-age-matched volunteers from friends and relatives of the authors, the staff and the patients in the Department of Neuro-Ophthalmology at the University of Tübingen.

To be included in the study, all participants were required to be at least 18 years old, to have best corrected monocular (near and distant) visual acuity of at least 20/25 and normal function and morphology of the anterior visual pathways as evaluated by ophthalmological tests (fundus and slit-lamp examinations, ocular alignment, ocular motility). The group-age-matched control subjects should additionally have normal visual fields and no history of brain injury, physical or cognitive impairment. Patients should have a homonymous visual field defect, varying from complete homonymous hemianopia to homonymous paracentral scotomas, due to a unilateral vascular brain lesion, which was documented by neuroradiological examinations(magnetic resonance imaging or computerized tomography). Exclusion criteria for patients were as follows: visual hemi-neglect as determined by horizontal line bisection, copying of figures, and by means of the "Bells test" (Gauthier et al., 1989), evidence of cognitive decline, aphasia, apraxia, visual agnosia or physical impairment, cerebral tumor, multiple sclerosis, Alzheimer's disease, Parkinson's disease, and previous scanning training. The time span between the brain lesion and the examination date should comprise at least six months.

The research study was approved by the Institutional Review Board of the University of Tübingen (Germany) and was performed according to the Declaration of Helsinki. Following verbal and written explanation of the experimental protocol all subjects gave their written consent, with the option of withdrawing from the study at any time.

Of the 41 potential participants with hemianopia or quadrantanopia, two patients with unilateral neglect and seven patients with bilateral homonymous defects were excluded. Two further patients withdrew after experiencing symptoms of motion sickness. Thirty eligible patients with HVFDs (20 with hemianopia and 10 with quadrantanopia) and 30 normal-sighted group-age-matched control subjects were finally enrolled in the study.

The etiology of the HVFD was in all cases a unilateral cerebrovascular lesion due to ischemia (21 patients), hemorrhage (one patient), rupture of intracerebral aneurysm (two patients), arteriovenous malformation (two patients) or hemorrhage after trauma (four patients). Time since lesion onset was at least six months (median: 20 months, range: 6 months-18 years). There were 15 patients with right-hemispheric and 15 patients with left-hemispheric lesions, which were in the majority of cases located in the occipital lobe. The demographic characteristics of each of the 30 patients are listed in Appendix 1.

2.2 Visual field assessment

Visual fields of patients were assessed with monocular threshold-related, slightly supraliminal automated static perimetry (sAS) within the central 30° visual field, binocular slightly supraliminal automated static perimetry (sAS) within the 90° visual field as well as binocular semi-automated 90° kinetic perimetry (SKP), each obtained with the OCTOPUS 101 Perimeter (Fa. HAAG-STREIT, Koeniz, Switzerland). Visual fields of control subjects were assessed with binocular slightly supraliminal automated static perimetry (sAS) within the 90° and binocular semi-automated 90° kinetic perimetry (SKP). Visual fields within the central 30° were performed with appropriate near correction. In the patient group – in accordance with a recent study of Wood et al. (2009) – homonymous visual field loss was classified as left vs. right, complete vs. incomplete, and whether macular sparing was present according to standard definitions (Schiefer et al., 2007; Kline, 2008). For patients with quadrantanopia, field loss was further classified in superior vs. inferior.

2.3 Experimental setup

Performance in the collision avoidance task was assessed under VR conditions. The VR environment was displayed on a cone-shaped projection screen. This screen provided a horizontal field of view of 150^{o} and a vertical one of 70^{o}. Subjects were seated upright with the back tightly on the chair and with their head in the axis of the conical screen. Eye level was set at 1.2 m altitude and distance to the screen at 1.62 m (Fig. 1).

Figure 1. Image of the experimental set-up. Study participant performing collision avoidance in front of the projection screen.

The visual environment and the experimental procedures were programmed in the SGI OpenGL Performer^{TM}. The spatial resolution of the projected images was 2048 x 768 pixels displayed with a frame rate of 60 Hz.

2.4 Experimental task

The subject was instructed to "drive" along a straight road (Fig. 2A and 2B) and finally to drive through a virtual intersection with cross traffic without causing a collision.

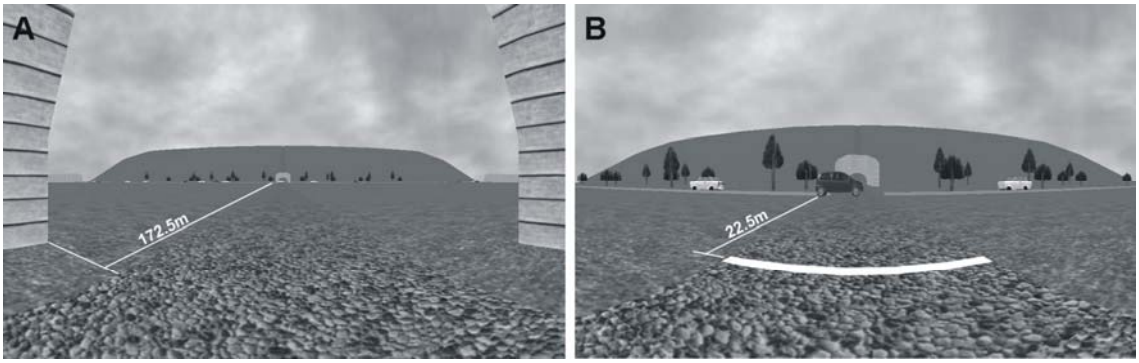

Figure 2. A) Start position of the virtual vehicle in the tunnel. The distance to the intersection (172.5 m) is depicted. B) End position of the virtual drive at the white line 22.5 m before the intersection. The cross traffic at that moment is depicted (two cars driving from right to left and one car driving to the right) .

The virtual driving distance to the intersection was 172.5 m and only straightforward movement of the virtual vehicle was possible. Subjects started each trial in a tunnel (Fig. 2A). After leaving the tunnel they could adjust their driving speed between 18 and 61.2 km/h (11.2-38 mph) by means of a joystick in order to avoid a collision with the cross traffic at the intersection. During the driving period it was not possible to stop the car. The subject should therefore estimate the time interval when the oncoming vehicle will arrive at the intersection. At the same time, the subject also needed to estimate the time interval that it will take for his vehicle to cross the road at the intersection (Matsumiya & Kaneko, 2008) and could adjust his speed in order to achieve the goal of preventing a collision. When subjects reached a white line 22.5 m before the intersection (Fig. 2B), they weren't allowed to adjust their speed anymore. After this line they were automatically driven across the intersection with the last adjusted speed without further visual input. A potential collision was then calculated by the simulation program and was delivered to the examiner at the end of the experiment. Even in case of a collision, participants did not experience a virtual crash and did not receive any feedback about their performance, in order to maintain identical conditions for each trial.

All cars of the cross traffic had a constant speed of 50 km/h (31.1 mph) and on average there were equal numbers of vehicles from the left and right side. The experiment was programmed at two traffic density levels of ascending difficulty, which would generate collisions in 50% or 75% of the trials respectively – in case that

the subjects would begin the trial at a random position within the first 150 meters and would drive with a constant random speed.

Subjects performed 30 trials: 15 trials for each density level in the same randomized order – and were free to perform head and eye movements. Prior to the start of the experiment all subjects underwent a training session lasting 5-10 minutes in order to understand the experimental demands and become familiar with the use of the equipment and the joystick. The experiment started after the participant reported that he/she has understood the task and has completed at least three "collision-free" trials at each of the two density levels. After each trial the simulation program recorded if there was a collision or not. Participants were not given feedback about their performance until the end of the experiment. Participants were encouraged to take breaks at will; testing resumed when the participant indicated they were ready. The time to complete the whole experiment ranged from 40 to 50 minutes.

2.5. Statistical methods

2.5.1 Visual field evaluation

From the binocular semi-automated 90° kinetic perimetry (SKP) we calculated the area of sparing within the affected hemifield (A-SPAR in degrees^2) for the stimulus III 4e (background luminance 10 cd/m2, angular velocity 3°/s, Fig. 3). A software tool available on the OCTOPUS 101 Perimeter enables automatic calculation of the area within a specific isopter (in degrees^2). In order to calculate the area of sparing for subjects with normal vision, they were arbitrarily assigned the right hemifield as the "affected" one, since any difference between the two hemifields in this case would be negligible. We used the binocular visual field, because it is assumed to provide more realistic information about the visual field a patient uses for performing daily activities (Schiefer et al., 2000).

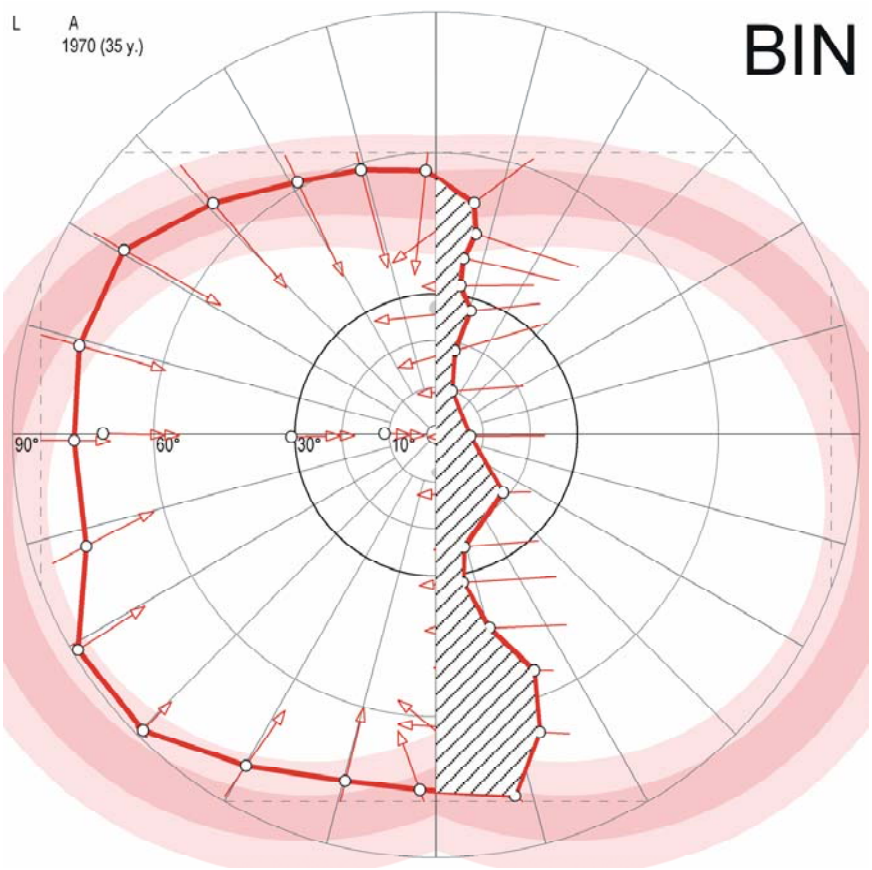

Figure 3. Binocular visual field of a patient with a homonymous hemianopia to the right: Graphic representation of the area of sparing within the affected hemifield (A-SPAR as *hatched region*, obtained with stimulus III4e, angular velocity 3^{o}/s).

2.5.2 Data analysis and statistics

Overall performance in the task was quantitatively assessed as the number of collisions for the 15 trials per density level. Data were analyzed using the statistical software JMP® (SAS Institute Inc., Cary, NC, USA) [www.jmp.com]. Since the number of collisions followed a Poisson distribution we applied a square root transformation in order to stabilize variances. We applied multifactorial analyses of variance with fixed factors group and traffic density and as random factor the individual nested under the factor group. The factor group refers to the division of participants in patients and normal subjects. Since the interaction terms between the fixed factors turned out to be non-significant, they were not included into the final models. The results are given as Hölder means together with the corresponding 95% confidence intervals. In our case the Hölder mean is the square of the arithmetic mean

of the square roots of the observations. Further statistical models are described under Results.

3. Results

3.1 Demographic data

The demographic summary statistics of patients and controls are given in Table 2. There were no differences in age ($p = 0.79$, t-test) and gender ($p = 0.79$, Fisher's exact test) between patients and control subjects, reflecting group-matching with respect to age and gender. The ratio males/females for patients was 2.0 and for control subjects it was 1.5.

	Hemianopia (n_1=20)	Quadrantanopia (n_2=10)	Combined (N=30)	Controls (N_o=30)
Age, mean (SD)	45.9 (16.4)	46.9 (16.1)	46.2 (16.0)	45.1 (15.4)
Gender, N (%)				
Female	5 (25)	5 (50)	10 (33)	12 (40)
Male	15 (75)	5 (50)	20 (67)	18 (60)
Side of lesion, N (%)				
Right	9 (45)	6 (60)	15 (50)	
Left	11 (55)	4 (40)	15 (50)	
Macular sparing, N (%)				
	10 (50)	7 (70)	17 (57)	

Table 2: Demographic summary statistics (age and gender) of patients with HVFDs and control subjects.

3.2 Task performance analysis

The number of collisions of all subjects is shown in Figure 4 separately for each traffic density level. Increasing the traffic density from 50 to 75% increases the mean number of accidents for controls by about 6 and for patients by about 7 ($p < 0.0001$). The difference between the controls and patients is about 1 for 50% density and 2 for 75% density ($p = 0.0061$).

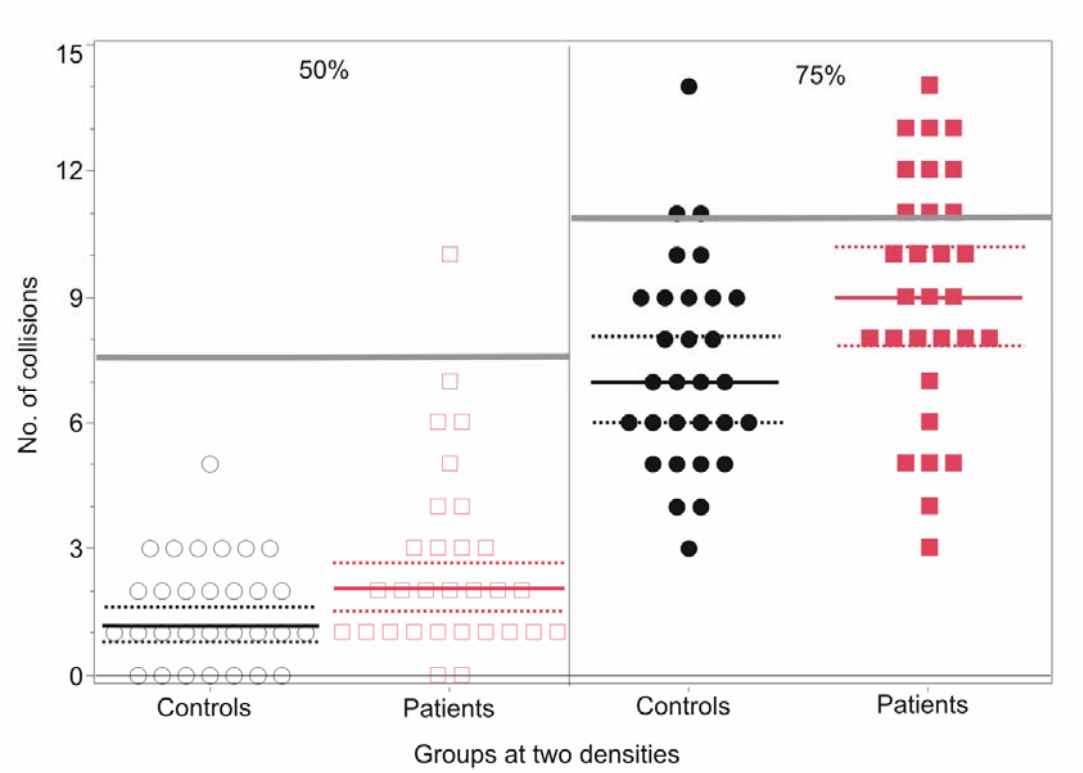

Figure 4. Scatterplots of the number of virtual collisions at the 50% and 75% traffic density. The continuous lines show the Hölder means and the dashed lines show the corresponding 95% confidence intervals. The red squares correspond to patients and the black circles refer to control subjects. The markers are open for density 50% and closed for density 75%. Increasing the traffic density from 50 to 75% increases the mean number of accidents for controls by about 6 and for patients by about 7 ($p < 0.0001$). The difference between the controls and patients is about 1 for 50% density and 2 for 75% density ($p = 0.0061$). The grey lines show the expected number of collisions in case that the subjects began the trials at a random time point and drove with random speed (i.e. with closed eyes): 7.5 collisions for 50% density and 11.25 collisions for 75% density.

Patients with hemianopia had significantly higher collision rates than controls in both traffic density levels, while there were neither significant differences in the collision rates of quadrantanopia patients compared with normal subjects nor with hemianopia patients (Fig. 5).

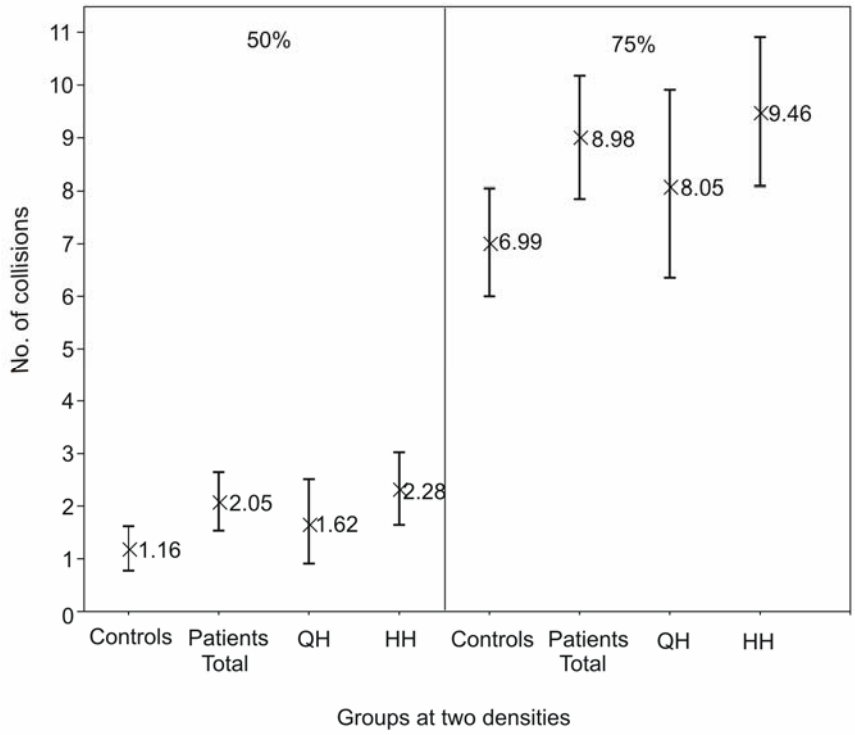

Figure 5. Hölder mean number of collisions in controls, in the total patient group ("patients total"), in patients with homonymous quadrantanopia (QH) and patients with homonymous hemianopia (HH) together with 95% confidence intervals. The means were estimated by a multifactorial analysis of variance with the fixed factors "group" (three levels) and "density" (two levels) and the random factor "individual", nested under the factor "group." The interaction between the two fixed factors was not significant ($p = 0.4546$) and was therefore ignored in the final model.

3.3 Area of sparing and side of collision

In order to identify factors that might affect performance of patients, the effect of A-SPAR, age, gender, and density on the number of collisions was investigated by means of fitting an analysis of covariance model stepwise by starting with the full model, setting the critical p-values at 5%, and eliminating all non-significant factors and their interactions. In order to stabilize the variances we took the square roots of the number of collisions. For Poisson distributed variables this results in a constant standard deviation of 0.5. The observed root mean square error was 0.54, which agrees well with the expected value. The final result of this stepwise procedure yielded a simple model, which contained all four main effects but without their interactions.

The effect of A-SPAR (area of sparing within the affected hemifield) on collision rate is presented in Figure 6 as scatterplot of the number of collisions by A-SPAR. There are large individual differences within our sample. It is noteworthy, that there are patients with almost identical A-SPAR but considerably different collision rates. Furthermore, there are also some patients with even low A-SPAR, who exhibit similar performance with that of normal-sighted control subjects.

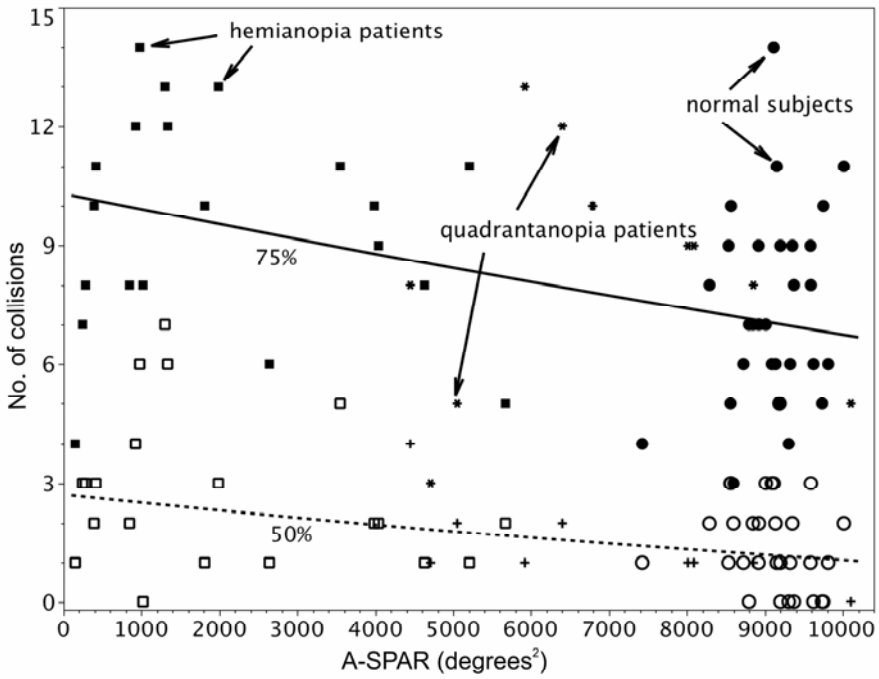

Figure 6. Number of collisions by area of sparing within the affected hemifield (A-SPAR in degrees^2), data and regression curves for both traffic densities. The dots are labeled according to type and density. For 50% densities all labels are open and for 75% density they are filled. Normal subjects are shown by circles, hemianopia patients by squares and quadrantanopia patients by stars for 75% density vs. crosses for 50% density. Because the intercepts differ for the two densities, the slopes of the linear component of the two curves are different though for the square roots the slopes are identical: -0.6/10000 A-SPAR (95% CI -0.9 to -0.3/10000 A-SPAR).

Table 3 summarizes all results with respect to the side of the HVFD. The table contains the collision rates (number of collisions divided by the number of patients at risk) together with their exact 95% CI based on the Poisson distribution (The data from four participants with respect to the side of collision were not available). In order

to compare rates of different groups we applied a likelihood ratio test based on a Poisson model (Gu et al., 2008). For comparisons of two hemifields within the same group we used the exact sign test.

Number of group	Traffic density	Participant group	Side of HVFD	Side of collision	Number of participants	Sum of collisions	Rate	Lower 95% CL	Upper 95% CL	Test	p-value
1	50%	Patients	Left	same	14	22	1.57	0.98	2.38	3 with 6	0.314
2		Patients	Left	opposite	14	23	1.64	1.04	2.47	2 with 6	0.020
3		Patients	Right	same	15	17	1.13	0.66	1.81	1 with 5	0.002
4		Patients	Right	opposite	15	16	1.07	0.61	1.73	4 with 5	0.073
5		Controls	-	left	27	15	0.56	0.31	0.92	9 with 12	0.002
6		Controls	-	right	27	22	0.81	0.51	1.23	8 with 12	0.145
7	75%	Patients	Left	same	14	83	5.93	4.72	7.35	7 with 11	0.031
8		Patients	Left	opposite	14	57	4.07	3.08	5.28	10 with 11	0.071
9		Patients	Right	same	15	76	5.07	3.99	6.34	1+3 with 2+4	1.000
10		Patients	Right	opposite	15	48	3.20	2.36	4.24	7+9 with 8+10	0.001
11		Controls	-	left	27	117	4.33	3.58	5.19	5 with 6	0.320
12		Controls	-	right	27	84	3.11	2.48	3.85	11 with 12	0.024

Table 3: Summary of results with respect to the side of the HVFD.

3.4 Age and gender

The effect of age and gender on the total number of collisions is exhibited in Fig. 7. The data were modeled by square root transformed numbers of collisions. Backward stepwise regression analysis with fixed factors group (patient or normal), density (50% or 75%), gender and age, revealed non-significant interaction terms between them. All the main effects were significant: The number of collisions increases quadratically with age. The age effect is highly significant ($p = 0.0001$). The effects of group ($p=0.0007$) and density ($p<0.0001$) are discussed in Section 3.2. The gender effect is marginally significant ($p=0.0456$). The age effect is not influenced by the other main factors (group, density and gender).

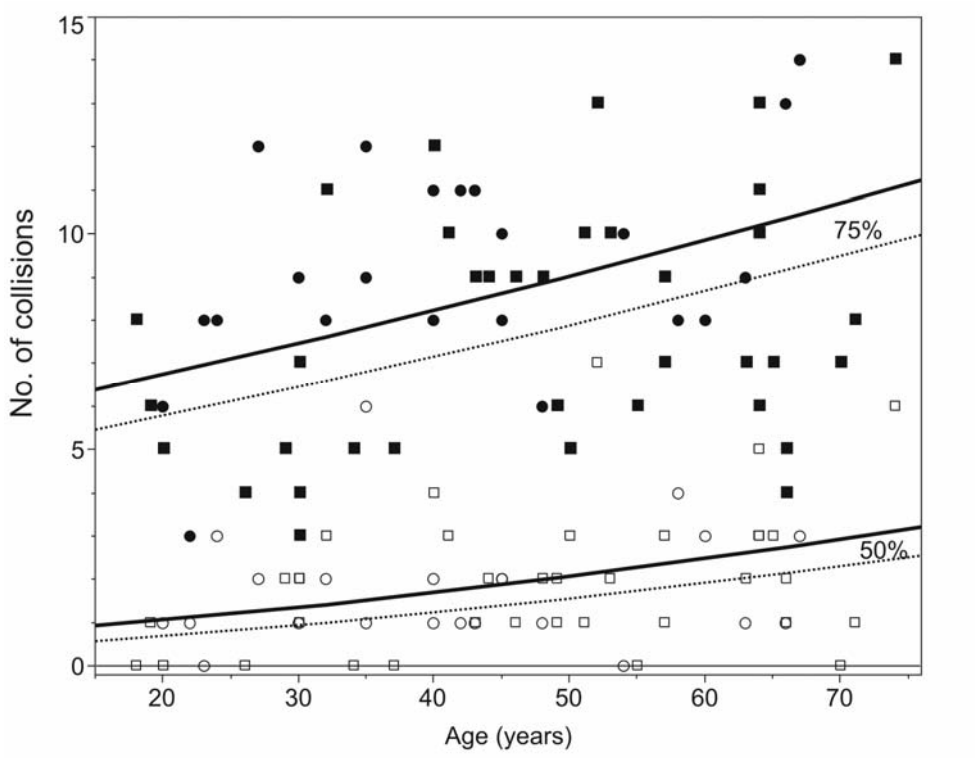

Figure 7. The effect of age and gender on the number of collisions by traffic density in the total study population. Open markers refer to 50% density and closed markers to 75% density. Females are denoted by a circle and males by a square. The continuous theoretical curves refer to females and the dashed lines to males. The number of collisions increases quadratically with age and is not influenced by gender, density and group.

3.5 Brain lesion and macular sparing

Patients were divided into two subgroups by the median of their performance in both density levels using the median split method (Cohen, 2003): "performance above average" and "performance below average". Above average patients were compared with below average patients regarding the time span since brain lesion, side of brain lesion and macular sparing (t-test and Fisher's exact test for log transformed continuous and dichotomous variables, respectively). None of these parameters was significantly different between the two patient subgroups. Data regarding the effect of brain lesion site on collision avoidance are reported elsewhere (Papageorgiou et al., submitted).

3.6 Learning effect

Performance of participants over time was investigated, in order to find out if participants decrease their collision rate over time. A learning effect was revealed for both patients and control subjects only in density 75%. The learning effect is exhibited in Fig. 8. The learning effect was not influenced by age and gender (Data not shown).

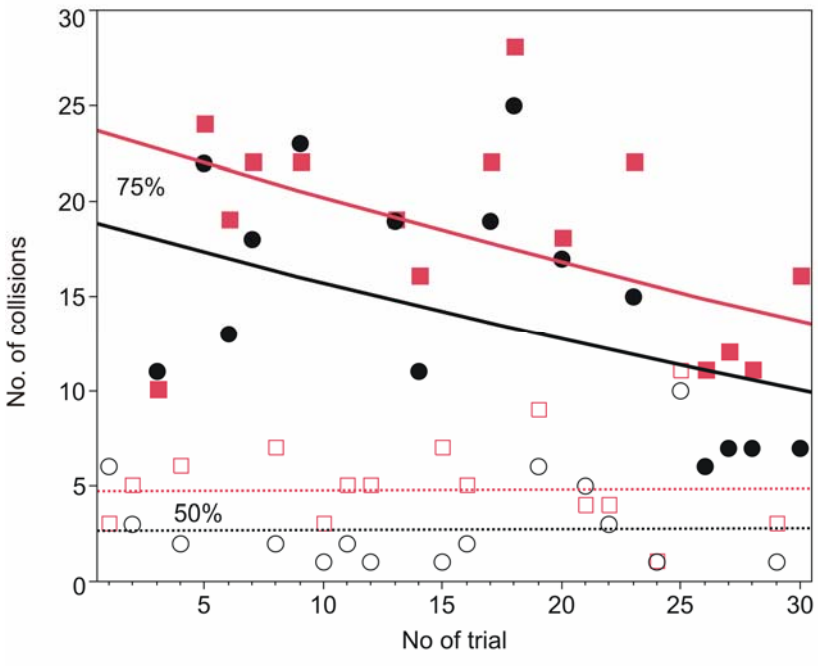

Figure 8. A learning effect could only be seen at density 75% for patients and control subjects alike. The data were modeled by square root transformed numbers of collisions. The red squares correspond to patients and the black circles refer to control subjects. The markers are open for density 50% and closed for density 75%.

4. Discussion

The goal of this study was twofold. First, it was designed to examine differences in performance between patients with HVFDs and normal-sighted control subjects in a collision avoidance task with moving obstacles. Second, it was designed to investigate the impact of the extent of the HVFD on collision avoidance, with the hypothesis that performance would not be solely explained by visual field-related parameters. Therefore we expected contribution of additional factors, e.g. age, gender, presence of macular sparing, side of brain lesion and time span since lesion onset. We have tried to eliminate potential problems encountered previously by using standardized, repeatable VR conditions and by examining a large homogenous patient group (regarding cause of HVFD) in comparison to an age-matched control group.

4.1 Effect of HVFD

As hypothesized, subjects with HVFDs experienced more collisions with vehicles approaching from the blind side than the seeing side and had on average more collisions than subjects with normal vision. These results suggest that patients with HVFDs are less efficient and experience difficulties in collision avoidance under VR conditions. This finding was more obvious when we increased the density of the cross traffic (i.e. 75% density) and therefore the visual and cognitive demands of the task. Our results are partly in accordance with a recent study of Bowers et al. (2009). They examined the effect of HH on detection of pedestrian figures within the controlled environment of a driving simulator. They concluded that detection rates of HH drivers for pedestrians on the blind side were significantly lower than detection rates for pedestrians on the seeing side and were significantly lower than those of drivers with normal vision. However, the experimental task in the study of Bowers et al. (2009) included detection of stationary pedestrians. Therefore the authors assumed that this may have resulted in lower detection rates than if the detection 'target' had been a moving car. In the present study, moving vehicles at an intersection were used in order to achieve more realistic circumstances in terms of collision avoidance. For this reason probably performance differences between patients and normal-sighted subjects were not as large in our sample as in the study of Bowers et al. (2009). Therefore, our results suggest that patients with HVFDs may achieve better ratings on collision avoidance tasks with moving obstacles than on detection of stationary targets at intersections. This may be related to the Riddoch phenomenon of statokinetic dissociation, whereby patients perceive moving but not static objects (Schiller et al., 2006). Statokinetic dissociation is often noted in recovering occipital lesions and has been commonly attributed to preserved islands of function within the occipital cortex. Variable degrees of dissociation of perception between moving and nonmoving stimuli have been also demonstrated in normal subjects and in patients with compression of the anterior visual pathways (Safran & Glaser, 1980). An additional explanation is provided by the division of the retino-cortical projection in two parallel pathways, the parvo- and the magno-cellular system (Nassi & Callaway, 2009). Magno-cellular neurons predominate in retinal periphery and are believed to mediate fast flicker and motion detection (Merigan & Maunsell, 1990; Merigan et al., 1991). Therefore, peripheral vision is much more sensitive to flicker perception than foveal

vision, and this phenomenon might underlie our findings as well (Schiller et al., 1990; Chapman et al., 2004).

However, our findings cannot be directly contrasted to the results of Bowers et al. (2009), because the task requirements and the expected responses are different. In the study of Bowers et al. (2009) the subjects had to indicate detection of pedestrians by honking the car horn without any time constraints (i.e. even after they completed a turn at an intersection), while steering the virtual vehicle, operating all vehicle controls and interacting with other traffic. We rather investigated subjects' ability to detect moving obstacles and avoid a collision with them in a strictly timely manner. Estimates of collision avoidance involve primarily perception of time-to-contact (Lee, 1976), i.e. the amount of time before a perceived object would reach the observer, the ability to detect the potential collision object and switch attention towards it, the ability to determine an appropriate avoidance response, and the ability to actually control the vehicle to avoid the collision under continuous demand on working memory (Horrey et al., 2007; Olson, 2002). Therefore, we did not offer the possibility of bringing the vehicle to a halt at the intersection. At most intersections without traffic lights, drivers would normally have to obey either a yield or a stop sign, which means that they would slow down on approach to the intersection and make a gap judgment either as they were slowing down (yield sign) or from a stationary position (stop sign). They would then choose an appropriate speed and time point at which to go through the intersection. While the inability to stop the vehicle might be a limitation in the study design, it was adopted in order to investigate how subjects perform in time-constrained collision avoidance situations and to quantify performance as the number of collisions by eliciting a "forced choice response."

One might argue about the choice of collisions as indicator/measure of performance, because collisions are relatively rare events in real-world situations; however, intersections are challenging even for normal subjects (Bowers et al., 2009) and the available period to react, namely to perceive the size of the gap in terms of time to act (Simpson et al., 2003), is not always unlimited even in real world. In 2007, at least 22% of fatal accidents in the USA occurred at intersections (Fatality Analysis Reporting System Encyclopedia, 2007). Injury accidents at intersections account for 41,2 % in Germany, which is quite close to the European median (43%), and 50,1 % in the UK. This is due mainly to the fact that accident scenarios at intersections are

among the most complex ones, since different categories of road users interact in these limited areas with crossing trajectories (Cooperative Intersection Safety, 2009)

4.2 Effect of the area of sparing (A-SPAR)

The presence and extent of the HVFD, as expressed by a lower area of sparing in the affected hemifield (A-SPAR), is associated with worse performance in the present collision avoidance task. This is additionally illustrated by the finding that patients with hemianopia displayed worse performance than those with quadrantanopia (Fig. 5). However, the relationship between A-SPAR and the number of collisions is extremely weak, as shown by the slope of the regression curve for the square roots (Fig. 6): -0.6/10000. Therefore, we suggest that perimetric findings per se seem to be inadequate in predicting collision avoidance of patients with HVFDs under VR-conditions. Few studies have assessed the impact of the extent of the HVFD on performance by using different performance measures and study designs. Hence, comparing our results with previous findings may only provide indicative data. Racette et al. (2005) reviewed the occupational therapists' assessments of 131 patients with visual field loss, who had undergone an on-road driving test, including 20 patients with HVFDs. They concluded that hemianopia tended to have a worse impact on driving performance than quadrantanopia, and quadrantanopic drivers obtained no "unsafe" driving outcomes. We also found that patients with quadrantanopia did not differ in their performance from normal-sighted subjects (Fig. 5). Furthermore, in the present study 23 out of 30 patients with HVFDs (76,7%) performed within the range of normal subjects in both difficulty levels (Fig. 4), if the outlier normal subject with excessively high collision rates is excluded. These findings are consistent with a recent on-road study (Wood et al., 2009). Although the authors found significant differences in the Esterman binocular field test (% seen) and the mean sensitivity in the Humphrey 24-2 field test (dB) between safe and unsafe drivers, 88% of quadrantanopic patients against 73% of patients with HVFDs received safe ratings (Wood et al., 2009). On the other hand, our results appear to be at odds with the on-road study of Tant et al. (2002), who found that only 14% of patients with HVFDs received safe ratings. However, in this study only patients whose driving was suspected to be unsafe by the caregiver or the patients themselves were recruited. Similarly, in the study of Kooijman et al. (2004), where only four out of 28 patients with HVFDs passed the practical fitness to drive test, subjects were referred having a

question related to their fitness to drive. Finally, the discrepancy observed between our study and the studies of Bowers et al. (2009) and Lövsund et al. (1991), where only a low percentage of patients received safe ratings, is probably explained by the fact that these authors used static stimuli. Our findings also seem to be inconsistent with a previous study suggesting no differences in driving performance between HH and normal-sighted drivers (Schulte et al., 1999). Except for the small patient sample in this study (n=6), it seems likely that the experimental task was less demanding than the present one. It could be that HH patients should not scan so much due to the restricted field of view (16^{o}x21^{o}) offered by a 28-inch monitor or that study included insufficient unexpected events (e.g. the appearance of a single deer in 3 minutes of test driving).

4.3 Variability among patients with HVFDs and among various studies

The predictive power of A-SPAR is additionally limited by the fact that large individual variability occurs and performance of some patients was similar to that of normal subjects (Fig. 6). A high degree of between-subject variability in patients with HVFDs in VR or on-road driving tasks has been reported in other studies as well, and may reflect aging processes (see Section 4.4), individual compensation capacity and working memory availability (see Section 4.6, Hardiess et al., 2010; Bowers et al., 2009; Lövsund et al., 1991; Racette et al., 2005; Wood et al., 2009). These large individual differences demand a thorough observation of the clinical data in addition to the descriptive statistics and may partly interfere with the variety of results obtained in several studies.

Possible factors that may account for the great variability in the performance of patients with HVFDs among studies are the differences in the experimental setup (naturalistic tasks, virtual reality or on-road driving assessments) and the performance measures, the presence of a normal-sighted control group, the sample sizes and the inclusion criteria of subjects, i.e. time after lesion onset, presence of hemi-neglect. Szlyk et al. (1993) reported significantly worse performance on an interactive driving simulator for six patients with HVFDs after brain damage compared to visually intact subjects. However, three of the patients were additionally diagnosed as having hemi-spatial neglect and the examination was performed two months after their stroke, so the recovery process was probably still active. The reason for participation in the study should also be considered. For example, Wood et al. (2009) included patients

who had a driving license and were current drivers or wished to return to driving. The results of the interstate drive in the same study did not include patients who preferred not to drive on the interstate or were deemed unsafe (Wood et al., 2009). Our subject group was relatively large and free of selection bias, since there were no safety concerns and our study did not include a driving test, but rather an assessment of performance in a cognitively challenging task under repeatable VR conditions. The observed variability obviates the need for development of a standardized procedure, in order to provide objective measures of functional performance (Bowers et al., 2008). Such a quantitative approach would also enhance the evaluation of peripheral enhancement devices and improve the efficacy of rehabilitation training programs (Szlyk et al., 2005).

4.4 Age effect

Increasing age in the present collision avoidance task was associated wih worse performance. Previous studies have reported deterioration in simulated tasks or on-road assessments with increasing age (Lövsund et al., 1991; Szlyk et al., 1993; Wood, 2002). However, there is little work investigating how age affects performance in time-constrained collision-avoidance situations. Bowers et al. (2009) found that older HH drivers had lower pedestrian detection rates than younger HH drivers, indicating a reduction in the ability to compensate for the field loss with increasing age. Szlyk et al. (1993) also suggested that age-related losses, when compounded by stroke-associated impairments, significantly influenced visuo-spatial driving-related skills. A recent study suggested that collision avoidance situations are increasingly difficult with advancing age and older adults are less efficient at perceiving an affordable gap when spatiotemporal relations are of importance (Lobjois et al., 2007). Our findings confirm these results and extend the age effect in collision avoidance tasks for patients with HVFDs as well. Interestingly, there was no interaction of age and the presence of HVFDs, thus indicating a similar (highly significant) age effect in both patients and normal-sighted subjects. Age-related changes, like a decline in cognitive abilities, a slowing down of information processing or even a deterioration of exploration ability, may probably affect object detection and subsequent reaction ability in such interactive scenarios (Ryan et al., 1998).

4.5 Learning effect

An improvement in performance over time, which was identical for both patients and normal-sighted control subjects, could be demonstrated in the more challenging task of higher traffic density. Usually, performance over time in patients with HVFDs is studied before and after training interventions, such as saccadic visual search training, in order to investigate the ability of patients to develop compensatory abilities (Kerkhoff, 2000; Pambakian et al., 2004). However, the similar learning curves in our study suggest that patients' performance improvement over time should rather be attributed to task learning – as in the normal subjects – than to compensatory behavior. Additionally, the duration of the experiment was relatively short for the development of compensatory mechanisms.

4.6 Brain lesion

Consistent with previous findings (Bowers et al., 2009), we did not find any differences in the time span since the brain lesion between patients with "performance above average" and "performance below average". The reason is probably that our patient group was homogenous regarding cause of the brain lesion and the time span after lesion onset was at least six months. Recent studies suggest that six months postinjury is the time span, after which spontaneous recovery of visual field is unusual in vascular lesions and patients have adapted a different compensatory eye movement strategy (Pambakian et al., 2004; Zhang et al., 2006).

Concerning the side of the brain damage, one might expect that patients with right-hemispheric lesions would perform worse, presumably because of a higher incidence of visuo-spatial deficits like neglect (Korner-Bitensky et al., 2000; Meerwaldt & Harskamp, 1982). However, no differences in performance were revealed between patients with left- and right-hemispheric lesions in agreement with earlier studies (Bowers et al., 2009, Szlyk et al., 1993, Wood et al., 2009, Zihl, 1995). This may be due to the fact that patients with clinical evidence of neglect or signs of impaired lateralized attention in the paper-and-pencil tests were excluded from the present study. As suggested recently (Bowers et al., 2009), this possibly indicates that the tests used (horizontal line bisection, copying of figures and the "Bells test") are sufficient to detect neglect symptoms. Another possible explanation is that both hemispheres play equivalent roles in the spatial guidance of visual searching (Ratcliff & Newcombe, 1973; Zihl, 1995). A reason accounting for the unexpected – though statistically non-significant – finding of higher collision rates to the left side in normal

subjects might be the right of way for vehicles approaching from the right side at an intersection.

4.7 Macular sparing

In conjunction with earlier studies (Kooijman et al., 2004; Wood et al., 2009) the presence of macular sparing was not different between patients with "performance above average" and "performance below average". Although macular sparing of at least 2^{o} to either side is a prerequisite for fluent reading (Schiefer et al., 2007), it is less obvious how it could be so important for driving (Tant et al., 2002). In contrast, Tant et al. (2002) found a positive correlation between macular sparing and visual performance during driving. He suggested that macular sparing could be associated with the ease of identification of individual objects, and hence with the creation of a spatial representation during driving. While we have not found contribution of sparing to performance on our task, we agree that studies should attempt to measure the saccadic amplitude into the blind field, in order to detect if such saccades are under the direction of immediate visual input (Martin et al., 2007).

5. Conclusion

Our results for patients with HVFDs seem to extend the findings of a recent study on impaired detection of stationary objects (Bowers et al., 2009), to impaired collision avoidance of moving obstacles at intersections as well. However, the extent of HVFDs is weakly associated with performance in the present collision avoidance task under VR conditions. Performance of some patients is similar to that of normal subjects, which may be probably attributed to the development of compensatory viewing behavior (Hardiess et al., 2010). Due to this wide between-subject variability, generalization of the findings regarding the impact of HVFDs is misleading and individualized approaches of compensatory functional behavior of patients with HVFDs are necessary. In future studies we will attempt to find predictors of visual compensation in realistic tasks and measure not only the extent of the visual field defect, but also the extent to which impaired individuals adopt compensatory viewing strategies. Assessment of visual exploration (head and eye movements), functioning in everyday life and multimodal approaches (performance in different tasks) may play an important role in determining the visual capacities of patients with homonymous field loss (Hardiess et al., 2010).

Acknowledgements

The authors are thankful to Mrs. Simone Bahlo (Bad Urach Rehabilitation Centre) for assisting with the recruitment of patients.

Grants: This work was supported by the following grants: European Union (PERACT-Marie Curie Early Stage Research Training, MEST-CT-2004-504321), Deutsche Forschungsgemeinschaft (SFB 550-A4), GRK 778.

Disclosure: Ulrich Schiefer is consultant of HAAG-STREIT, Inc., Koeniz, Switzerland, he holds patents, related to the semi-automated kinetic perimetry.

References

Bowers, A. R., Keeney, K., & Peli, E. (2008). Community-based trial of a peripheral prism visual field expansion device for hemianopia. *Archives of Ophthalmology*, 126(5), 657-664.

Bowers, A. R., Mandel, A. J., Goldstein, R. B., & Peli, E. (2009). Driving with hemianopia: 1. Detection performance in a driving simulator. *Investigative Ophthalmology and Visual Science*, 50(11), 5137-5147.

Bowers, A. R., Mandel, A. J, Goldstein, R. B., & Peli, E. (2010). Driving with hemianopia, II: lane position and steering in a driving simulator. *Investigative Ophthalmology and Visual Science*, 51(12), 6605-6613

Chapman, C., Hoag, R., & Giaschi, D. (2004). The effect of disrupting the human magnocellular pathway on global motion perception. *Vision Research*, 44(22), 2551-2557.

Cohen, J. (2003). *Applied Multiple Regression/Correlation Analysis for the Behavioral Sciences (3 rd ed.).* Routledge: Lawrence Erlbaum Associates.

Cooperative Intersection Safety, 2009. User needs and operational requirements for a cooperative intersection safety system. Deliverable D3.1 – European Commission.

Retrieved 12 Dec, 2010, from http://www.intersafe-2.eu/public/public-documents/deliverables/d3_1_intersafe-2_user_needs_and_requirements_v1-05-final.pdf

Fatality Analysis Reporting System Encyclopedia, 2007. Fatal crashes by relation to junction and traffic control device - USA. Retrieved 03 Mar, 2009, from http://wwwfars.nhtsa.dot.gov/Crashes/CrashesLocation.aspx

Gall, C., Lucklum, J., Sabel, B. A., & Franke, G. H (2009). Vision- and health-related quality of life in patients with visual field loss after postchiasmatic lesions. *Investigative Ophthalmology and Visual Science,* 50(6), 2765-2776.

Gauthier, L., Dehaut, F., & Joannette Y. (1989). The bells test: A quantitative and qualitative test for visual neglect. *International Journal of Clinical Neuropsychology*, 11, 49-54.

Gu, K., Ng, H. K. T., Tang, M. L., & Schucany WR. (2008). Testing the ratio of two Poisson rates. Biometrical Journal, 50 (2), 283-298

Hardiess, G., Papageorgiou, E., Schiefer, U., Mallot, H. A. (2010). Functional compensation of visual field deficits under the influence of different task demands. *Vision Research*, 50(12), 1158-72.

Horrey, W. J., Simons, D. J., Lleras, A., & Scott, D. L. (2007). Estimates of crash avoidance: Discrepancies between drivers' judgments and actual performance. *Human Factors Division, Institute of Aviation.* Technical Report HFD-07-01.

Johnson, C. A., & Keltner, J. L. (1983). Incidence of visual field loss in 20.000 eyes and its relationship to driving performance. *Archives of Ophthalmology*, 101(3), 371-375.

Kerkhoff G (2000). Neurovisual rehabilitation: recent developments and future directions. *Journal of Neurology Neurosurgery and Psychiatry*, 68(6):691-706.

Kline, L. B. (2008). Visual fields. In L. B. Kline (Ed.). *Neuro-Ophthalmology Review Manual (pp.* 1–44). Thorofare, NJ: Slack Inc.

Kooijman, A. C., Brouwer, W. H., Coeckelbergh, T. R. M., Tant, M., Cornelissen, F., Bredewoud, R., et al. (2004). Compensatory viewing training improves practical fitness to drive of subjects with impaired vision. *Visual Impairment Research*, 6(1), 1-27.

Korner-Bitensky, N. A., Mazer, B. L., Sofer, S., Gelina, I., Meyer, M. B., Morrison, C., et al. (2000). Visual testing for readiness to drive after stroke: a multicenter study. *American journal of physical medicine & rehabilitation,*79(3), 253-259.

Lee, D. N. (1976). A theory of visual control of braking based on information about time-to-collision. *Perception*, 5(4), 437-459.

Lobjois, R., Benguigui, N., Bertsch, J., & Broderick, M. P. (2008). Collision avoidance behavior as a function of aging and tennis playing. *Experimental Brain Research*, 184(4), 457-468.

Lövsund, P., Hedin, A., & Törnros, J. (1991). Effects on driving performance of visual field defects: a driving simulator study. *Accident; analysis and Prevention,* 23(4), 331-342.

Mandel, A. J., Bowers, A. R., Goldstein, R. B., & Peli, E. (2007). Analysis of driving behavior where it matters. *Driving Simulation Conference 2007*, North America, Iowa City.

Martin, T., Riley, M. E., Kelly, K. N., Hayhoe, M., & Huxlin, K. R. (2007). Visually-guided behavior of homonymous hemianopes in a naturalistic task. *Vision Research,* 47(28), 3434-3446.

Matsumiya, K., & Kaneko, H. (2008). Judgment in Crossing a Road between Objects Coming in the Opposite Lane. *Optical Review*, 15(3), 133-135.

Meerwaldt, J. D., & Van Harskamp, F. (1982). Spatial disorientation in right-hemisphere infarction. *Journal of Neurology Neurosurgery and Psychiatry,* 45(7), 586-590.

Merigan, W. H., & Maunsell, J. H. (1990) Macaque vision after magnocellular lateral geniculate lesions. *Visual Neuroscience*, 5(4), 347-352.

Merigan, W. H., Byrne, C. E., & Maunsell, J. H. (1991). Does primate motion perception depend on the magnocellular pathway? *The Journal of Neuroscience*, 11(11), 3422-3429.

Nassi, J. J., & Callaway, E. M. (2009). Parallel processing strategies of the primate visual system. *Nature Reviews. Neuroscience*, 10(5), 360-372.

Oh, S., & Kim, M. (2004). The role of spatial working memory in visual search efficiency. *Psychonomic Bulletin and Review*, 11(2), 275–281.

Olson, P. (2002). Driver perception-response time. In R.E. Dewar & P.L. Olson (Eds.). *Human Factors in Traffic Safety* (pp. 43-76). Tucson, AZ: Lawyers & Judges.

Pambakian, A. L., Wooding, D. S., Patel, N., Morland, A., Kennard, C., & Mannan, S. (2000). Scanning the visual world: a study of patients with homonymous hemianopia. *Journal of Neurology Neurosurgery and Psychiatry,* 69(6), 751-759.

Pambakian, A. L., Mannan, S. K., Hodgson, T. L., & Kennard, C. (2004). Saccadic visual search training: a treatment for patients with homonymous hemianopia. *Journal of Neurology Neurosurgery and Psychiatry,* 75(10), 1443-1448.

Papageorgiou, E., Hardiess, G., Schaeffel, F., Wiethoelter, H., Karnath, H. O., Mallot, H., et al. (2007). Assessment of vision-related quality of life in patients with homonymous visual field defects. *Graefe's Archive for Clinical and Experimental Ophthalmology*, 245(12), 1749-1758.

Papageorgiou, E., Hardiess, G., Wiethoelter, H., Ackermann, H., Dietz, K., Mallot., H., et al. (2011). The neural correlates of impaired collision avoidance in hemianopic patients. *Acta Ophthalmologica,* submitted.

Racette, L., & Casson, E. J. (2005). The impact of visual field loss on driving performance: evidence from on-road driving assessments. *Optometry and Vision Science,* 82(8), 668-674.

Ratcliff, G., & Newcombe, F. (1973). Spatial orientation in man: effects of left, right, and bilateral posterior cerebral lesions. *Journal of Neurology Neurosurgery and Psychiatry,* 36(3), 448-454.

Ryan, G. A., Legge, M., & Rosman, D. (1998). Age related changes in drivers' crash risk and crash type. *Accident; Analysis and Prevention,* 30(3), 379-387.

Safran, A. B., & Glaser, J. S. (1980). Statokinetic dissociation in lesions of the anterior visual pathways. A reappraisal of the Riddoch phenomenon. *Archives of Ophthalmology*, 98(2), 291-295.

Schiefer, U., Hofer, R., Vischer, P. M., & Wilhelm, H. (2000). Perimetry findings and driving performance: "How much visual field" does a motorist need? *Der Ophthalmologe,* 97(7), 491-497.

Schiefer, U., Wilhelm, H., & Hart, W. (2007). *Clinical Neuro-Ophthalmology*. Berlin, Heidelberg, New York: Springer.

Schiff, W., & Detwiler, M. L. (1979). Information used in judging impending collision. *Perception*, 8(6), 647-658.

Schiff, W., & Oldak, R. (1990). Accuracy of judging time to arrival: effects of modality, trajectory, and gender. *Journal of Experimental Psychology. Human Perception and Performance*, 16(2), 303-316.

Schiller, P. H., Logothetis, N. K., & Charles, E. R. (1990). Role of the color-opponent and broad-band channels in vision. *Visual Neuroscience*, 5(4), 321-346.

Schiller, J., Paetzold, J., Vonthein, R., Hart, W. M., Kurtenbach, A., & Schiefer, U. (2006). Quantification of stato-kinetic dissociation by semi-automated perimetry. *Vision Research,* 46(1-2), 117–128.

Schulte, T., Strasburger, H., Muller-Oehring, E. M., Kasten, E., & Sabel, B. (1999). Automobile driving performance of brain-injured patients with visual field defects. *American journal of physical medicine & rehabilitation*, 78(2), 136-142.

Simpson, G., Johnston, L., & Richardson, M. (2003). An investigation of road crossing in a virtual environment. *Accident; Analysis and Prevention,* 35(5), 787–796.

Soto, D., & Humphreys, G. W. (2008). Stressing the mind: The effect of cognitive load and articulatory suppression on attentional guidance from working memory. *Attention, Perception & Psychophysics*, 70(5), 924–934.

Szlyk, J. P., Brigell, M., & Seiple, W. (1993). Effects of age and hemianopic visual field loss on driving. *Optometry and Vision Science,* 70(12), 1031-1037.

Szlyk, J. P., Seiple, W., Stelmack, J., & McMahon, T. (2005). Use of prisms for navigation and driving in hemianopic patients. *Ophthalmic & Physiological Optics*, 25(2), 128-135.

Tant, M. L. M., Brouwer, W. H., Cornelissen, F. W., & Kooijman, A. C. (2002). Driving and visuospatial performance in people with hemianopia. *Neuropsychological rehabilitation*, 12(5), 419-437.

Taylor, J. F. (1982). Vision and driving. *Practitioner,* 226(1367), 885-889.

Trauzettel-Klosinski, S., & Reinhard, J. (1998). The vertical field border in hemianopia and its significance for fixation and reading. *Investigative Ophthalmology and Visual Science,* 39(11), 2177–2186.

Voyer, D., Voyer, S., & Bryden, M. P. (1995). Magnitude of sex differences in spatial abilities: a meta-analysis and consideration of critical variables. *Psychological Bulletin*, 117, 250–270.

Wolf, C. C., Ocklenburg, S., Oren, B., Becker, C., Hofstätter, A., Bös, C., et al. (2010). Sex differences in parking are affected by biological and social factors. *Psychological Research*, 74(4), 429-435.

Wood, J. M. (2002). Age and visual impairment decrease driving performance as measured on a closed-road circuit. *Human Factors*, 44(3), 482-494.

Wood, J. M., McGwin, G. Jr., Elgin, J., Vaphiades, M. S., Braswell, R. A., DeCarlo, D. K., et al. (2009). On-road driving performance by persons with hemianopia and quadrantanopia. *Investigative Ophthalmology and Visual Science,* 50(2), 577-585.

Wood, J. M., McGwin, G. Jr., Elgin, J., Vaphiades, M. S., Braswell, R. A., Decarlo, D. K., et al. (2011) Hemianopic and quadrantanopic field loss, eye and head movements, and driving. *Investigative Ophthalmology and Visual Science,* 52(3), 1220-1225.

Zhang, X., Kedar, S., Lynn, M. J., Newman, N. J., & Biousse, V. (2006). Natural history of homonymous hemianopia. *Neurology,* 66(6), 901-905.

Zihl, J. (1995). Visual scanning behavior in patients with homonymous hemianopia. *Neuropsychologia*, 33(3), 287-303.

Zihl, J. (2000). *Rehabilitation of visual disorders after brain injury*. Hove, UK: Psychology Press.

Zihl, J (2003). Recovery and rehabilitation of cerebral visual disorders. In M. Fahle & M. W. Greenlee (Eds). *The neuropsychology of vision* (pp. 319-338). Oxford: Oxford University Press.

Appendix 1: Demographic characteristics of the patient group. Patient identification (Pat-ID), gender, age at time of examination (Age), time span between brain lesion and neuro-ophthalmological examination (Δt), pathogenesis of brain lesion, site and extent of lesion, side of brain lesion (R=right, L=left), type of homonymous visual field defect (HVFD), A-SPAR (area of sparing within the affected hemifield in degrees^2), visual field classification, No. of collisions (as absolute number in 50% and 75% density).

Appendix: Demographic characteristics of the patient group

Patient identification (Pat-ID), gender, age at time of examination (Age), time span between brain lesion and neuro-ophthalmological examination (Δt), pathogenesis of brain lesion, site and extent of lesion, side of brain lesion (R=right, L=left), type of homonymous visual field defect (HVFD), A-SPAR (area of sparing within the affected hemifield in degrees^2), visual field classification, No. of collisions (as absolute number in 50% and 75% density).

Pat-ID	Gender Age [yrs.]	Δt [yrs.]	Pathogenesis Site / Extent of lesion Side of brain lesion	HVFD (90 ° eccentricity, both eyes)	A-SPAR [degrees^2]	Visual field classification	No. of collisions 50%	No. of collisions 75%
01	w 35	11.2	Ischemia occipital, PCA L	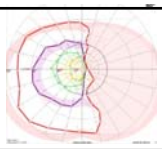	1335	Right complete hom. hemianopia with macular sparing	6	12
02	m 32	3.5	Brain surgery (AV malformation) parieto-occipital, MCA & PCA R	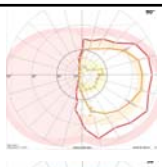	414	Left complete hom. hemianopia without macular sparing	3	11
03	m 51	3.5	Ischemia parieto-temporo-occipital R	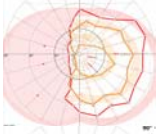	1301.1	Left incomplete hom. hemianopia with macular sparing	7	13
04	m 70	1	Ischemia occipital, PCA L	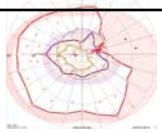	4632	Right incomplete hom. hemianopia with macular sparing	1	8
05	w 21	3.9	Ischemia parieto-occipital, MCA L	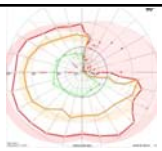	4710.7	Right complete hom. superior quadrantanopia without macular sparing	1	3
06	m 66	1	Ischemia temporo-occipital, PCA & MCA R	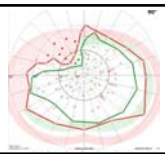	5052.3	Left incomplete hom. superior quadrantanopia with macular sparing	2	5
07	m 48	1	Ischemia occipital L	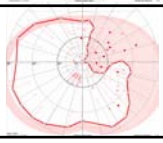	4041.7	Right incomplete hom. hemianopia without macular sparing	2	9
08	w 65	9.9	Hemorrhage (Aneurysm) occipital, PCA & MCA R	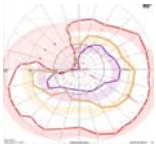	5920.6	Left complete hom. superior quadrantanopia with macular sparing	1	13
09	w 58	2.5	Hemorrhage temporo-occipital, MCA R		4450.2	Left complete hom. superior quadrantanopia without macular sparing	4	8
10	m 64	0.5	Ischemia occipital, PCA L	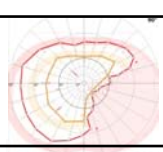	1986.6	Right incomplete hom. hemianopia with macular sparing	3	13
11	m 57	7	Ischemia occipital, PCA L	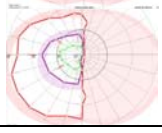	243.1	Right complete hom. hemianopia without macular sparing	3	7

12	w 40	2.7	Ischemia occipital, PCA L	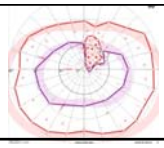	8853.2	Right incomplete hom. superior quadrantanopia without macular sparing	1	8
13	m 37	0.5	Ischemia occipital, PCA L		10105	Right incomplete hom. inferior quadrantanopia with macular sparing	0	5
14	m 64	1.6	Ischemia occipital, PCA R		3549.7	Left incomplete hom. hemianopia with macular sparing	5	11
15	m 51	0.7	Ischemia parieto-temporo-occipital, R	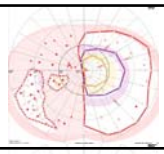	1810.3	Left incomplete hom. hemianopia without macular sparing	1	10
16	m 29	1.8	Ischemia occipital, PCA R		5671.3	Left incomplete hom. hemianopia with macular sparing	2	5
17	w 27	0.8	Ischemia occipital, PCA R	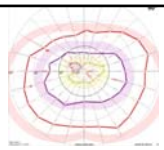	6401.8	Left incomplete hom. superior quadrantanopia with macular sparing	2	12
18	m 46	1	Ischemia temporo-occipital, PCA L	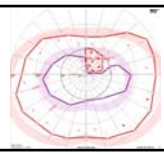	8090.4	Right incomplete hom. superior quadrantanopia with macular sparing	1	9
19	m 30	1.6	Hemorrhage (Aneurysm) parietal, MCA L	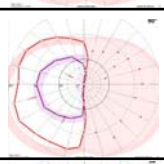	149.4	Right complete hom. hemianopia without macular sparing	1	4
20	m 19	1.7	Hemorrhage (Trauma) parieto-occipital L	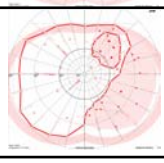	2640.4	Right incomplete hom. hemianopia with macular sparing	1	6
21	m 40	4.9	Brain surgery (AV malformation) occipital, MCA & PCA R	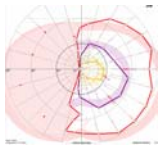	923.7	Left complete hom. hemianopia without macular sparing	4	12
22	w 45	16	Hemorrhage (Trauma) parieto-occipital L	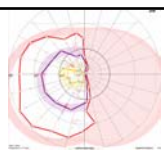	391	Right complete hom. hemianopia without macular sparing	2	10
23	w 32	1.1	Ischemia occipital L	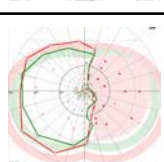	845.5	Right complete hom. hemianopia with macular sparing	2	8
24	m 43	1	Ischemia occipital, PCA R	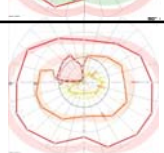	8013.7	Left incomplete hom. superior quadrantanopia with macular sparing	1	9
25	m 64	0.7	Ischemia occipital R		6790.6	Left incomplete hom. superior quadrantanopia with macular sparing	10	10

26	m 73	1.1	Ischemia occipital, PCA L	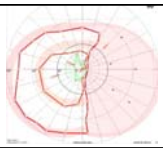	976.7	Right complete hom. hemianopia with macular sparing	6	14
27	w 43	5.9	Hemorrhage (Trauma) occipital R	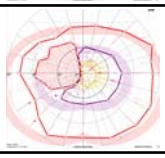	5208.6	Left incomplete hom. hemianopia without macular sparing	1	11
28	m 18	1.8	Hemorrhage (Trauma) Parieto-temporo-occipital R	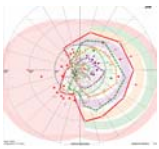	1019	Left incomplete hom. hemianopia with macular sparing	0	8
29	m 53	2	Ischemia occipital R	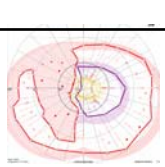	3987.2	Left incomplete hom. hemianopia with macular sparing	2	10
30	w 60	1.1	Ischemia occipital L	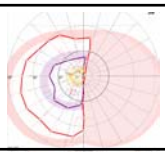	280.2	Right complete hom. hemianopia without macular sparing	3	8

Gaze patterns predicting successful collision avoidance in patients with homonymous visual field defects

Authors: Eleni Papageorgiou[1], Gregor Hardiess[2], Hanspeter Mallot[2], Ulrich Schiefer[1]

Affiliations: [1]Center for Ophthalmology, Institute for Ophthalmic Research, University of Tübingen, Germany, [2]Department of Neurobiology, Lab of Cognitive Neuroscience, University of Tübingen, Germany

Corresponding author: Papageorgiou Eleni, Department & Institute for Ophthalmology, University of Tübingen, Schleichstraße 12-16, 72076, Tübingen, Germany, e_papage@yahoo.com
Tel: +49-7071-29-80726, Fax: +49-7071-29-5038

Study funding*:* Supported by the following grants: European Union (PERACT-Marie Curie Early Stage Research Training, MEST-CT-2004-504321), Deutsche Forschungsgemeinschaft (SFB 550-A4), Graduiertenkolleg 778.

Abstract

Purpose: To identify efficient compensatory gaze patterns applied by patients with homonymous visual field defects (HVFDs) under virtual reality (VR) conditions.

Methods: Thirty patients with HVFDs due to vascular brain lesions and 30 normal subjects performed a collision avoidance task with moving objects at an intersection under two difficulty levels. Based on their performance (i.e. the number of collisions), patients were assigned to either an "adequate" ($HVFD_A$) or "inadequate" ($HVFD_I$) subgroup by the median split method. Eye and head tracking data were available for 14 patients and 19 normal subjects. Saccades, fixations, mean number of gaze shifts, scanpath length and the area under the curve, defined as the area scanned by eye and head movements, were compared between $HVFD_A$, $HVFD_I$ patients and normal subjects by one-way ANOVA and post-hoc Tukey's HSD test. For non-normally distributed data, the Kruskal-Wallis and the Mann-Whitney U tests were used.

Results: For both difficulty levels, the gaze pattern of $HVFD_A$ patients (N=5) in comparison to $HVFD_I$ patients (N=9) was characterized by more gaze shifts, longer saccadic amplitudes towards both the affected and the intact side, more fixations/s on vehicles but fewer fixations/s on the intersection, longer scanpaths and larger area under the curve ($p<0.05$, Tukey's HSD test). Both patient groups displayed more fixations and larger area under the curve in the affected compared to the intact hemifield ($p<0.05$, unpaired t-test). Scanpath length and number of gaze shifts were similar between $HVFD_A$ patients and normal subjects (Tukey's HSD test).

Conclusions: Patients with HVFDs who adapt successfully to their visual deficit, display distinct gaze patterns characterized by increased exploratory eye and head movements, particularly towards moving objects of interest on their blind side. In the context of a dynamic environment, detection of moving objects from patients with HVFDs requires continuous updating of spatial representation by means of gaze movements.

Introduction

Homonymous visual field defects (HVFDs) represent the most frequent type of visual deficits after acquired brain injury (Zihl, 1999), affecting nearly 80% of patients with unilateral postchiasmal brain damage (Zihl, 1995). Sufficient spontaneous recovery of the visual field is seldom and may occur within the first six months (Zhang et al., 2006). In the majority of patients, HVFDs are chronic manifestations that create a marked amount of subjective inconvenience in everyday life (Papageorgiou et al., 2007; Gall et al., 2009). Patients typically complain of difficulties with reading (i.e. hemianopic dyslexia) and visual exploration (Zihl, 2000; Schuett et al., 2008). The visual exploration impairment is characterized by the disability to gain a quick overview of the visual scene especially in unfamiliar surroundings or complex situations (Zihl, 1995; Mort et al., 2003). As a consequence, patients may collide with obstacles and omit details on their blind side leading to difficulties in visual orientation and navigation. (Zihl, 1999). Impaired visual exploration is associated with longer visual search times, shorter saccades, numerous refixations, target omissions, and longer, unsystematic scanpaths (Pambakian et al., 2000; Tant et al., 2002; Zihl, 1995; Mort et al., 2003).

However, some patients develop adaptive eye- and head-movements allowing them to efficiently compensate for the visual field loss. When viewing simple patterns patients with HVFDs spend most of their time looking toward their blind hemifield in order to bring more of the visual scene into their seeing hemifield (Ishiai et al., 1987). This deviation of the fixation point towards the hemianopic side was considered to be an efficient compensatory strategy and has since been observed in numerous other tasks, including dot-counting (Zihl, 1995; Hardiess et al., 2010; Tant et al., 2002), viewing of natural and degraded images (Pambakian) and visual search paradigms (Hardiess et al., 2010). However, to date, hemianopic gaze patterns have been assessed with dot-counting and visual search tasks on stationary displays, usually limiting the field of view to a computer screen. Although the most demanding tasks for hemianopic patients arise within dynamic – commonly time-constrained – situations in our constantly changing visual world (Zihl, 1995), little is known about the exploration strategy applied by those patients when confronted with moving stimuli. Recent evidence suggests that efficient oculomotor adaptation to visual field loss is highly specific and task-dependent (Schuett et al, 2009, Hardiess et al., 2010), therefore specialized approaches seem necessary in order to assess visual behavior of

hemianopic patients towards dynamic objects in contrast to stationary targets. Some clues to visual behavior of heminopes in dynamic, naturalistic environments have been provided by on-road experiments; however, the use of accurate eye and head tracking systems under such scenarios is still not established (Wood et al., 2009).

Moreover, most of the previous studies assessed hemianopic patients as a group in contrast to normal subjects. Given however that some of the patients compensate for their visual deficit, it might be more appropriate to identify these patients according to functional performance measures, and study their gaze patterns in comparison to patients with inadequate compensation and normal subjects as well (Hardiess et al., 2010; Wood et al., 2009; Zihl, 1999). Therefore, the aim of the present study was to identify efficient compensatory gaze patterns applied by patients with HVFDs in a collision avoidance task with moving stimuli under virtual reality (VR) conditions. We hypothesized that patients with high success rates in completing the task will demonstrate compensatory scanning patterns, characterized by increased gaze movements especially towards moving objects of interest on their blind side and that this gaze strategy will be more evident in the more difficult task.

Material and Methods

Participants

Thirty eligible patients with HVFDs (20 with hemianopia and 10 with quadrantanopia) and 30 normal-sighted group-age-matched control subjects were enrolled in the study. All participants were at least 18 years old, had best corrected monocular (near and distant) visual acuity of at least 20/25 and normal function and morphology of the anterior visual pathways as evaluated by ophthalmological tests (fundus and slit-lamp examinations, ocular alignment, ocular motility). The group-age-matched control subjects additionally showed normal visual fields and no history of brain injury, physical or cognitive impairment. Patients had a homonymous visual field defect, varying from complete homonymous hemianopia to homonymous paracentral scotomas, due to a unilateral vascular brain lesion, which was documented by neuroradiological findings (magnetic resonance imaging or computerized tomography). The time span between the brain lesion and the examination date comprised at least six months. Exclusion criteria for patients were as follows: visual hemi-neglect as determined by horizontal line bisection, copying of figures, and by means of the “Bells test” (Gauthier et al., 1989), evidence of cognitive decline,

aphasia, apraxia, visual agnosia or physical impairment, cerebral tumor, multiple sclerosis, Alzheimer's disease, Parkinson's disease, and previous scanning training. The research study was approved by the Institutional Review Board of the University of Tübingen and was performed according to the Declaration of Helsinki. Following verbal and written explanation of the experimental protocol all subjects gave their written consent, with the option of withdrawing from the study at any time.

Experimental procedure

The VR environment was displayed on a large cone-shaped projection screen (horizontal field of view:150^{o}, vertical: 70^{o}) allowing for more natural viewing behavior (Hardiess et al., 2010; Hardiess et al., 2008). Subjects were seated upright with the back tightly on the chair and with their head in the axis of the conical screen (eye level: 1.2 m altitude, distance to the screen: 1.62 m). The virtual environment and the experimental procedures were programmed in C++ using the SGI OpenGL Performer^{TM} (spatial resolution of the generated images: 2048 x 768 pixels). To illuminate the whole projection screen, two video projectors each with 1024 by 768 pixel resolution and a fixed 60 Hz frame rate were used. The light in the experimental lab was dimmed nearly to complete darkness in order to avoid disturbing cues from the surround.

Eye-in-head movement recordings were realized with an infrared light based, head mounted and lightweight eye tracker (bright pupil type, model 501 from Applied Science Laboratories, Bedford, USA). The tracker uses the pupil-corneal-reflection method and enables an accuracy two degrees or better, depending on the eccentricity of the eye position. Real time delay was 50 ms. To record head-in-space movements, an infrared light based tracker system (ARTtrack/DTrack from ART GmbH, Weilheim, Germany) with 6 degrees of freedom, 0.1^{o} accuracy, and a real time delay of 40 ms was used. A configuration of four light reflecting balls fixed to the eye tracker device and thus to the head provided the tracking target for the head tracking system. Both trackers had a fixed temporal sampling frequency of 60 Hz. The online position recordings from eyes and head were transmitted via socket connection to an experimental PC for storage.

We used a nine-point grid for equipment calibration which was carried out at the beginning of the experiment. Subjects started each trial in a tunnel. Prior to each

trial, patients initially fixated a central cross for 5 s to ensure that their gaze commenced at the centre of the projection screen (point of origin). All gaze (eye and head) measurements are reported relative to this point of origin. After leaving the tunnel they could adjust their driving speed between 18 and 61.2 km/h (11.2 - 38 mph) by means of a joystick in order to avoid a collision with the cross traffic at the intersection. During the driving period it was not possible to stop the car. The subjects were instructed to "drive" along a straight road (**Figs. 1a and 1b**) and finally to cross a virtual intersection without causing a collision. Since a lateralization effect has been suggested for patients with HVFDs – in terms of failing to detect stationary objects in the hemianopic side (Bowers et al., 2009) – collision avoidance was assessed at an intersection in order to elicit visual scanning by eye and head movements and detect participants' potential to compensate. The driving distance to the intersection was 172.5 m and the only possible movement of the virtual vehicle was straight ahead. When subjects reached a white line 22.5 m before the intersection (**Fig. 1b)**, they were automatically driven across the intersection at the last adjusted speed without further visual input. A potential collision was then calculated by the simulation program and was delivered to the examiner at the end of the experiment. Even in case of a collision the participants did not experience a virtual crash and did not receive any feedback about the result during the experiment, in order to maintain identical conditions for each trial. All cars of the cross traffic had a constant speed of 50 km/h (31.1 mph), were either red Renault Twingo or white Trabant vehicles with equal numbers of cars approaching from the left and right side. Recent evidence suggests that functional compensation of hemianopes differs according to the specific task demands (Hardiess et al., 2010; Schuett et al., 2009); hence the experiment was performed at two traffic density levels of ascending difficulty, which would generate collisions in 50% or 75% of the trials respectively – assuming that a subject would begin the trial in a random time point and would drive with random speed (i.e. with closed eyes). Subjects performed 30 trials in the same randomized order (i.e. 15 trials for each density level) and were free to perform head and eye movements. Prior to the start of the experiment all subjects underwent a training session lasting 5-10 minutes. The time to complete the whole experiment ranged from 40 to 50 minutes.

Visual fields of patients were assessed with monocular threshold-related, slightly supraliminal automated static perimetry (sAS) within the central 30° visual field, binocular slightly supraliminal automated static perimetry (sAS) within the 90°

visual field as well as binocular semi-automated 90° kinetic perimetry (SKP), each obtained with the OCTOPUS 101 Perimeter (Fa. HAAG-STREIT, Koeniz, Switzerland). Visual fields of control subjects were assessed with binocular slightly supraliminal automated static perimetry (sAS) within the 90° and binocular semi-automated 90° kinetic perimetry (SKP).

Data analysis and statistics

The MATLAB software (MathWorks Company, Natick, USA) was used to analyze the recorded head and eye tracking data. The gaze vector was calculated as resultant of the head and eye vectors. Thus, the gaze vector combines both the head-in-space and the eye-in-head vectors. Fixations were defined as sections of the gaze trajectory where gaze velocity did not exceed $100\,^{o}$/s for at least 120 ms. A gliding window procedure was used to distinguish such gaze fixations (stable gaze position related to the processed stimulus region) from gaze saccades (Hardiess et al., 2008). Since gaze position was calculated from the sum of *eye*-in-head plus head-in-space positions, the terms "saccades" and "fixations" used in the text refer to gaze saccades and gaze fixations respectively.

Statistical analysis was conducted using the statistical software JMP® (SAS Institute Inc., Cary, NC, USA) [www.jmp.com]. Task performance was quantitatively assessed as the number of collisions for the 15 trials per density level. A distinction between "adequate" ($HVFD_A$) and "inadequate" ($HVFD_I$) patients was based on their task performance (i.e. number of collisions) in both difficulty levels by means of the median split method, thus introducing an intrinsic functional criterion (Cohen, 2003; Hardiess et al., 2010; Machner et al., 2009; Altgassen et al., 2007). The square roots of the number of collisions for each density level were used to span a two-dimensional co-ordinate system, where each point represents a patient (**Fig. 2**). The square root transformation of the data was used in order to stabilize the variance for Poisson distributed variables.

For the assessment of visual exploration we calculated the following gaze-related parameters: number of fixations/s, mean duration of fixations (ms), number of fixations/s to vehicles, number of "straight-ahead" fixations/s (i.e. fixations on the intersection), number of gaze shifts (i.e. gaze transitions between left and right hemifield) and scanpath length (i.e. the sum of all saccadic amplitudes). In addition,

we performed hemispace and directional analyses (Tant et al., 2002; Zihl, 1995). The hemifield is defined in terms of the vertical center of the screen (Tant et al., 2002). Hemispace analysis was performed on the proportion (%) of fixations spent in the left and right hemifield, which are referred to as fixations in the blind and seeing hemifield in case of patients. Directional analysis was performed on the mean amplitude (^{o}) of saccades which landed in the left or right half of the screen, which corresponds to the blind and the seeing hemifield for patients. Finally, we calculated the "area under the curve" (pixels) and the proportion (%) of the area under the curve in the left and right hemifield. The "area under the curve" corresponds to the area enclosed by the trajectory of the scanpath, which has been actually scanned by eye and head movements (**Fig. 3**). In accordance with an earlier study (Zihl, 1995), the terms "visual exploration", "visual searching" and "visual scanning" are used synonymously.

In order to identify gaze patterns associated with successful collision avoidance, the above gaze-related parameters were compared across the three participant groups (adequate patients $HVFD_A$, inadequate patients $HVFD_I$ and normal subjects N) by one-way ANOVA. Subsequent post-hoc comparisons were performed using the Tukey's HSD test. In order to test for hemispace preferences and the influence of task difficulty, t-tests were conducted between hemifields (left and right for normal subjects, blind and seeing for patients) and between the levels of "traffic density" (50% and 75%). As multiple tests were carried out, the significance level was adjusted using a Bonferroni correction to an alpha-level of 0.05 for multiple comparisons. All data sets were tested for normality by the Shapiro-Wilk test; for non-normally distributed data, the Kruskal-Wallis test for multiple comparisons and the Mann-Whitney U test were used.

Results

Thirty patients with HVFDs (20 patients with homonymous hemianopia, 10 patients with homonymous quadrantanopia) with a mean age of 46.2$\pm$16 years and 30 normal subjects with a mean age of 45.1$\pm$15.4 years were included in the study. Mean time since lesion onset was 2.7 years and exceeded 1 year in the vast majority of cases (26 out of 30 patients). There were 15 patients with right-hemispheric and 15 patients with left-hemispheric lesions. There were no differences in age ($p=0.79$, t-test) and gender ($p=0.79$, Fisher's exact test) between patients and control subjects, reflecting

group-matching with respect to age and gender. As we have reported elsewhere, the mean number of collisions was on average higher for patients and was weakly related to the extent of the HVFD (Papageorgiou under revision). However, wide variability in performance among patients suggested that visual-field related parameters per se are insufficient in predicting successful collision avoidance; hence gaze strategies might be more decisive in compensating for HVFDs (Papageorgiou under revision). According to the median split method, patients were divided into two subgroups by the median of their performance in both density levels: 15 "adequate" ($HVFD_A$) and 15 "inadequate" ($HVFD_I$) patients (**Fig. 2**). Zihl was the first to introduce this method, by dividing patients into two subgroups either according to their subjective reports of disability in everyday life (Zihl, 1999) or depending on whether their search times exceeded the highest value found in normal subjects (Zihl, 1995). Fourteen patients (five $HVFD_A$ and nine $HVFD_I$) and 19 normal subjects (N) were finally evaluable, since 27 participants with insufficient eye and head tracking data have to be excluded. There were no differences between the two patient subgroups regarding age ($p=0.65$, t-test), the time span since brain lesion ($p=0.69$, Mann-Whitney U test) and the degree of macular sparing ($p=0.35$, Mann-Whitney U test). The relatively high rate of missing gaze tracking data is due to the large projection screen (horizontal view 150^o). Such errors occur when either the corneal reflection or the pupil moves out of the range of the eye camera, i.e. in case of saccadic movements to peripheral stimuli. The offaxis movements are often brief and, therefore, not fully followed by a head movement to recenter the eye within the tracking range (Reimer et al., 2006).

In order to identify gaze strategies associated with successful collision avoidance, relevant gaze-related parameters are depicted graphically as a function of participant group ($HVFD_A$ patients, $HVFD_I$ patients and normal subjects) for density 50% (**Figure 4**) and density 75% (**Figure 5**). Hemispace parameters and results of the analysis of area under the curve are shown for both densities in Figure 6 and 7. The effect of "group" under both traffic densities was significant for all examined parameters except for fixation duration (**Table 1**). Results of post-hoc tests are presented in **Table 2** (density 50%) and **Table 3** (density 75%). In comparison to $HVFD_I$ patients, visual exploration of $HVFD_A$ patients concerning both traffic densities was characterized by significantly longer scanpaths, more gaze shifts, a larger area under the curve, more fixations on virtual vehicles, less "straight-ahead" fixations on the intersection (**Fig. 4 and 5**) and higher saccadic amplitudes towards

both hemifields (Fig 8 and Table 7). There were no significant differences between $HVFD_A$ and $HVFD_I$ patients regarding fixation duration (**Fig. 4 and 5**), proportion of fixations and of the area under the curve to the blind hemifield (**Fig. 6**). Overall, the visual exploration behavior was intensified in the subgroup of adequately performing patients.

All patients showed increased fixational behavior compared to normals; however, $HVFD_A$ patients invested additional fixations in looking more often to vehicles, while $HVFD_I$ patients explored the straight ahead direction more intensified. Thus, in comparison to normal subjects, $HVFD_A$ patients exhibited an overall higher number of fixations, fewer fixations on the intersection, a larger area under the curve, shorter saccadic amplitudes, a higher proportion of fixations and of the area under the curve to the blind hemifield and more fixations on moving objects in the more demanding task. Interestingly, when the area under the curve is analyzed as a function of the distance to the intersection, divided into three parts, $HVFD_I$ patients display a similar area under the curve with normal subjects in the middle part of the route (**Fig. 7a**). During the last part of the route, i.e. close to the intersection, $HVFD_I$ patients even achieve a larger area under the curve (i.e. more scanning activity) than normal subjects (**Fig. 7**). However, gaining an initial overview seems to be more important.

The effect of task difficulty on scanning strategies was investigated by comparing gaze-related parameters between the two traffic densities (**Table 4**). Under more challenging task conditions (i.e. traffic density 75%), $HVFD_A$ patients and normal subjects significantly increased their number of gaze shifts, scanpath length, area under the curve and fixations on vehicles; fixation duration, total fixations and fixations on the intersection were decreased. The tendency for larger saccadic amplitudes to the blind side with increasing traffic density in $HVFD_A$ patients did not reach statistical significance (**Table 4**). Interestingly, normal subjects exhibited more fixations on their right than their left hemifield for density 50%, while under more demanding experimental conditions the area under the curve was larger to their left than their right hemifield (**Table 5**). $HVFD_I$ patients also displayed adaptive visual behavior to the higher traffic density; however, the trend for decreasing number of fixations and fixations on the intersection failed to reach significance. The proportion of fixations and the proportion of the area under the curve to the blind side under more challenging conditions were significantly decreased for $HVFD_I$ patients, and there was also a declining trend for $HVFD_A$ patients.

Finally, the data were analyzed to specifically assess whether the blind hemifield was explored more than the seeing hemifield in terms of fixations and the area under the curve (hemispace analysis, **Table 5**). Indeed, both $HVFD_A$ and $HVFD_I$ patients showed similar (increased) numbers of fixations and a higher proportion of the area under the curve in the blind hemifield compared to their intact hemifield under both traffic densities. However, they differed in their fixation distribution. $HVFD_A$ patients devoted more fixations on vehicles and fewer fixations on the intersection than $HVFD_I$ patients under both traffic densities. In the more difficult task all three participant subgroups increased their fixations on vehicles as expected. $HVFD_A$ patients exhibited more fixations on vehicles even than normal subjects, resulting in identification of the collision-relevant ones and successful collision avoidance. Interestingly, normal subjects displayed more fixations in the right than the left hemifield for the easier task, and a higher proportion of the area under the curve in the left than the right hemifield for the more difficult task. Directional analysis revealed that the mean saccadic amplitude towards the blind hemifield was significantly shorter in comparison to the seeing hemifield for both patient subgroups, while there were no differences for normal subjects (**Fig. 8**).

Discussion

We investigated the scanning strategies of patients with HVFDs and normal subjects under dynamic VR conditions. We found that the subgroup of patients who adapt successfully to their visual deficit, display distinct gaze patterns characterized by increased exploration, particularly towards moving objects of interest on their blind side. This compensatory behavior becomes especially evident during the more demanding task. A gaze bias to the blind hemifield – in terms of proportion of fixations and the area under the curve – is observed in both patient subgroups; however, adequately compensating patients undertake larger saccadic amplitudes and more gaze shifts than inadequate patients, leading to a scanned area that is even larger than that of normal subjects.

These findings are to some extent consistent with previous studies demonstrating that compensatory efforts of patients with HVFDs in stationary scenarios include increased numbers of fixations, longer search times and more time looking towards their blind hemifield (Ishiai et al. 1987; Hardiess et al., 2010; Tant et al., 2002; Pambakian et al., 2000). According to our results, under dynamic, time-

constrained situations, the deviation of fixation distribution towards the blind side is sufficient only when combined with appropriate "goal-relevant" gaze movements in order to extract all the necessary information for completion of the current task in a timely manner. Increased gaze scanning led to a more efficient fixation pattern for $HVFD_A$ patients, who exhibited more fixations on vehicles and fewer fixations on the intersection than $HVFD_I$ patients. This strategy resulted in identification of the collision-relevant vehicles and successful collision avoidance. Experiments on visual behavior of hemianopes in naturalistic tasks have indeed revealed that in dynamic or complex environments, where patients cannot exclusively rely on their spatial working memory in order to locate salient objects (Martin et al., 2007, Hardiess et al., 2010), compensation is possible by means of exploratory gaze movements. This is reflected in the increased scanpath length, number of gaze shifts and especially in the area under the curve of $HVFD_A$ patients compared to $HVFD_I$ patients. The area under the curve for $HVFD_A$ patients implies increased scanning of the visual scene and exceeds even that of normal subjects, although they show similar scanpath lengths and gaze shifts. A possible explanation for this finding is that $HVFD_A$ patients perform hypometric but more numerous saccades/s to their blind side in comparison to normal subjects, as indicated by the increased number of fixations/s on their blind hemifield especially on moving vehicles. Similar results were obtained from on-road tests (Wood et al., 2009; Koojman et al., 2004) showing that patients rated as safe to drive compensated by making more head movements into their blind field and received superior ratings regarding eye movements. In accordance with an earlier study (Kooijman et al., 2004), we also observed that $HVFD_A$ patients started to scan the visual scene at a larger distance to the intersection, resulting in a higher area under the curve in the first part of the route and finally in efficient collision avoidance (Kooijman et al., 2004). This strategy offers the advantage of capturing more visual elements by performing shorter saccades and also having more time to plan the motor response.

In addition to gaze compensation, recent studies have pointed to increased involvement of spatial working memory as a compensatory strategy for patients with HVFDs when assembling wooden models under naturalistic conditions (Martin et al., 2007) or during a dot-counting task and a comparative visual search task (Hardiess et al., 2010). In some cases no gaze bias towards the blind hemifield or adaptive gaze behavior were observed. It was hypothesized that these findings reflected the static

nature or the relative simplicity of the task, which afforded an opportunity for greater reliance on visuo-spatial memory (Martin et al., 2007; Hardiess et al., 2010). In the present dynamic task gaze adaptation of $HVFD_A$ patients was evident in both difficulty levels and became more prominent in the more complex situation. Therefore, in contrast to experiments with stationary displays, the dynamic nature of the present task forces $HVFD_A$ patients to adopt appropriate gaze strategies. Recent evidence (Schuett et al., 2009) further suggests that efficient oculomotor adaptation to visual field loss is highly specific and task-dependent; therefore the dissociation in compensational strategies between various tasks should be interpreted in the light of their cognitive demand. Dot-counting restricts visual scanning to the processes of visual sampling without any further identification component (Zihl, 1999) and a low demand for working memory. The visual search for targets among distractors requires additional object recognition. Comparative visual search is more challenging, since a comparator mechanism is further involved (Hardiess et al., 2010). Collision avoidance is a cognitively even more complex task, involving processes such as oculomotor adaptation, speed estimation, selection of collision relevant obstacles, storage in visual working memory and visuo-motor calibration (Lee et al., 1976; Simpson et al., 2003), therefore a distinct compensatory strategy is expected.

Although our findings suggest, that gaze adaptation is the primary compensatory mechanism to achieve collision avoidance, implementation of intact working memory should be also considered. $HVFD_A$ patients efficiently avoided collisions at the intersection, although they performed fewer fixations on it than $HVFD_I$ patients and normal subjects. Storage in unimpaired working memory may hence play a role for stationary elements of the visual scene (Hardiess et al., 2010; Martin et al., 2007; Machner et al., 2009). Since the present study included only a straight route ending at the intersection and no turns at all, the location of the intersection was steady throughout the experiment. $HVFD_I$ patients attempted to compensate by increased working memory involvement as indicated by longer – though statistically non-significant – fixations compared to $HVFD_A$ patients and normal subjects. Additionally, they devoted a high proportion of their fixations on the intersection probably due to reduced working memory capacity and inability to create an adequate spatial representation even of stationary elements.

The need to compensate by gaze scanning in the context of a dynamic scenario and visual field loss is further reflected in the finding that $HVFD_A$ patients exhibit

even fewer fixations on the intersection than normal subjects. When normal subjects look straight ahead, input from the peripheral visual field possibly combined with spatial memory information, enables them to use the concluding milliseconds of a fixation (Pambakian et al., 2000) to program their next saccade in order to gather information critical for the execution of the current task (Hayhoe et al., 2005). Preplanning of future saccades based on peripheral information has the advantage of locating the objects of interest through accurate saccades, without investing much effort in exploring irrelevant elements. However, $HVFD_A$ patients lack unilateral peripheral visual input that could guide their saccades, so they must explore even irrelevant parts of the visual scene, in order to increase their possibilities of detecting an object of interest. Tant has also pointed to the absence of an immediately available spatial representation in homonymous hemianopia and the need to usually fully explore all parts of the projection screen (Tant et al., 2002). $HVFD_A$ patients achieve this goal by means of numerous gaze movements. This suggestion may also explain the finding reported in most of the studies (Zihl, 1999; Hardiess et al., 2010; Pambakian et al., 2000; Machner et al., 2009; Tant et al., 2002; Chedru et al., 1973) and the present study as well, that patients perform more fixations even on irrelevant locations in comparison to normal subjects. Normal subjects are able to parafoveally perceive and spatially represent large areas. Therefore, they organize their exploration economically by guiding their saccades to task-relevant objects, clustering neighboring stimuli and omitting empty or irrelevant parts (Tant et al., 2002; Zihl, 1999).

Regarding task difficulty, in the more complex task both $HVFD_A$ patients and normal subjects significantly reduce their fixations on the intersection in favor of gaze movements. This finding in combination with shorter fixation duration supports a greater reliance on gaze adaptation in order to solve the more difficult task. Fixation duration has been shown to reflect ongoing processing in scene viewing (Henderson et al., 2008) and shorter fixation duration has been associated with lower memory load (Velichkovsky et al., 1995). Therefore, $HVFD_A$ patients and normal subjects seem to reduce their working memory load, as indicated by the fewer fixations on the intersection and their shorter duration, and increase their gaze adaptation in the more complex task. A possible explanation is that the plethora of moving objects does not allow the maintenance of a reliable spatial representation. Although $HVFD_I$ patients also reduce fixation duration in the more complex task, they fail to undertake

scanning movements and continue fixating on the intersection to the same degree. Decreased gaze activity and reduced working memory availability result in their inability to solve the task.

Interestingly, although distinct differences were observed in fixation position, fixation duration was similar across the three participant groups in both difficulty levels and in the more demanding task all three participant groups significantly reduced their fixation duration. Our results are in general accord with studies reporting that the mean fixation duration during visual search is 275 msec (Rayner et al., 1998). Some authors have reported increased fixation duration for patients with HVFDs in comparison to normal subjects when performing dot-counting (Zihl, 1999), search for targets among distractors (Machner et al., 2009) and comparative visual search tasks (Hardiess et al., 2010). This finding might be attributed to the lack of time constraints and the need to rely more on working memory in order to achieve object recognition in terms of color, form or spatial location. However, in cases of brief presentation of images (Pambakian et al., 2000) patients with HVFDs demonstrated shorter fixations than normal subjects. In the present task, to visually avoid a collision, visual information on the location and speed of moving vehicles and the crossing distance is essential (Cheong et al., 2008; Lee et al., 1976; Simpson et al., 2003). In contrast to previous studies with stationary images, the processing of motion by the faster magnocellular channel (Livingstone et al., 1988) in combination with time constraints in our paradigm, where participants did not have the possibility to stop the vehicle, may explain the adoption of fixations with similar duration to those of normal subjects. Our results are in accordance with a study reporting eye movements of drivers while they watched films of dangerous driving situations. Similarly, the authors found that the least visually complex rural roads attracted the longest fixations durations, while the most visually complex urban roads attracted the shortest fixation durations (Chapman et al., 1998). Additionally, one might expect, that fixation duration would be prolonged in $HVFD_I$ patients in their attempt to increase the involvement of visual working memory so as to avoid gaze saccades while memorizing larger chunks of information (Zihl, 1999; Hardiess et al., 2008; Tant et al., 2002; Hardiess et al., 2010). $HVFD_I$ patients demonstrated in both difficulty levels longer fixations, but this difference did not reach significance and poor performance of $HVFD_I$ patients was mainly attributed to deficient implementation of gaze saccades resulting in short scanpaths, scarce gaze shifts and

subsequent underdetection of moving objects of interest. Hence, our results are in accordance with a recent study suggesting that saccadic metrics account for much more of the variability and improvement in performance than did fixation duration in a visual search task of one-dimensional dense, regular columns of stimuli (Phillips et al., 2009). The authors hypothesize that the speed of visual scanning depends upon how much is perceived during a single fixation, rather than how long it takes to process what is seen during that fixation.

In terms of saccadic metrics, saccadic amplitudes of patients with HVFDs to their blind field were shorter than those made into their seeing field and those of normal subjects in general accord with previous reports (Ishiai et al., 1987; Zihl, 1995; Zihl, 1999; Hardiess et al., 2010; Tant et al., 2002; Pambakian et al., 2000). The overshooting / corrective saccade strategy towards the blind hemifield – as described previously (Meienberg et al., 1981; Zangemeister et al., 1995) – was not observed in the present study, as it would result in longer saccades in the blind than in the seeing hemifield. However $HVFD_A$ patients performed significantly longer saccades to both hemifields than $HVFD_I$ patients. There were no differences in macular sparing between the two patient subgroups, so it is unlikely that $HVFD_A$ patients received visual input from their remaining intact visual field. Saccades into the blind hemifield are based on spatial memory and allow for normal saccadic accuracy towards static targets (Martin et al., 2007). However in case of numerous moving stimuli with constantly changing locations, we assume that creating and updating of a spatial representation interferes with scanning due to apparent difficulties in accurately predicting the location of moving objects within the blind field. As discussed above, given that working memory is intact in $HVFD_A$ patients, implementation of memory-guided saccades may explain the finding that $HVFD_A$ patients perform hypometric saccades to the blind side, which however are larger than those of $HVFD_I$ patients.

In conclusion, the assignment of patients into two subgroups on the basis of their performance in a collision avoidance task, allowed associating certain compensatory mechanisms with functional outcomes. Striking differences were revealed between adequately ($HVFD_A$) and inadequately ($HVFD_I$) compensating patients and normal subjects. Successful compensation was associated with increased exploration in terms of more gaze shifts, increased scanpath length and longer saccades especially towards objects of interest in the blind side. While in stationary displays compensation might be possible by means of increased working memory

involvement, our findings suggest that in the context of a dynamic environment gaze adaptation is the primary compensatory mechanism in patients with HVFDs, since detection of moving objects requires continuous updating of their spatial representation by means of gaze movements.

Grants: This work was supported by the following grants: European Union (PERACT-Marie Curie Early Stage Research Training, MEST-CT-2004-504321), Deutsche Forschungsgemeinschaft (SFB 550-A4), GRK 778.

References

1. Altgassen M, Phillips L, Kopp U, Kliegel M. Role of working memory components in planning performance of individuals with Parkinson's disease. Neuropsychologia 45 (2007) 2393–2397.

2. Bowers AR, Mandel AJ, Goldstein RB, Peli E. Driving with hemianopia, I: Detection performance in a driving simulator. Invest Ophthalmol Vis Sci. 2009;50:5137-47.

3. Chapman PR, Underwood G. Visual search of dricing situations: danger and experience. Perception 1998;27(8):951-64

4. Chédru F, Leblanc M, Lhermitte F. Visual searching in normal and brain-damaged subjects (contribution to the study of unilateral inattention). Cortex. 1973;9:94-111.

5. Cheong AM, Geruschat DR, Congdon N. Traffic gap judgment in people with significant peripheral field loss. Optom Vis Sci. 2008;85:26-36.

6. Cohen, J. (2003). Applied Multiple Regression/Correlation Analysis for the Behavioral Sciences (3rd ed.). Routledge: Lawrence Erlbaum Associates.

7. Gall C, Lucklum J, Sabel BA, Franke GH. Vision- and health-related quality of life in patients with visual field loss after postchiasmatic lesions. Invest Ophthalmol Vis Sci. 2009;50:2765-76.

8. Gauthier, L., Dehaut, F., & Joannette Y. (1989). The bells test: A quantitative and qualitative test for visual neglect. International Journal of Clinical Neuropsychology, 11, 49-54.

9. Hardiess G, Gillner S, Mallot HA. Head and eye movements and the role of memory limitations in a visual search paradigm. J Vis. 2008;8:7.1-13.

10. Hardiess G, Papageorgiou E, Schiefer U, Mallot HA. Functional compensation of visual field deficits in hemianopic patients under the influence of different task demands. Vision Res. 2010;50:1158-72.

11. Hayhoe M, Ballard D. Eye movements in natural behavior. Trends Cogn Sci. 2005;9:188-94.

12. Henderson, J. M., & Pierce, G. L. (2008). Eye movements during scene viewing: Evidence for mixed control of fixation durations. Psychonomic Bulletin & Review, 15, 566–573.

13. Ishiai S, Furukawa T, Tsukagoshi H. Eye-fixation patterns in homonymous hemianopia and unilateral spatial neglect. Neuropsychologia. 1987;25:675-9.

14. Kooijman, A. C., Brouwer, W. H., Coeckelbergh, T. R. M., Tant, M., Cornelissen, F., Bredewoud, R., et al. (2004). Compensatory viewing training improves practical fitness to drive of subjects with impaired vision. Visual Impairment Research, 6(1), 1-27.

15. Lee, D. N. (1976). A theory of visual control of braking based on information about time-to-collision. Perception, 5, 437-459.

16. Livingstone M, Hubel D. Segregation of form, color, movement, and depth: anatomy, physiology, and perception. Science. 1988;240(4853):740-9.

17. Machner B, Sprenger A, Kömpf D, Sander T, Heide W, Kimmig H, Helmchen C. Visual search disorders beyond pure sensory failure in patients with acute homonymous visual field defects. Neuropsychologia. 2009;47:2704-11.

18. Martin T, Riley ME, Kelly KN, Hayhoe M, Huxlin KR. Visually-guided behavior of homonymous hemianopes in a naturalistic task. Vision Res. 2007;47:3434-46.

19. Meienberg O, Zangemeister WH, Rosenberg M, Hoyt WF, Stark L. Saccadic eye movement strategies in patients with homonymous hemianopia. Ann Neurol. 1981;9:537-44.

20. Mort DJ, Kennard C. Visual search and its disorders. Curr Opin Neurol. 2003;16:51-7.

21. Pambakian AL, Wooding DS, Patel N, Morland AB, Kennard C, Mannan SK. Scanning the visual world: a study of patients with homonymous hemianopia. J Neurol Neurosurg Psychiatry. 2000;69:751-9.

22. Papageorgiou E, Hardiess G, Schaeffel F, Wiethoelter H, Karnath HO, Mallot H, Schoenfisch B, Schiefer U. Assessment of vision-related quality of life in patients with homonymous visual field defects. Graefes Arch Clin Exp Ophthalmol. 2007;245:1749-58.

23. Papageorgiou E, Hardiess G, Ackermann H, Wiethoelter H, Dietz K, Mallot HA, Schiefer U. Collision avoidance in persons with homonymous visual field defects under virtual reality conditions. [submitted]

24. Papageorgiou E, Hardiess G, Wiethoelter H, Ackermann H, Dietz K, Mallot HA, Schiefer U. The neural correlates of impaired collision avoidance in hemianopic patients. [submitted]

25. Phillips MH, Edelman JA. The dependence of visual scanning performance on search direction and difficulty. Vision Res. 2008;48:2184-92.

26. Rayner, K. (1998). Eye movements in reading and information processing: 20 years of research. Psychological Bulletin, 124, 372-422.

27. Reimer B, Sodhi M. Detecting eye movements in dynamic environments. Behav Res Methods. 2006;38(4):667-82.

28. Schuett S, Heywood CA, Kentridge RW, Zihl J. The significance of visual information processing in reading: Insights from hemianopic dyslexia. Neuropsychologia. 2008;46:2445-62.

29. Schuett S, Kentridge RW, Zihl J, Heywood CA. Adaptation of eye-movements to simulated hemianopia in reading and visual exploration: Transfer or specificity? Neuropsychologia. 2009;47:1712-20.

30. Simpson, G., Johnston, L., & Richardson, M. (2003). An investigation of road crossing in a virtual environment. Accident; Analysis and Prevention, 35, 787–796.

31. Tant ML, Cornelissen FW, Kooijman AC, Brouwer WH. Hemianopic visual field defects elicit hemianopic scanning. Vision Res. 2002;42:1339-48.

32. Velichkovsky BM, Challis BH, Pomplun M. [Working memory and work with memory: visual-spatial and further components of processing]. Z Exp Psychol. 1995;42:672-701

33. Wood J, Elgin J, McGwin Jr. J, Vaphiades M, Kline L, Owsley C. Head and Eye Movements and Lane Keeping in Drivers With Hemianopia and Quadrantanopia Compared to Controls. Invest Ophthalmol Vis Sci 2009;50: E-Abstract 3204.

34. Zangemeister WH, Meienberg O, Stark L, Hoyt WF.Eye-head coordination in homonymous hemianopia. J Neurol. 1982;226:243-54.

35. Zhang X, Kedar S, Lynn MJ, Newman NJ, Biousse V. Natural history of homonymous hemianopia. Neurology. 2006;66:901-5.

36. Zihl J. Oculomotor scanning performance in subjects with homonymous visual field disorders. Visual Impairment Research 1 (1999), pp. 23–31.

37. Zihl J. (2000). Rehabilitation of visual disorders after brain injury. Hove, UK: Psychology Press.

38. Zihl J. Visual scanning behavior in patients with homonymous hemianopia. Neuropsychologia. 1995;33:287-303.

Figures and legends

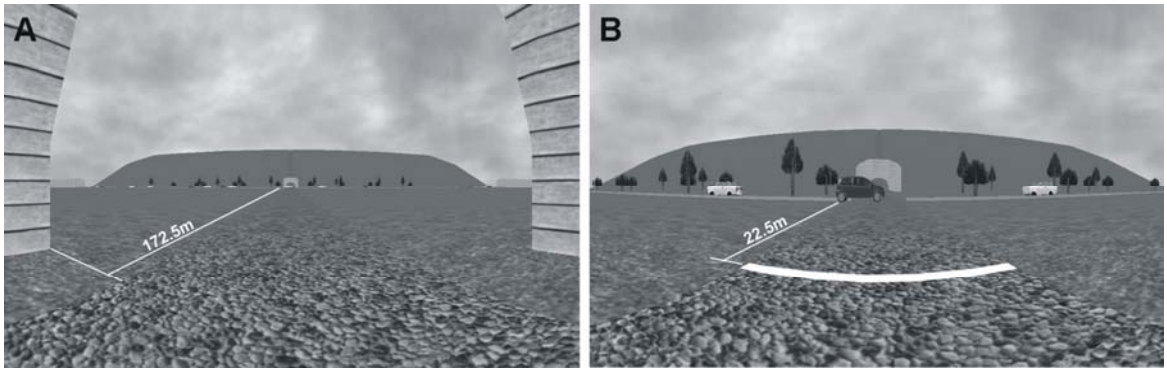

Fig. 1 Start and end positions of the virtual drive. (**a**) Start position of the virtual vehicle in the tunnel. The distance to the intersection is also depicted. (**b**) End position of the virtual drive at the white line 22.5m before the intersection.

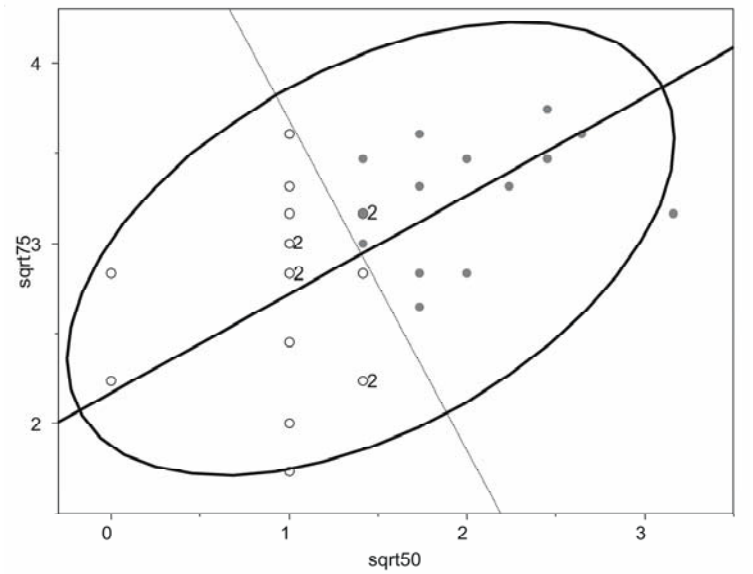

Fig. 2 Median split method. The square roots of the number of collisions for the density levels 50% (x axis) and 75% (y axis) were used to span a two-dimensional co-ordinate system, where each point represents a patient. The ellipse contains 95% of the bivariate normal distribution. The continuous line is the principal axis of the ellipse. Based on its slope, the formula for the weighted sum "wsum" is calculated from both square roots: 1.83sqrt50 + sqrt75. The median is 5.55. Patients with wsum>median are shown as grey dots and were denoted as "inadequate" (i.e. more collisions or $HVFD_I$), while all remaining patients (with wsum<median) are shown as white dots and were denoted as "adequate" (i.e. fewer collisions or $HVFD_A$). The label "2" on some positions indicates coinciding values. By this method, an intrinsic

criterion based on the experimental results was applied in order to divide patients into two subgroups each one consisting of 15 patients.

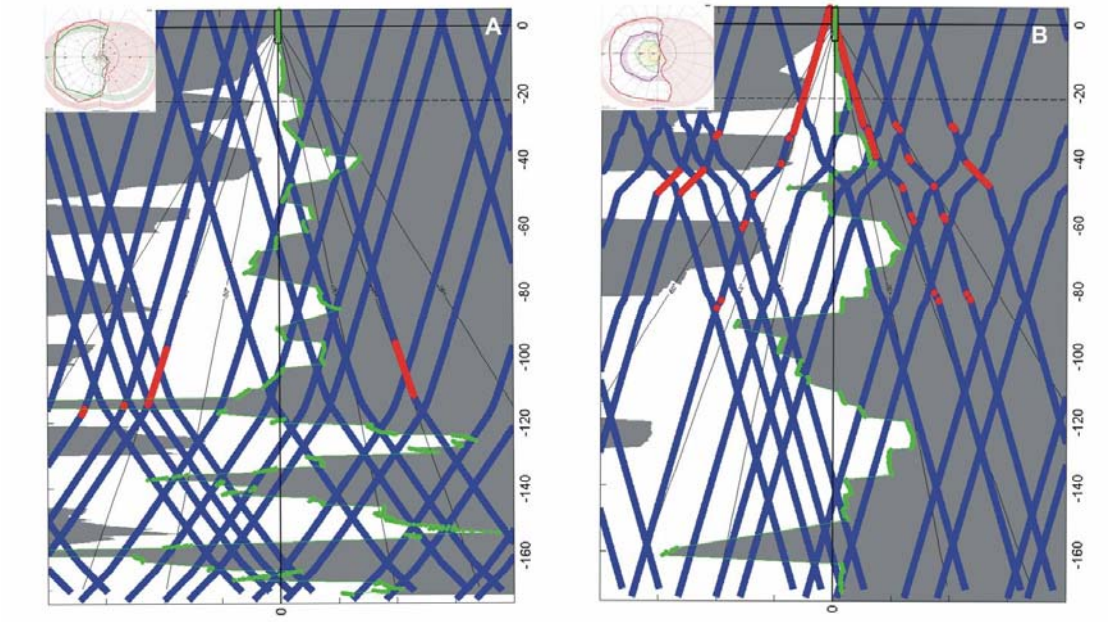

Fig. 3: Visualization of gaze (green line) during an entire trial from position -160 (bottom=start) to position 0 (top=end of intersection) in the vertical axis. A: $HVFD_A$ patient with right homonymous hemianopia, and B: $HVFD_I$ patient with right homonymous hemianopia of comparable size (grey area: "blind" area, blue lines: courses of the cross traffic vehicles, red lines: vehicles on collision route). Binocular semi-automated 90° kinetic perimetry (SKP) is shown on the left top corner of each display. The gaze pattern of the $HVFD_A$ patient is characterized by numerous gaze shifts and saccades with larger amplitudes especially in the initial part of the route, while the $HVFD_I$ patient demonstrates decreased gaze activity resulting in a collision.

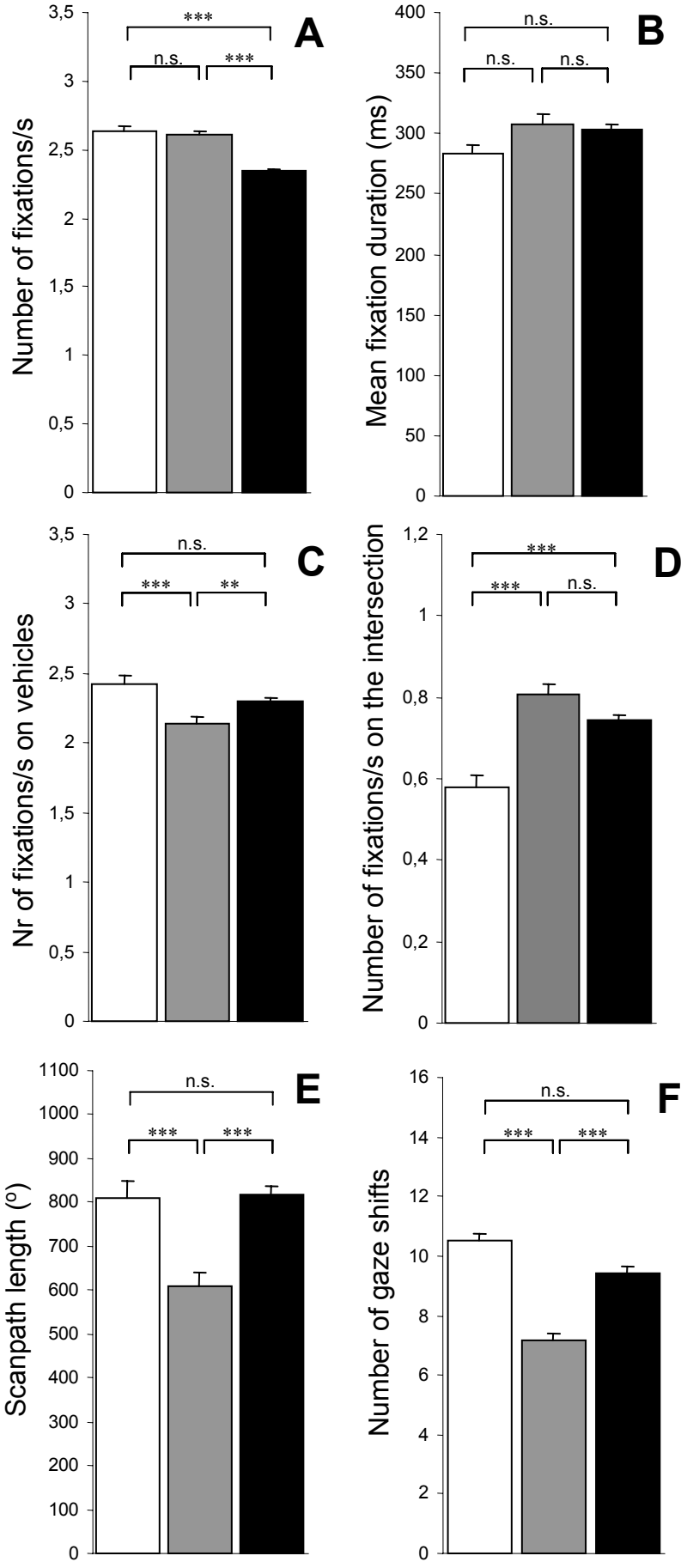
A
Number of fixations/s
3,5
3
2,5
2
1,5
1
0,5
0
***
n.s.
***
B
Mean fixation duration (ms)
400
350
300
250
200
150
100
50
0
n.s.
n.s.
n.s.
C
Nr of fixations/s on vehicles
3,5
3
2,5
2
1,5
1
0,5
0
n.s.
***
**
D
Number of fixations/s on the intersection
1,2
1
0,8
0,6
0,4
0,2
0
***
***
n.s.
E
Scanpath length (°)
1100
1000
900
800
700
600
500
400
300
200
100
0
n.s.
***
***
F
Number of gaze shifts
16
14
12
10
8
6
4
2
0
n.s.
***
***

Fig. 4 Gaze-related parameters of all participant-groups for traffic density of 50%. Comparisons were performed between normal subjects (black bars) and both patients subgroups ($HVFD_A$ patients: white bars, $HVFD_I$ patients: grey bars) regarding the number of fixations/s (A), mean fixation duration (B), the number of fixations/s to vehicles (C), the number of fixations/s to the intersection (D), the scanpath length (E), and the number of gaze shifts (F). Tukey's post-hoc test was conducted in order to detect significant differences between normal subjects and each of the patient subgroups (* $p<0.05$, ** $p<0.01$, *** $p<0.001$, n.s. indicates non-significant comparisons). Error bars indicate standard error of the mean (sem).

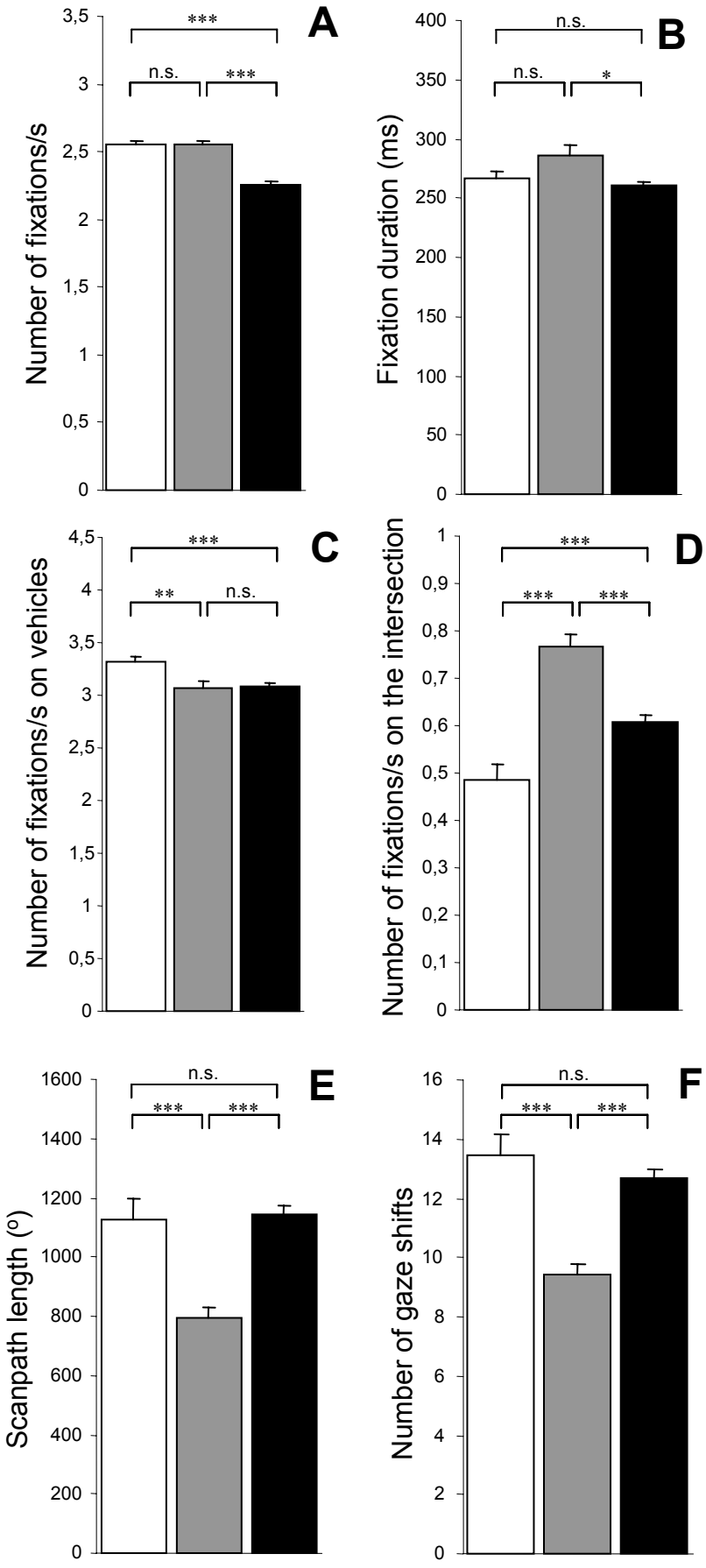
A
Number of fixations/s
3,5
3
2,5
2
1,5
1
0,5
0
***
n.s.
***
B
Fixation duration (ms)
400
350
300
250
200
150
100
50
0
n.s.
n.s.
*
C
Number of fixations/s on vehicles
4,5
4
3,5
3
2,5
2
1,5
1
0,5
0
***
**
n.s.
D
Number of fixations/s on the intersection
1
0,9
0,8
0,7
0,6
0,5
0,4
0,3
0,2
0,1
0
***
***
***
E
Scanpath length (°)
1600
1400
1200
1000
800
600
400
200
0
n.s.
***
***
F
Number of gaze shifts
16
14
12
10
8
6
4
2
0
n.s.
***
***

Fig. 5 Gaze-related parameters of all participant-groups for traffic density of 75%. Comparisons were performed between normal subjects (black bars) and both patients subgroups ($HVFD_A$ patients: white bars, $HVFD_I$ patients: grey bars) regarding the number of fixations/s (A), mean fixation duration (B), the number of fixations/s to vehicles (C), the number of fixations/s to the intersection (D), the scanpath length (E), and the number of gaze shifts (F). Tukey's post-hoc test was conducted in order to detect significant differences between normal subjects and each of the patient subgroups (* $p<0.05$, ** $p<0.01$, *** $p<0.001$, n.s. indicates non-significant comparisons). Error bars indicate standard error of the mean (sem).

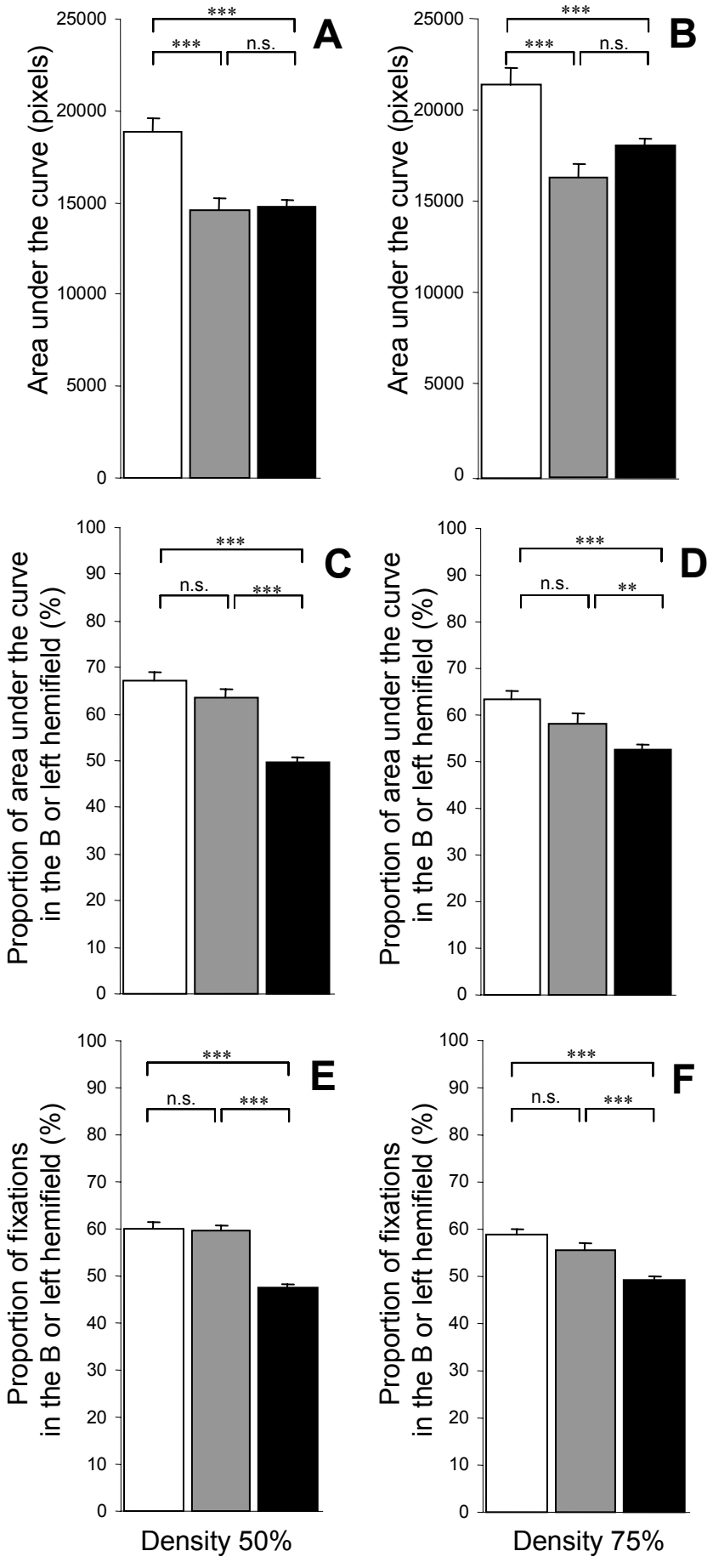
A
B
C
D
E
F
Area under the curve (pixels)
Proportion of area under the curve in the B or left hemifield (%)
Proportion of fixations in the B or left hemifield (%)
***
n.s.
**
Density 50%
Density 75%

Fig. 6 Area under the curve and hemispace analyses of all participant-groups for both density conditions. Comparisons were performed between normal subjects (black bars) and both patients subgroups ($HVFD_A$ patients: white bars, $HVFD_I$ patients: grey bars) regarding the area under the curve in 50% (A), the area under the curve in 75% (B), the proportion of the area under the curve due to the blind hemifield of patients or the left hemifield of normal subjects in density 50% (C), the proportion of the area under the curve due to the blind or the left hemifield in density 75% (D), the proportion of fixations due to the blind or the left hemifield in density 50% (E), and the proportion of fixations due to the blind or the left hemifield in density 75% (F). Tukey's post-hoc test was conducted in order to detect significant differences between normal subjects and each of the patient subgroups (* $p<0.05$, ** $p<0.01$, *** $p<0.001$, n.s. indicates non-significant comparisons). Error bars indicate standard error of the mean (sem).

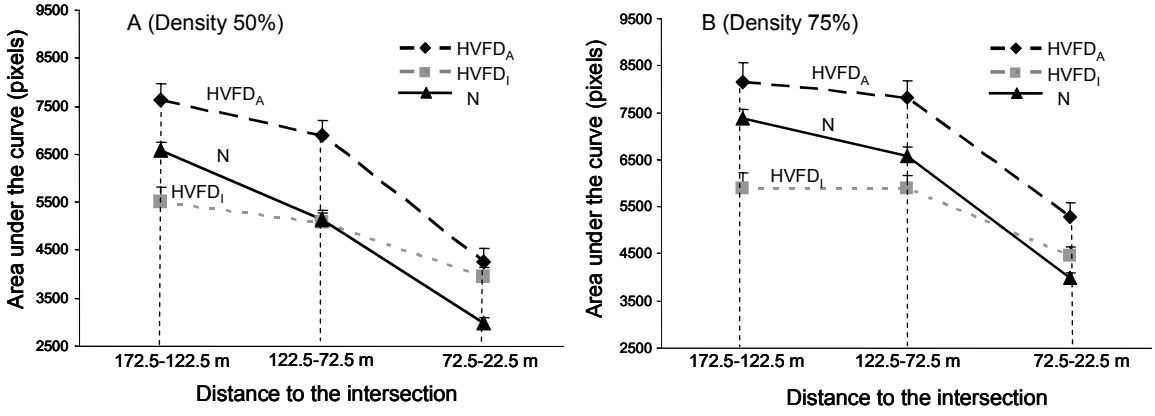

Fig.7 Area under the curve of all participant groups as a function of distance to the intersection for both densities. Values are depicted for the first (172.5-122.5 m), the second (122.5-72.5 m) and the third (72.5-22.5 m) part of the route in density 50% (A) and density 75% (B).

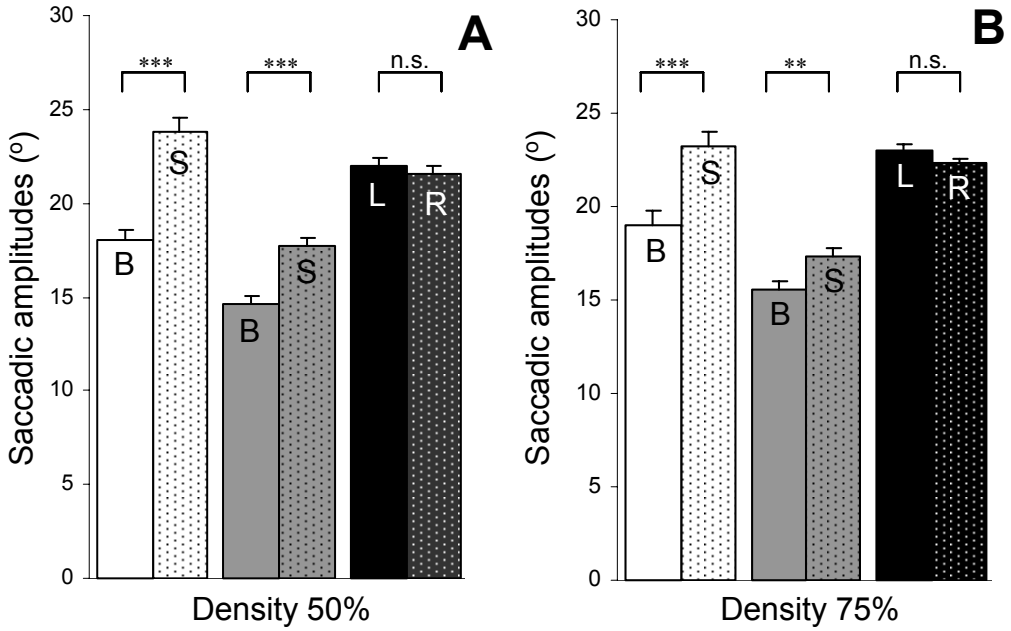

Fig.8 Mean gaze amplitudes of all participant-groups for both densities. Unpaired t-tests were performed between the blind (B) and seeing (S) hemifield of patients, and between the left (L) and right (R) hemifield of normal subjects ($HVFD_A$ patients: white bars, $HVFD_I$ patients: grey bars, normal subjects: black bars) in density 50% (A) and density 75% (B) (Bonferroni: * $p<0.05$, ** $p<0.01$, *** $p<0.001$, n.s. indicates non-significant comparisons). Error bars indicate standard error of the mean (sem).

Table 1: Statistical results of the ANOVA-test for all examined parameters in density 50% and density 75%.
[a] Kruskall-Wallis test

	Density 50%		Density 75%	
Gaze-related parameter	**Statistical data**	**Significance**	**Statistical data**	**Significance**
Number of fixations/s	F (2, 492) = 36.91	$p < 0.0001$	F (2, 492) = 45.34	$p < 0.0001$
Fixation duration (ms)[a]	H = 4.59, 2 d.f.	n.s.	H = 6.58, 2 d.f.	$p < 0.05$
Percentage of fixations on vehicles	F (2, 492) = 18.01	$p < 0.0001$	F (2, 492) = 21.03	$p < 0.0001$
Percentage of fixations on the intersection	F (2, 492) = 20.16	$p < 0.0001$	F (2, 492) = 36.9	$p < 0.0001$
Scanpath length (^{o})	F (2, 492) = 17.94	$p < 0.0001$	F (2, 492) = 28.18	$p < 0.0001$
Number of gaze shifts	F (2, 492) = 21.67	$p < 0.0001$	F (2, 492) = 27.06	$p < 0.0001$
Area under the curve (pixels)	F (2, 492) = 13.26	$p < 0.0001$	F (2, 492) = 10.95	$p < 0.0001$
Directional analysis				
Saccadic amplitude (^{o}) to the blind or left hemifield	F (2, 492) = 69	$p < 0.0001$	F (2, 492) = 77.78	$p < 0.0001$
Saccadic amplitude (^{o}) to the seeing or right hemifield	F (2, 492) = 28.34	$p < 0.0001$	F (2, 492) = 44.87	$p < 0.0001$
Hemispace analysis				
Proportion of fixations (%) in the blind or left hemifield	F (2, 492) = 46.64	$p < 0.0001$	F (2, 492) = 20.05	$p < 0.0001$
Proportion of area under the curve (%) in the blind or left hemifield	F (2, 492) = 36.04	$p < 0.0001$	F (2, 492) = 10.97	$p < 0.0001$

Table 2: Gaze-related parameters, directional and hemispace analyses for $HVFD_A$, $HVFD_I$ patients, and normal subjects (N) for density 50%. Data are presented as mean (standard error of the mean). Statistical comparisons were made between $HVFD_A$ - $HVFD_I$ patients, $HVFD_A$ patients – N and $HVFD_I$ patients – N (Tukey's HSD test).
* $p<0.05$, ** $p<0.01$, *** $p<0.001$, n.s. indicates non-significant comparisons

Gaze-related parameter	$HVFD_A$		$HVFD_I$		N		$HVFD_A$-$HVFD_I$ (p)	$HVFD_A$-N (p)	$HVFD_I$-N (p)
Number of fixations/s	2.64	(0.04)	2.61	(0.03)	2.34	(0.02)	n.s.	***	***
Fixation duration (ms)	283.91	(6.06)	307.71	(8.35)	302.87	(4.84)	n.s.	n.s.	n.s.
Percentage of fixations on vehicles (%)	64.59	(1.39)	54.54	(1.04)	59.82	(0.71)	***	**	***
Percentage of fixations on the intersection (%)	15.16	(0.9)	22.08	(0.67)	18.52	(0.46)	***	***	***
Scanpath length (^{o})	810.83	(38.45)	610.76	(28.17)	816.31	(20.4)	***	n.s.	***
Number of gaze shifts	10.5	(0.44)	7.16	(0.31)	9.42	(0.24)	***	n.s.	***
Area under the curve (pixels)	18873.3	(763.4)	14597	(664.48)	14771.8	(337.93)	***	***	n.s.
Directional analysis									
Saccadic amplitude (^{o}) to the blind or left hemifield	18.06	(0.51)	14.58	(0.42)	22.03	(0.41)	***	***	***
Saccadic amplitude (^{o}) to the seeing or right hemifield	23.77	(0.76)	17.69	(0.46)	21.58	(0.38)	***	**	***
Hemispace analysis									
Proportion of fixations (%) in the blind or left hemifield	59.88	(1.53)	59.52	(1.24)	47.47	(0.82)	n.s.	***	***
Proportion of area under the curve (%) in the blind or left hemifield	67	(1.96)	63	(1.93)	49.70	(1.12)	n.s.	***	***

Table 3: Gaze-related parameters, directional and hemispace analyses for $HVFD_A$, $HVFD_I$ patients, and normal subjects (N) for density 75%. Data are presented as mean (standard error of the mean). Statistical comparisons were made between $HVFD_A$ - $HVFD_I$ patients, $HVFD_A$ patients – N and $HVFD_I$ patients – N (Tukey's HSD test).
[a] Mann-Whitney U test
* $p<0.05$, ** $p<0.01$, ** $p<0.001$, n.s. indicates non-significant comparisons

Gaze-related parameter	$HVFD_A$		$HVFD_I$		N		$HVFD_A$-$HVFD_I$ (p)	$HVFD_A$-N (p)	$HVFD_I$-N (p)
Number of fixations/s	2.55	(0.03)	2.55	(0.03)	2.26	(0.02)	n.s.	***	***
Fixation duration (ms)[a]	267.39	(4.89)	285.46	(8.88)	261.34	(2.75)	n.s.	n.s.	*
Percentage of fixations on vehicles (%)	80.22	(1.32)	69.65	(0.98)	72.4	(0.68)	***	***	n.s.
Percentage of fixations on the intersection (%)	12.16	(0.72)	18.45	(0.53)	13.42	(0.37)	***	n.s.	***
Scanpath length (^{o})	1126.21	(71.15)	793.38	(33.82)	1146.08	(26.19)	***	n.s.	***
Number of gaze shifts	13.45	(0.7)	9.40	(0.41)	12.71	(0.25)	***	n.s.	***
Area under the curve (pixels)	21355.7	(923.68)	16297.6	(758.96)	18027.9	(394.01)	***	***	n.s.
Directional analysis									
Saccadic amplitude (^{o}) to the blind or left hemifield	19.05	(0.74)	15.59	(0.38)	22.99	(0.36)	***	***	***
Saccadic amplitude (^{o}) to the seeing or right hemifield	23.23	(0.75)	17.35	(0.41)	22.28	(0.32)	***	n.s.	***
Hemispace analysis									
Proportion of fixations (%) in the blind or left hemifield	58.71	(1.36)	55.45	(1.41)	49.19	(0.72)	n.s.	***	***
Proportion of area under the curve (%) in the blind or left hemifield	63.29	(1.78)	58.04	(2.14)	52.70	(0.93)	n.s.	***	**

Table 4: Gaze-related parameters, directional and hemispace analyses for $HVFD_A$, $HVFD_I$ patients, and normal subjects (N) for both density conditions (mean). Statistical comparisons were made between density 50% - density 75% (matched pairs t-test).
Bonferroni: * $p<0.05$, ** $p<0.01$, *** $p<0.001$, n.s. indicates non-significant comparisons
[a] Mann-Whitney U test (paired samples)

	$HVFD_A$			**$HVFD_I$**			**N**		
Gaze-related parameters	**Density 50%**	**Density 75%**	**p**	**Density 50%**	**Density 75%**	**p**	**Density 50%**	**Density 75%**	**p**
Number of fixations/s	2.64	2.55	*	2.61	2.55	n.s.	2.34	2.26	***
Fixation duration (ms)[a]	283.91	267.39	**	307.71	285.45	**	302.87	261.34	***
Percentage of fixations on vehicles (%)	64.59	80.22	***	54.54	69.65	***	59.82	72.4	***
Percentage of fixations on the intersection (%)	15.16	12.16	***	22.08	18.45	***	18.52	13.42	***
Scanpath length (°)	810.83	1126.21	***	610.76	793.38	***	816.31	1146.08	***
Number of gaze shifts	10.1	13.45	***	7.16	9.4	***	9.42	12.71	***
Area under the curve (pixels)	18873.3	21355.7	***	14597	16297.6	***	14771.8	18027.9	***
Directional analysis									
Saccadic amplitude (°) to the blind or left hemifield	18.06	19.05	n.s.	14.58	15.59	**	22.03	22.99	**
Saccadic amplitude (°) to the seeing or right hemifield	23.77	23.23	n.s.	17.69	17.35	n.s.	21.58	22.28	n.s.
Hemispace analysis									
Proportion of fixations (%) in the blind or left hemifield	59.88	58.71	n.s.	59.52	55.45	**	47.47	49.19	n.s.
Proportion of area under the curve (%) in the blind or left hemifield	67.08	63.29	n.s.	63.45	58.04	**	49.7	52.70	*

Table 5: Directional and hemispace analyses for $HVFD_A$, $HVFD_I$ patients, and normal subjects (N) in both hemifields [mean]. Statistical comparisons were made between blind (B) and seeing (S) hemifield for patients, and between left (L) and right (R) hemifield for normal subjects (unpaired t-tests).
Bonferroni: * $p<0.05$, ** $p<0.01$, *** $p<0.001$, n.s. indicates non-significant comparisons

	$HVFD_A$				**$HVFD_I$**				**N**			
	Density 50%	**p**	**Density 75%**	**p**	**Density 50%**	**p**	**Density 75%**	**p**	**Density 50%**	**p**	**Density 75%**	**p**
Saccadic amplitude (°) to the B or S (L or R)	18.06 / 23.77	***	19.05 / 23.23	***	14.58 / 17.69	***	15.59 / 17.35	**	22.03 / 21.58	n.s.	22.99 / 22.28	n.s.
Proportion of fixations (%) in the B or S (L or R)	59.88 / 40.12	***	58.71 / 41.29	***	59.52 / 40.48	***	55.45 / 44.55	***	47.47 / 52.53	***	49.19 / 50.81	n.s.
Proportion of area under the curve (%) in the B or S (L or R)	67.08 / 32.92	***	63.29 / 36.71	***	63.45 / 36.55	***	58.04 / 41.96	***	49.70 / 50.30	n.s.	52.70 / 47.3	***

The pupillary light reflex pathway

Cytoarchitectonic probabilistic maps in hemianopic patients

E. Papageorgiou, MD
L.F. Ticini
G. Hardiess, PhD
F. Schaeffel, PhD
H. Wiethoelter, MD
H.A. Mallot, PhD
S. Bahlo
B. Wilhelm, MD
R. Vonthein, PhD
U. Schiefer, MD
H.-O. Karnath, MD, PhD

Address correspondence and reprint requests to Prof. Dr. med. U. Schiefer, Centre for Ophthalmology, Schleichstrasse 12-16, 72076, Tuebingen, Germany
Ulrich.Schiefer@uni-tuebingen.de

ABSTRACT

Objective: The anatomy of the human pupillary light reflex (PLR) pathway is a matter of debate. The aim of this study was twofold: namely, to investigate the association of a relative afferent pupillary defect (RAPD) in acquired suprageniculate lesions with the location and extent of the cerebral lesions. Further, we suggest a new strategy of lesion analysis by combining established techniques with the stereotaxic probabilistic cytoarchitectonic atlas developed by the Jülich group.

Methods: Twenty-three patients with homonymous visual field defects participated in this study. The RAPD was quantified clinically by two independent examiners with graded neutral density filters (swinging flashlight test). Using MRI in each individual, cerebral regions commonly affected in patients with a RAPD but spared in patients without a RAPD were determined and subsequently assessed by using cytoarchitectonic probabilistic maps.

Results: A RAPD was present in 10/23 patients. Comparison of patients showing a RAPD vs those not showing a RAPD revealed that a region including the course of the optic radiation at its early beginning in the temporal white matter is commonly associated with a RAPD.

Conclusions: It was demonstrated that the pupillary light reflex (PLR) depends on the input of suprageniculate neurons, thus supporting the involvement of a cortical pathway also. The site of integration of cortical signals in relation to the PLR into the pupillomotor pathway may be located suprageniculately in the vicinity of the lateral geniculate nucleus. Moreover, the suggested combination of established lesion analysis techniques with the probabilistic cytoarchitectonic atlas turned out to be a very helpful amelioration of stroke data analyses. ***Neurology*® 2008;70:956–963**

GLOSSARY

CG = ciliary ganglion; **DWI** = diffusion-weighted imaging; **FLAIR** = fluid-attenuated inversion-recovery; **HVFD** = homonymous visual field defect; **IN** = intercalated neurons; **LGN** = lateral geniculate nuclei; **MNI** = Montreal Neurological Institute; **N.III** = oculomotor nerve; **NEW** = nucleus Edinger-Westphal; **ON** = optic nerve; **OT** = optic tract; **PLR** = pupillary light reflex; **PT** = pretectal area; **RAPD** = relative afferent pupillary defect; **SCN** = short ciliary nerves.

The neural pathway of the pupillary light reflex (PLR) was first described by Wernicke in the 1880s.[1] Afferent fibers from the retina travel in the optic nerve and undergo hemidecussation at the chiasm before entering the optic tract. In the posterior third of the optic tract, the fibers branch medial to the lateral geniculate nucleus (LGN) and synapse in the ipsilateral pretectal nucleus. Intercalated neurons from each pretectal nucleus then project to both Edinger-Westphal nuclei and parasympathetic fibers from the Edinger-Westphal nuclei innervate the iris pupillary sphincter muscle.

A relative afferent pupillary defect (RAPD) is characterized by diminished pupillary constriction on direct illumination with a normal consensual response to illumination of the contralateral eye. It is typically related to lesions within the anterior visual pathways and is almost always present in unilateral or asymmetric bilateral optic nerve disease. A

Supplemental data at www.neurology.org

From Centre for Ophthalmology (E.P., F.S., B.W., U.S.), Section Neuropsychology, Center for Neurology (L.F.T., H.-O.K.), and Department of Medical Biometry (R.V.), University of Tuebingen; Department of Zoology (G.H., H.A.M.), Lab of Cognitive Neuroscience, Tuebingen; Department of Neurology (H.W.), Buerger Hospital, Stuttgart; and Bad Urach Rehabilitation Center (S.B.), Germany.

Supported by the following grants: European Union (PERACT-Marie Curie Early Stage Research Training, MEST-CT-2004-504321), Bundesministerium für Bildung und Forschung (BMBF-Verbundprojekt "Räumliche Orientierung" 01GW0641), GRK 778.

Disclosure: Dr. Ulrich Schiefer receives royalties from some of the equipment of this study, which do not exceed $10,000/year.

RAPD contralateral to the side of the lesion is also observed in optic tract lesions, which are characterized by incongruent homonymous visual field defects (HVFDs) and asymmetric bilateral optic disc atrophy.[2] The proposed pathogenesis for the presence of a contralateral RAPD in an optic tract lesion is based on the greater nasal photoreceptor density, a ratio of crossed to uncrossed fibers in the chiasm of 53:47 and a temporal visual field 61% to 71% larger than the nasal field.[3] A tract lesion disrupts fibers from the contralateral nasal retina and the ipsilateral temporal retina, thus disproportionally diminishing input from the contralateral eye and producing a corresponding RAPD.[4] Furthermore, a RAPD has also been described in patients with congenital occipital hemianopia. The suggested mechanism is transsynaptic optic tract atrophy after intrauterine or perinatal damage to the suprageniculate visual pathway, which presumably affects also the afferent pupillary fibers to the pretectal area of the mesencephalon.[5,6] Therefore, the detection of a RAPD in acute homonymous hemianopias has been commonly used in differentiating infrageniculate from suprageniculate lesions, since neither optic atrophy nor a RAPD should occur in acquired affections of the optic radiation or the visual cortex.[3,7-9]

However, the presence of a RAPD in acquired suprageniculate lesions and the underlying anatomic pathway are still a matter of debate, mainly because of numerous studies, reporting disturbances of the PLR in patients with HVFDs due to lesions not involving the optic tract. In the early 1940s and later elaborated investigations by several authors had already shed some doubt on the validity of Wernicke's model of a direct retinal-pretectal connection.[1] Furthermore, pupillary hemihypokinesia—that is, reduced or absent pupillary reaction to perimetric stimuli in the blind part of the visual field—was observed in all kinds of postchiasmal lesions.[10-13] These early clinical reports were later confirmed by other groups using modern pupillometric techniques.[14-17] In addition to the former studies, a clinically relevant RAPD, as a response to full-field light stimulation, was also reported in suprageniculate lesions, if the damaged area is close to the LGN.[18] Many theories have been developed to explain these phenomena, the most prominent pointing out that the integrity of the pupillomotor response depends upon or is influenced also by the occipital cortex.[19-22] However, the anatomic evidence is still limited to make any clear conclusions.

The aims of this study thus were 1) to assess the presence and magnitude of the RAPD in patients with HVFDs due to cerebrovascular lesions in the posterior and middle cerebral artery territories, and 2) to analyze the association of the pupillary findings with the location and extent of the cerebral lesions. Further, the present study suggests 3) a new strategy of lesion analysis by combining established techniques with the stereotaxic probabilistic cytoarchitectonic atlas developed by the Jülich group.[23,24] In contrast to the reference brain of the Talairach and Tournoux atlas,[25] or the Montreal Neurological Institute (MNI) single subject or group templates,[26,27] these probabilistic cytoarchitectonic maps provide stereotaxic information on the location and variability of cortical areas in the MNI reference space. They are based on the analysis of the cytoarchitecture in a sample of 10 human postmortem brains and already are available for various brain regions (http://www.fz-juelich.de/ime/ime_brain_mapping).

METHODS Twenty-three patients with HVFDs (16 men and 7 women), with a mean age of 50.5 years (age range: 21 to 74 years, SD 17 years) were enrolled in this study (appendix e-1 on the *Neurology*® Web site at www.neurology.org). Patients were recruited from the Centre for Ophthalmology at the University of Tübingen (Germany), the University Neurology Clinic of Tübingen, as well as the Neurology Clinic of Buerger Hospital in Stuttgart and the Bad Urach Rehabilitation Center. All patients had a homonymous visual field defect, varying from a complete homonymous hemianopia to homonymous paracentral scotomas. The cause was a unilateral vascular brain lesion in the territories of the posterior or middle cerebral arteries, which was documented by MRI. There were 12 patients with right-sided and 11 patients with left-sided lesions. Best-corrected monocular (near and distant) visual acuity was at least 16/20. Patients with unilateral cataract, marked anisocoria, amblyopia,

strabismus, ocular motility disorders, optic nerve diseases, glaucoma, advanced diseases of the retina, or funduscopic signs of bilateral asymmetric optic disc atrophy, which could indicate an optic tract involvement, were excluded from this study.

The median time since lesion onset and the neuro-ophthalmologic investigation used for the present analysis was 1 year (range 0.3 to 11.2 years, appendix e-2). The RAPD was assessed clinically by means of the swinging flashlight test. This test was selected because it represents an easy-to-apply, clinical examination, which provides reliable results about visual sensory dysfunction immediately.[28] The aim was to detect the degree of asymmetry between both eyes regarding the pupillary light reflex, which is independent of the absolute pupillary responses. Therefore only the relationship of responses between both sides (RAPD) was investigated: in a dark room an indirect ophthalmoscope as a light source was held below the level of the line of sight, with its light beam elevated at about a 45 degree angle. Initially pupil size was assessed under two different ambient light conditions in order to detect the presence of anisocoria. If no anisocoria was found and the pupils responded well to the light stimulus, then one eye was illuminated, and after 2 to 3 seconds, the light was shifted quickly to the contralateral eye. The process was repeated four or five times. A RAPD was defined in case of a pathologic swinging flashlight test: if the consensual response of the pupil was better than the direct, an ipsilateral RAPD was diagnosed, while if the direct response was better than the consensual, a contralateral RAPD was diagnosed. Using neutral density filters of varying strength, we measured the magnitude of a RAPD, by weakening the light stimulus as it was presented to the better eye. The filters were separated in 0.3 log unit steps from 0.3 to 1.8 log units. A RAPD was defined as any asymmetry of 0.3 log units or more, while any asymmetry below 0.3 log units was defined as a RAPD 0. In order to test the reproducibility and reliability of the results, all pupil examinations were carried out by two independent examiners, a senior neuro-ophthalmologist (U.S.) and a resident (E.P.). Both ophthalmic examiners were blinded to the perimetric and the imaging results. Agreement between examiners regarding the presence and magnitude of a RAPD was 0.74 (SE 0.13), assessed by Cohen's kappa. All analyses were performed according to the findings of the senior neuro-ophthalmologist (appendix e-1, Examiner 1).

Mapping and analysis of lesion location was carried out by two experimenters (H.-O.K. and L.F.T.) without knowledge of test results and clinical features of the patients. For lesion delineation, diffusion-weighted imaging (DWI) was used within the first 48 hours post-stroke and weighted fluid-attenuated inversion-recovery (FLAIR) sequences when imaging was conducted 48 hours or later after stroke. Two cases with marked perifocal edema or marked hemorrhage leading to a significant shift of anatomic structures were excluded. The median time between stroke and imaging used for the present analyses was 4.5 days (range 0 to 200 days, appendix e-2). In one subject (No. 15) the original scans were of low quality such that new MRI scans were obtained at 11.2 years after the brain lesion. Brain imaging had typically preceded the neuro-ophthalmologic examination (median time between imaging and neuro-ophthalmologic examination 1 year, range 0.3 to 9.9 years, appendix e-2).

In 8 of the 23 patients with HVFDs, MR images were available in digital format. In these cases, the boundary of the lesion was delineated directly on every single transversal slice of the individual MRI using MRIcro software (http://www.mricro.com).[29] Both the scan and lesion shape were then transformed into stereotaxic space using the spatial normalization algorithm provided by SPM2 (http://www.fil.ion.ucl.ac.uk/spm/), using default settings. For determination of the transformation parameters, cost-function masking was employed.[30] In 15 of the 23 cases MRI data were not available in digital format. In these cases, MRIcro software was used to manually map the lesion on transversal slices of the T1-template MRI from the MNI (www.bic.mni.mcgill.ca/cgi/icbm_view) distributed with MRIcro. Lesions were mapped onto the slices that correspond to Z-coordinates −40, −32, −24, −16, −8, 0, 8, 16, 24, 32, 40, and 50 mm in MNI coordinates by using the identical or the closest matching transversal slices of each individual. Since the right and left visual pathway can be considered identical regarding anatomy and function, for the anatomic analysis the left-sided lesions were mirrored and superimposed on the right side of the brain template.

To identify the anatomic structures that were commonly affected in patients showing the disorder (here the RAPD) but were typically spared in patients without the disorder, we here used a new combination of the established lesion subtraction analysis[31] with the stereotaxic probabilistic cytoarchitectonic atlas, the latter developed by the Jülich group.[23,24] Subtraction plots directly contrast patients with stroke showing vs not showing the disorder. Since subtractions were made between groups of different sizes proportional values were used. Subsequently, the resulting subtraction image was plotted onto maps of the stereotaxic probabilistic cytoarchitectonic map of the optic radiation by Bürgel and coworkers.[32,33] This map illustrates the relative frequency with which a certain fiber tract of 10 normal human brains was present on a MNI reference brain in a voxel (e.g., a 50% value of a fiber tract in a certain voxel of the reference brain indicates that the fiber tract was present in that voxel in 5 out of 10 brains). The probabilistic cytoarchitectonic map thus serves as a measure of intersubject variability for each voxel of the reference space.

RESULTS A RAPD was present in 10 out of 23 patients and was located contralateral to the affected hemisphere in all 10 cases. The median magnitude was 0.3 log units (six patients) and the range was between 0.3 and 0.9 log units. A RAPD of 0.6 log units was demonstrated in three patients and one patient showed a RAPD of 0.9 log units. Patients 1, 7, 11, 12, and 17 were re-examined at least three times over a time span of 1 year after the brain lesion. The pupillary findings remained constant in all cases.

Figure 1A illustrates simple lesion overlay plots for the group of patients with a RAPD and the group without a RAPD. To identify the anatomic structures that were commonly affected in patients with a RAPD but were typically spared in patients without a RAPD, we subtracted the superimposed lesions of the group without a RAPD from the patient group with a RAPD, revealing percentage overlay plots. Figure 1B illustrates

Figure 1 Simple lesion overlay plots for the group of patients with relative afferent pupillary defect (RAPD positive) and the group without RAPD (RAPD negative) and subtraction of the superimposed lesions of the control group (without RAPD) from the overlap image of the group with RAPD

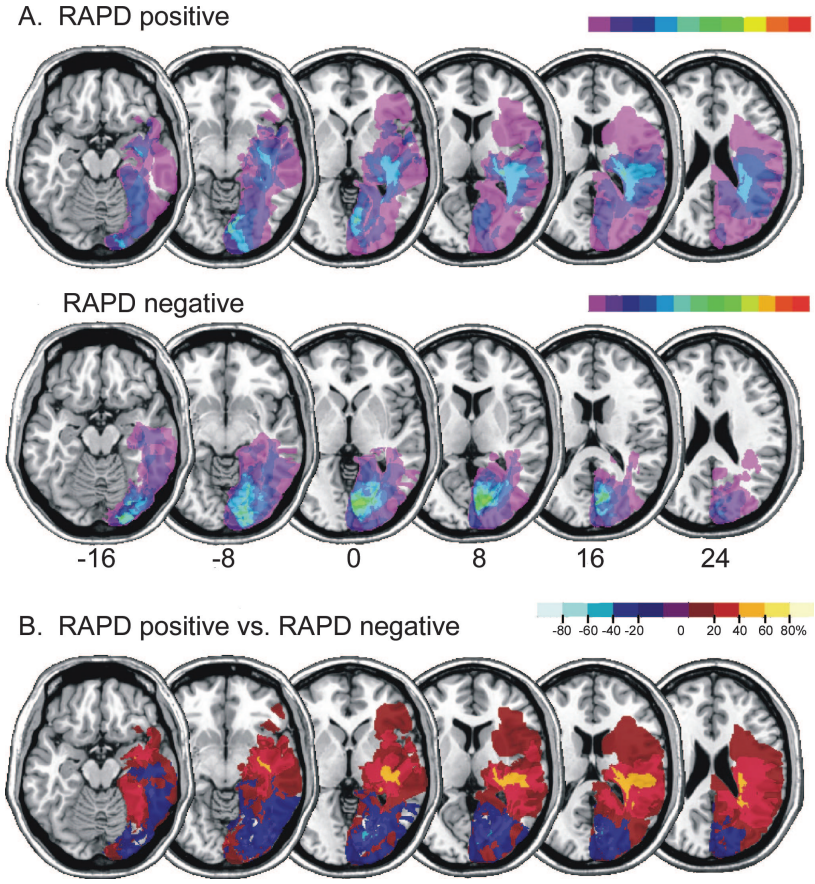

(A) Simple lesion overlay plots for the group of patients with RAPD (RAPD positive) and the group without RAPD (RAPD negative). Overlapping lesions are color-coded with increasing frequency from violet (n = 1) to red (n = 10 for RAPD positive; n = 13 for RAPD negative). MNI z-coordinates of each transverse section are given. (B) Subtraction of the superimposed lesions of the control group (without RAPD) from the overlap image of the group with RAPD. The center of the subtracted lesion overlap (orange area) indicates regions damaged at least 40% more frequently in patients with RAPD than in patients without RAPD.

these results. We found the center (orange) of the subtracted lesion overlap associated with a RAPD in the subcortical temporal white matter, extending further into superior temporal cortex. To analyze the anatomic relationship of this center with the location of the optic radiation, we plotted it onto the recently developed probabilistic cytoarchitectonic map of the optic radiation by Bürgel and coworkers.[32,33] Figure 2 illustrates the result. We found the region commonly affected in patients with a RAPD but typically spared in patients without a RAPD primarily at the early beginning of the course of the optic radiation in the temporal white matter. In absolute numbers 6 of the 10 patients with a RAPD (60%) had a lesion in this area, while in only 1 of the 13 patients without a RAPD (8%) this area was affected. The difference was significant (Fisher exact $p = 0.019$).

The mean percentage of left or right hemisphere tissue affected in patients with a RAPD was 10.6%, while it was 4.5% in patients without a RAPD. A statistical comparison revealed no significant difference in the lesion volume between both groups of patients ($t = 1.686$, $df = 11$, two-tailed $p = 0.12$, unpaired t test for unequal variances).

DISCUSSION The PLR has for a long time been associated with subcortical projections, and this was consistent with some clinical observations which suggest that the pupils continue to respond, even when the patients are cortically blind.[34,35] Wernicke's model of a direct retinal–pretectal interaction explained these observations well and the PLR was thought to be associated with a single subcortical neural pathway until the early 1940s. Since then, numerous studies have examined the effect of visual cortical lesions on the PLR. The results—either the presence of pupillary hemihypokinesia in the blind part of the visual field or a RAPD contralateral to the brain lesion, as a response to full-field light stimulation—often contradicted this classic belief and provided evidence that the PLR is not just a pure subcortical pathway.[18,22] However, the exact anatomic pathway remained unknown.

Using a new strategy of lesion analysis by combining established subtraction techniques[31] with the stereotaxic probabilistic cytoarchitectonic atlas developed by the Jülich group,[23,24,32,33] our findings suggest that a region in the early course of the optic radiation in the temporal white matter, close to the LGN, seems to be associated with the presence of the RAPD. This finding is consistent with the hypothesis that the connection between visual pathways and pretectal area in the dorsal midbrain is probably closely related to the LGN.[4,18,36-38] It has been found that a RAPD in suprageniculate homonymous hemianopsia occurred in approximately half of all patients with lesions closer than 10 mm to the LGN or involving it but sparing the optic tract.[18] In lesions further than 18 mm away from the LGN, a RAPD did not occur at all. The authors concluded that the RAPD was probably not caused by a lesion of the visual pathway itself, but by a lesion of the intercalated neurons between the visual pathway and the pupillomotor centers in the pretectal area of the midbrain. This assumption is strengthened by several cases of a RAPD with normal visual function in lesions close to the LGN or pretectal

Figure 2 Probabilistic cytoarchitectonic map of the optic radiation by Bürgel and coworkers[25,26]

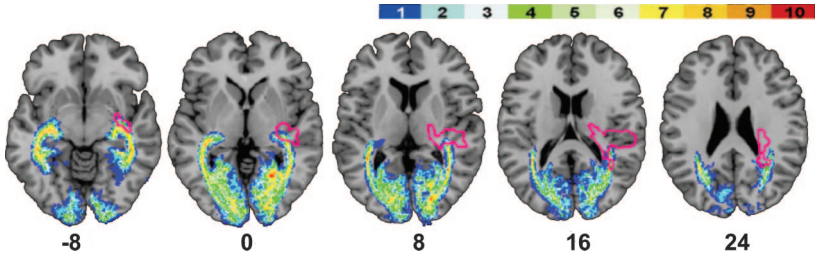

The color bar indicates the absolute frequency of voxels containing the optic radiation from 1 (dark blue) individual brain to 10 (red, overlap of all 10 [maximum] brains). The superimposed pink contour represents the center of the subtracted lesion overlap obtained in the present study (see orange area in figure 1B).

region as well as by reports of optic tract lesions without a RAPD.[4,28,37-44] The present findings also support the concept of cortical input into the PLR (figure 3), which may enter the PLR pathway via the area depicted in figures 1B and 2. Therefore, disturbed processing of signals along this part of the geniculostriate pathway can lead to a RAPD.

Figure 3 Schematic drawing of the pupillary light reflex pathway (figure modified from Wilhelm[21,52])

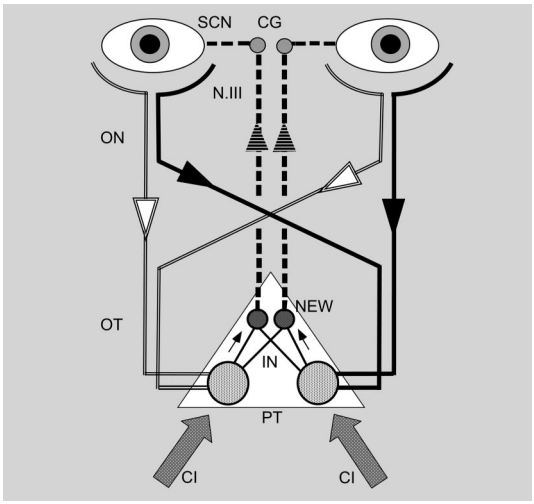

Afferent fibers from the retina travel in the optic nerve (ON) and undergo hemidecussation at the optic chiasm before entering the optic tract (OT). Close to the lateral geniculate nucleus (LGN) the fibers branch from the optic tract and pass through the brachium of the superior colliculus to reach the ipsilateral pretectal nucleus. However, there seems to be more input from suprageniculate neurons and the occipital cortex (CI). The exact anatomy of this connection is still unclear. Our data support that the site of integration of cortical signals in relation to the PLR into the pupillomotor pathway may be located suprageniculately in the early course of the optic radiation near the LGN (figure 2). Intercalated neurons (IN) from each pretectal nucleus then project to both Edinger-Westphal nuclei (NEW). Parasympathetic outflow from the Edinger-Westphal nuclei travels then with the oculomotor nerve (N.III) to the ciliary ganglion (CG) and via the short ciliary nerves (SCN) reaches the iris pupillary sphincter muscle. PT = pretectal area.

Another explanation could be that some afferent pupillomotor fibers of infrageniculate origin bypass the LGN and then travel through this critical area to the mesencephalon. Consistent with the aforementioned study, we draw a similar conclusion about a suprageniculate effect, although the site identified in the present study is located more distantly from the LGN.

Since the description of an impaired PLR in the blind field of subjects with definitely suprageniculate lesions a number of speculative suggestions have been offered to explain this finding.[10,12-14] It was hypothesized that transsynaptic degeneration could occur, either retrogradely across the geniculate synapse or into the pretectal area from the neocortical visual system, in line with former observations on cortico-pretectal interaction.[10,14,45-48] However, in the case of transsynaptic degeneration, one would expect that the RAPD would develop slowly, being found not earlier than months or years after the occipital lesion, and that in salient instances, optic disc atrophy should be observed. In the present study cohort, the RAPD in Patient 17 was demonstrated already a few days after the cerebral infarct and remained constant in the follow-up examinations, without any signs of optic disc atrophy. The pupillary findings in Patients 1, 7, 11, and 12 also remained constant in at least three re-examinations over a time span of 1 year after the brain lesion. Clinical observations have also provided evidence that transsynaptic degeneration in adults is still not convincing.[49] In our series, there were no funduscopic signs of partial optic atrophy in patients with a RAPD, thus indicating suprageniculate lesions. The time span between lesion and clinical examination exceeded 4 months in all cases; therefore the subsequent optic atrophy by a potential affection of the optic tract should already be visible, since the period necessary for retrograde degeneration following a pregeniculate lesion is estimated to be about 6 weeks.[49]

Potential models of cortico-pretectal interaction, which could be in accordance with our findings, have already been described.[50] It was observed that in patients with retrogeniculate hemianopsia the PLR in the blind hemifield was reduced but not absent. However, all the other specific, "higher" pupil responses to stimulus attributes, like stimulus color, structure, or motion, were completely lost. Therefore, it was considered that two or more distinct channels could serve the PLR: a more primitive "luminance channel," which connects the retina directly with the pretectal area and responds to diffuse light, and a

"pattern channel," which is mediated supragenic-ulately and responds to shifts in structured stimuli, like isoluminant grating, motion, and isoluminant color stimuli. According to the authors, the PLR is primarily mediated by the luminance channel and to a smaller extent by the "weaker," supragenic-ulate pattern channel. This explanation could possibly account for the comparatively small magnitude of the RAPD (predominantly 0.3 logU) in the majority of patients in the present study. Although these previous studies refer to pupillary hemihypokinesia, this model can also explain the presence of a RAPD in supragenic-ulate lesions of this critical region near the LGN. It is plausible that the critical area in the immediate vicinity of the LGN (figure 2) contains supragenic-ulate projections of the so-called "pattern channel" to the mesencephalon. A cortico-mesencephalic interaction should thus not be surprising, if one considers the selective loss of pupil color response in cerebral achromatopsia and the pupil near response, which must also be mediated by a similar cortical input to the Edinger-Westphal nuclei.[34] Recent studies assessing the various components of the pupil response that have been affected in subjects with damage to the dorsal midbrain (Parinaud syndrome) have also demonstrated that there was a small, residual PLR and preserved reactions to pattern and color stimuli as well as preserved pupillary sleepiness-related oscillations.[22] The authors suggested the existence of a cortical input to the pupillary pathway, since the retinal afferent input to the pretectal nuclei had been apparently damaged.[22]

The present results are still subject to interpretation, because our study has some limitations. One could stem from the resolution capacity of the imaging methods that are currently available. It cannot be excluded that our patients had additional, subclinical lesions affecting mesencephalic structures, i.e., the pretectal area or the vicinity of the oculomotor nucleus, which could possibly explain the presence of the RAPD. However, modern MRI techniques already provide anatomic information from living human beings with very high precision. By using FLAIR sequences, we excluded cases with marked perifocal edema or significant shift of anatomic structures. However, some tract or midbrain compression from secondary swelling may have occurred. Under-recognition of such cases, either due to slight effects or to changes undetectable with the current methods, is a further limitation of our study. Additionally, one could argue that the exclusion of patients with pregeniculate lesions was done funduscopically by two examiners (U.S. and E.P.), by detecting signs of bilateral asymmetric optic disc atrophy. However, it is very unlikely that the RAPD in all 10 patients was caused by an ophthalmoscopically and radiologically invisible pregeniculate or midbrain lesion, since special attention was paid in exactly excluding these cases. Secondly, it is well-known that lesions of the optic tract are seldom causes of homonymous visual field defects. Finally, interindividual variation in the connections between the visual pathway and the pupillomotor nuclei of the mesencephalon should be considered when trying to construct anatomic models.

Furthermore, the findings are based on the classification of patients according to a threshold of a RAPD of 0.3 log units. In a recent study, a RAPD of 0.3 log units was present in 2 of 102 healthy subjects.[51] Higher RAPDs were not found in the sample. These results, that were derived from a large number of normal subjects and were confirmed by means of modern pupillography, support the use of the threshold of 0.3 log units as a pathologic limit. On the other hand, a certain limitation of our study derives from a theoretically possible overlap between the groups with/without a RAPD. This may be due to the rather rough threshold of 0.3 log units used for the division into groups, which was assessed clinically with a certain variability of estimation. However, in order to increase the reliability of results, two independent examiners assessed the RAPD in all patients, resulting in substantial agreement. The use of neutral density filters with a transmission of 0.3 log units further aided in the detection and quantification of a RAPD. Moreover, according to the finding that 2 in 102 normal subjects show a RAPD of 0.3 log units, the expected number among the same number of normal subjects as patients in the present study would be less than one. Since there are six patients with a RAPD of 0.3 log units, it cannot be attributed to a normal pupillary system in more than one of the six cases and it seems therefore rather unlikely that RAPDs of 0.3 log units occurred independently of the brain lesion.[51] The fact that the RAPD in the present study as well as in previous ones was always located contralateral to the brain lesion further supports the belief that its presence is not coincidental.[18]

ACKNOWLEDGMENT

The authors thank Elke Krapp for careful construction of this manuscript as well as Prof. Helmut Wilhelm for providing an original version of figure 3.

Received April 4, 2007. Accepted in final form November 21, 2007.

REFERENCES

1. Wernicke C. Über hemianopische Pupillenreaktion. Fortschr Med 1883;1:49–53.
2. Savino PJ, Paris M, Schatz NJ, Orr LS, Corbett JJ. Optic tract syndrome: a review of 21 patients. Arch Ophthalmol 1978;96:656–663.
3. Bell RA, Thompson HS. Relative afferent pupillary defect in optic tract hemianopias. Am J Ophthalmol 1978;85:538–540.
4. King JT Jr, Galetta SL, Flamm ES. Relative afferent pupillary defect with normal vision in a glial brainstem tumor. Neurology 1991;41:945–946.
5. Tychsen L, Hoyt WF. Occipital lobe dysplasia: magnetic resonance findings in two cases of isolated congenital hemianopia. Arch Ophthalmol 1985;103:680–682.
6. Tychsen L, Hoyt WF. Relative afferent pupillary defect in congenital occipital hemianopia. Am J Ophthalmol 1985;100:345–346.
7. Lowenfeld IE. The pupil. Anatomy, Physiology and Clinical Applications Vol. 1. Detroit: Wayne State University Press; 1993.
8. Newman SA, Miller NR. Optic tract syndrome: neuro-ophthalmologic considerations. Arch Ophthalmol 1983;101:1241–1250.
9. Takahashi T, Hohki T, Entani S, Yamashita H, Shiba K. Optic tract syndrome with relative afferent pupillary defect. Jpn J Ophthalmol 1991;35:325–330.
10. Alexandridis E, Krastel H, Reuther R. [Disturbances of the pupil reflex associated with lesions of the upper visual pathway (author's transl).] Albrecht von Graefes Arch Klin Exp Ophthalmol 1979;209:199–208.
11. Frydrychowicz G, Harms H. Ergebnisse pupillomotorischer Untersuchungen bei Gesunden und Kranken. Ber Zusammenkunft Dtsch Ophthalmol Ges 1940;71–79.
12. Harms H. Grundlagen, Methodik und Bedeutung der Pupillenperimetrie für die Physiologie und Pathologie des Sehorgans. Albrecht von Graefes Arch Ophthalmologie 1949;149:1–68.
13. Harms H. Hemianopische Pupillenstarre. Klin Monatsbl Augenheilkd 1951;118:133–147.
14. Cibis GW, Campos EC, Aulhorn E. Pupillary hemiakinesia in suprageniculate lesions. Arch Ophthalmol 1975;93:1322–1327.
15. Hellner KA, Jensen W, Muller-Jensen A. Videoprocessing pupillographic perimetry in hemianopsia (author's transl). Klin Monatsbl Augenheilkd 1978;172:731–735.
16. Kardon RH, Kirkali PA, Thompson HS. Automated pupil perimetry. Ophthalmology 1991;98:485–496.
17. Kardon RH. Pupil perimetry. Ophthalmology 1992;3:565–570.
18. Wilhelm H, Wilhelm B, Petersen D, Schmidt U, Schiefer U. Relative afferent pupillary defects in patients with geniculate and retrogeniculate lesions. Neuro-Ophthalmology 1996;16:219–224.
19. Hamann KU, Hellner KA, Muller-Jensen A, Zschocke S. Videopupillographic and VER investigations in patients with congenital and acquired lesions of the optic radiation. Ophthalmologica 1979;149:348–356.
20. Wilhelm H, Kardon R. The pupillary light reflex pathway. Neuro-Ophthalmology 1997;6:219–224.
21. Wilhelm H. Pupille und retrogenikuläre Sehbahn. Ophthalmologe 1996;93:319–324.
22. Wilhelm BJ, Wilhelm H, Moro S, Barbur JL. Pupil response components: studies in patients with Parinaud's syndrome. Brain 2002;125(Pt 10):2296–2307.
23. Amunts K, Zilles K. Advances in cytoarchitectonic mapping of the human cerebral cortex. Neuroimaging Clin N Am 2001;11:151–169.
24. Zilles K, Schleicher A, Palomero-Gallagher N, Amunts K. Quantitative analysis of cyto- and receptor architecture of the human brain. In: Mazziotta JC, Toga A, eds. Brain Mapping: The Methods. Amsterdam: Elsevier; 2002:573–602.
25. Talairach J, Tournoux P. Co-Planar Stereotaxic Atlas of the Human Brain. Stuttgart: Thieme; 1988.
26. Collins DL, Neelin P, Peters TM, Evans AC. Automatic 3D intersubject registration of MR volumetric data in standardized Talairach space. J Comput Assist Tomogr 1994;18:192–205.
27. Evans AC, Marrett S, Neelin P, et al. Anatomical mapping of functional activation in stereotactic coordinate space. Neuroimage 1992;1:43–53.
28. Eliott D, Cunningham ET, Miller NR. Fourth nerve paresis and ipsilateral relative afferent pupillary defect without visual sensory disturbance. A sign of contralateral dorsal midbrain disease. J Clin Neuroophthalmol 1991;11:169–174.
29. Rorden C, Brett M. Stereotaxic display of brain lesions. Behav Neurol 2000;12:191–200.
30. Brett M, Leff AP, Rorden C, Ashburner J. Spatial normalization of brain images with focal lesions using cost function masking. Neuroimage 2001;14:486–500.
31. Rorden C, Karnath H-O. Using human brain lesions to infer function: a relic from a past era in the fMRI age? Nat Rev Neurosci 2004;5:813–819.
32. Bürgel U, Amunts K, Hoemke L, Gilsbach JM, Zilles K. White matter fiber tracts of the human brain: three-dimensional mapping at microscopic resolution, topography and intersubject variability. Neuroimage 2006;29:1092–1105.
33. Bürgel U, Schormann T, Schleicher A, Zilles K. Mapping of histologically identified long fiber tracts in human cerebral hemispheres to the MRI volume of a reference brain: position and spatial variability of the optic radiation. Neuroimage 1999;10:489–499.
34. Barbur JL. Learning from the pupil–Studies of basic mechanisms and clinical applications. In: Chalupa LM, Werner JS, eds. The Visual Neurosciences. Cambridge: MIT Press; 2004:641–656.
35. Brindley GS, Gautier-Smith PC, Lewin W. Cortical blindness and the functions of the non-geniculate fibres of the optic tracts. J Neurol Neurosurg Psychiatry 1969;32:259–264.
36. Behr C. Hemianopische Pupillenstarre ohne Hemianopsie. Z Prakt Augenheilkd 1926;58:398–406.
37. Girkin CA, Perry JD, Miller NR. A relative afferent pupillary defect without any visual sensory deficit. Arch Ophthalmol 1998;116:1544–1545.
38. Johnson RE, Bell RA. Relative afferent pupillary defect in a lesion of the pretectal afferent pupillary pathway. Can J Ophthalmol 1987;22:282–284.
39. Chen CJ, Scheufele M, Sheth M, Torabi A, Hogan N, Frohman EM. Isolated relative afferent pupillary defect secondary to contralateral midbrain compression. Arch Neurol 2004;61:1451–1453.

40. Ellis CJ. Afferent pupillary defect in pineal region tumour. J Neurol Neurosurg Psychiatry 1984;47:739–741.
41. Forman S, Behrens MM, Odel JG, Spector RD, Hilal S. Relative afferent pupillary defect with normal visual function. Arch Ophthalmol 1990;108:1074–1075.
42. Schiefer U, Dietrich TJ, Wilhelm B, Wilhelm H. Absence of relative afferent pupillary defect and pupillary hemiakinesia in a child with homonymous hemianopia due to (retro-)geniculate porencephaly. Br J Ophthalmol 1998;82:461–462.
43. Staubach F, Pieh C, Maier P, Lagrèze WA. Relative afferent pupillary defect with normal vision and vertical strabismus: implications for pupillary pathway anatomy. Graefes Arch Clin Exp Ophthalmol 2007;245:321–323.
44. Taguchi H, Kashii S, Kikuchi M, Yasuyoshi H, Honda Y. Superior oblique paresis with contralateral relative afferent pupillary defect. Graefes Arch Clin Exp Ophthalmol 2000;238:927–929.
45. van Buren JM. Trans-synaptic retrograde degeneration in the visual system of primates. J Neurol Neurosurg Psychiatry 1963;26:402–409.
46. Koerner F, Teuber HL. Visual field defects after missile injuries to the geniculo-striate pathway in man. Exp Brain Res 1973;18:88–113.
47. Sprague JM. Interaction of cortex and superior colliculus in mediation of visually guided behavior in the cat. Science 1966;153:1544–1547.
48. Szentagothai J. Die innere Gliederung des Oculomotoriuskernes. Arch Psychiat 1942;115:127–135.
49. Miller NR, Newman SA. Transsynaptic degeneration. Arch Ophthalmol 1981;99:1654.
50. Barbur JL, Keenleyside MS, Thomson WD. Investigation of central visual processing by means of pupillometry. In: Kulikowski JJ, Dickinson CM, Murray TJ, eds. Seeing Contour and Colour. Oxford: Pergamon Press; 1987:431–451.
51. Wilhelm H, Peters T, Lüdtke H. Relative afferent pupillary defect in normal subjects. J Neuroophthalmol 2007;27:263–267.
52. Wilhelm H. Neuro-ophthalmology of pupillary function-practical guidelines. J Neurol 1998;245:573–583.